

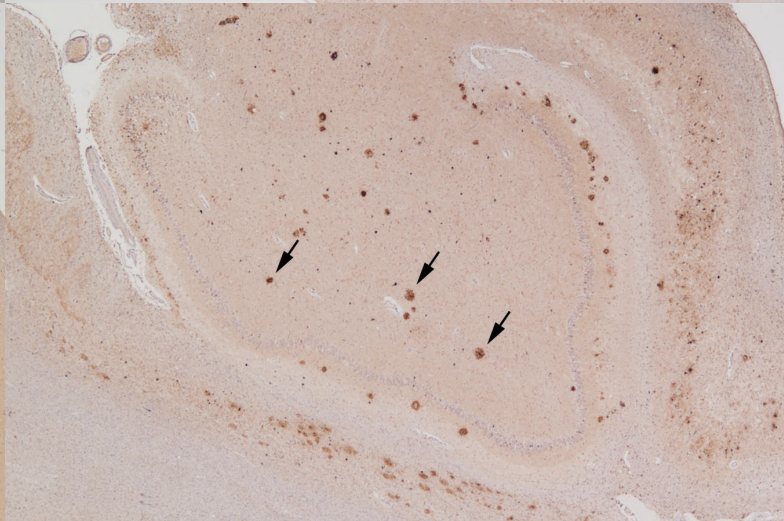
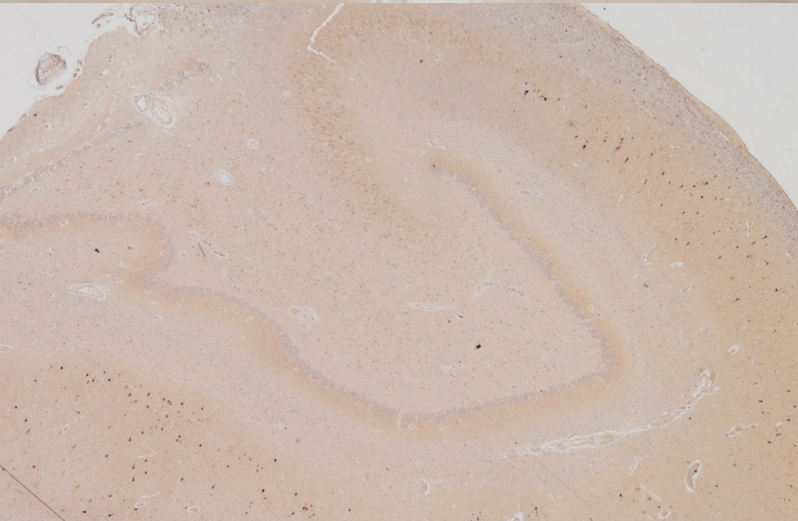
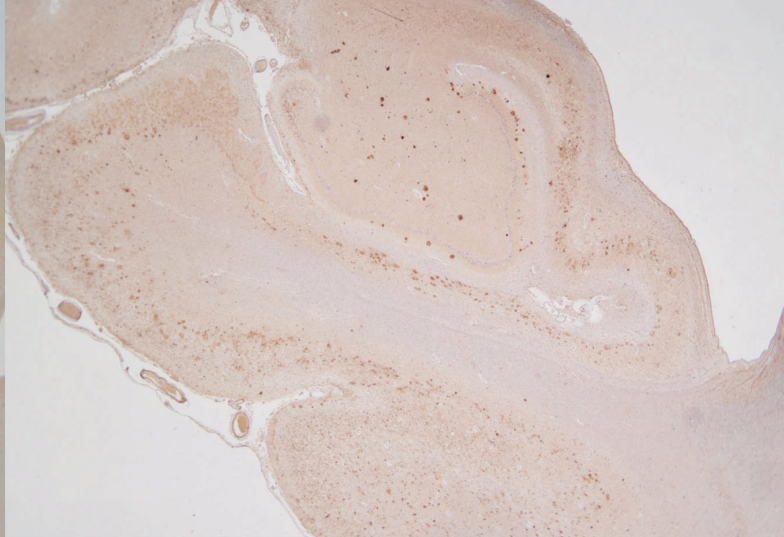
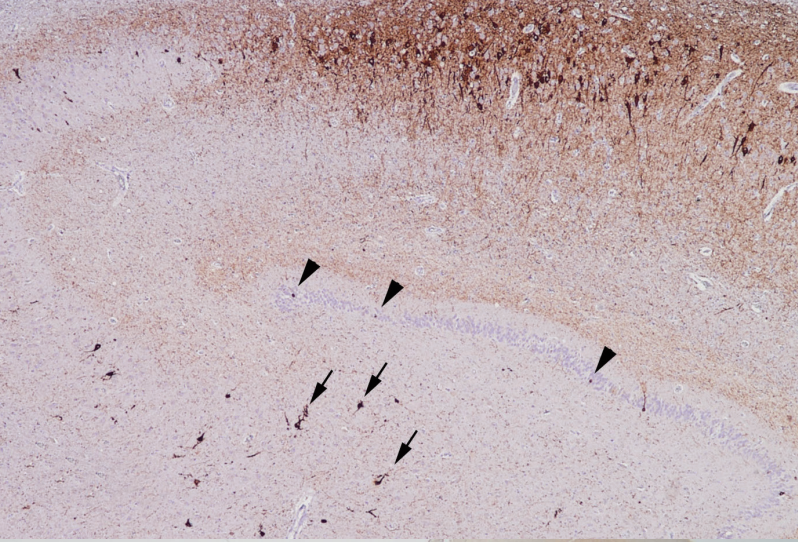
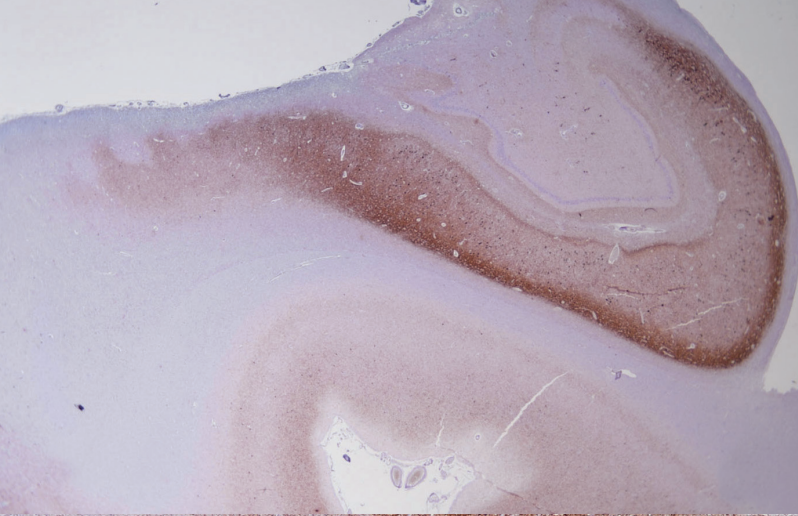
# JPTM

Journal of Pathology  
and Translational Medicine

May 2019  
Vol. 53 / No.3  
jpatholm.org  
pISSN: 2383-7837  
eISSN: 2383-7845



*Primary Age-Related  
Tauopathy*



## Aims & Scope

The *Journal of Pathology and Translational Medicine* is an open venue for the rapid publication of major achievements in various fields of pathology, cytopathology, and biomedical and translational research. The Journal aims to share new insights into the molecular and cellular mechanisms of human diseases and to report major advances in both experimental and clinical medicine, with a particular emphasis on translational research. The investigations of human cells and tissues using high-dimensional biology techniques such as genomics and proteomics will be given a high priority. Articles on stem cell biology are also welcome. The categories of manuscript include original articles, review and perspective articles, case studies, brief case reports, and letters to the editor.

## Subscription Information

To subscribe to this journal, please contact the Korean Society of Pathologists/the Korean Society for Cytopathology. Full text PDF files are also available at the official website (<http://jpatholm.org>). *Journal of Pathology and Translational Medicine* is indexed by Emerging Sources Citation Index (ESCI), PubMed, PubMed Central, Scopus, KoreaMed, KoMCI, WPRIM, Directory of Open Access Journals (DOAJ), and CrossRef. Circulation number per issue is 700.

## Editors-in-Chief

Jung, Chan Kwon, MD (*The Catholic University of Korea, Korea*) <https://orcid.org/0000-0001-6843-3708>

Park, So Yeon, MD (*Seoul National University, Korea*) <https://orcid.org/0000-0002-0299-7268>

## Senior Editors

Hong, Soon Won, MD (*Yonsei University, Korea*) <https://orcid.org/0000-0002-0324-2414>

Kim, Chong Jai, MD (*University of Ulsan, Korea*) <http://orcid.org/0000-0002-2844-9446>

## Associate Editors

Shin, Eunah, MD (*CHA University, Korea*) <http://orcid.org/0000-0001-5961-3563>

Kim, Haeryoung, MD (*Seoul National University, Korea*) <http://orcid.org/0000-0002-4205-9081>

## Editorial Board

Avila-Casado, Maria del Carmen (*University of Toronto, Toronto General Hospital UHN, Canada*)

Bae, Young Kyung (*Yeungnam University, Korea*)

Bongiovanni, Massimo (*Lausanne University Hospital, Switzerland*)

Choi, Yeong-Jin (*The Catholic University, Korea*)

Chung, Jin-Haeng (*Seoul National University, Korea*)

Fadda, Guido (*Catholic University of Rome-Foundation Agostino Gemelli University Hospital, Italy*)

Gong, Gyungyub (*University of Ulsan, Korea*)

Ha, Seung Yeon (*Gachon University, Korea*)

Han, Jee Young (*Inha University, Korea*)

Jang, Se Jin (*University of Ulsan, Korea*)

Jeong, Jin Sook (*Dong-A University, Korea*)

Kang, Gyeong Hoon (*Seoul National University, Korea*)

Kim, Aeree (*Korea University, Korea*)

Kim, Jang-Hee (*Ajou University, Korea*)

Kim, Jung Ho (*Seoul National University, Korea*)

Kim, Kyu Rae (*University of Ulsan, Korea*)

Kim, Se Hoon (*Yonsei University, Korea*)

Kim, Woo Ho (*Seoul National University, Korea*)

Ko, Young Hye (*Sungkyunkwan University, Korea*)

Koo, Ja Seung (*Yonsei University, Korea*)

Lee, C. Soon (*University of Western Sydney, Australia*)

Lee, Hye Seung (*Seoul National University, Korea*)

Lkhagvadorj, Sayamaa (*Mongolian National University of Medical Sciences, Mongolia*)

Moon, Woo Sung (*Chonbuk University, Korea*)

Park, Chan-Sik (*University of Ulsan, Korea*)

Park, Young Nyun (*Yonsei University, Korea*)

Shahid, Pervez (*Aga Khan University, Pakistan*)

Sung, Chang Ohk (*University of Ulsan, Korea*)

Than, Nandor Gabor (*Semmelweis University, Hungary*)

Tse, Gary M. (*The Chinese University of Hong Kong, Hong Kong*)

Tan, Puay Hoon (*National University of Singapore, Singapore*)

Yatabe, Yasushi (*Aichi Cancer Center, Japan*)

Yoon, Sun Och (*Yonsei University, Korea*)

Bychkov, Andrey (*Chulalongkorn University, Thailand Kameda Medical Center, Japan Nagasaki University Hospital, Japan*)

Chong, Yo Sep (*The Catholic University of Korea, Korea*)

Jain, Deepali (*All India Institute of Medical Sciences, India*)

Jun, Sun-Young (*The Catholic University of Korea, Korea*)

Lai, Chiung-Ru (*Taipei Veterans General Hospital, Taiwan*)

Liu, Zhiyan (*Shandong University, China*)

Paik, Jin Ho (*Seoul National University, Korea*)

Song, Joon Seon (*University of Ulsan, Korea*)

Zhu, Yun (*Jiangsu Institution of Nuclear Medicine, China*)

## Consulting Editors

Huh, Sun (*Hallym University, Korea*)

Kakudo, Kennichi (*Kindai University, Japan*)

Ro, Jae Y. (*Cornell University, The Methodist Hospital, U.S.A.*)

## Ethic Editors

Choi, In-Hong (*Yonsei University, Korea*)

## Statistics Editors

Kim, Dong Wook (*National Health Insurance Service Ilsan Hospital, Korea*)

Lee, Hye Sun (*Yonsei University, Korea*)

## Layout Editor

Chang, Soo-Hee (*InfoLumi Co., Korea*)

## Website and JATS XML File Producer

Cho, Yoosang (*M2Community Co., Korea*)

Im, Jeonghee (*M2Community Co., Korea*)

## Administrative Assistant

Jung, Ji Young (*The Korean Society Of Pathologists*)

Jeon, Anmi (*The Korean Society Of Cytopathology*)

## Contact the Korean Society of Pathologists/the Korean Society for Cytopathology

**Publishers:** Lee, Kyo Young, MD, Hong, Soon Won, MD

**Editors-in-Chief:** Jung, Chan Kwon, MD, Park, So Yeon, MD

**Published by the Korean Society of Pathologists/the Korean Society for Cytopathology**

## Editorial Office

Room 1209 Gwanghwamun Officia, 92 Saemunan-ro, Jongno-gu, Seoul 03186, Korea

Tel: +82-2-795-3094 Fax: +82-2-790-6635 E-mail: [office@jpatholm.org](mailto:office@jpatholm.org)

#1508 Renaissancetower, 14 Mallijae-ro, Mapo-gu, Seoul 04195, Korea

Tel: +82-2-593-6943 Fax: +82-2-593-6944 E-mail: [office@jpatholm.org](mailto:office@jpatholm.org)

**Printed by** iMiS Company Co., Ltd. (JMC)

Jungang Bldg. 18-8 Wonhyo-ro 89-gil, Yongsan-gu, Seoul 04314, Korea

Tel: +82-2-717-5511 Fax: +82-2-717-5515 E-mail: [ml@smileml.com](mailto:ml@smileml.com)

**Manuscript Editing by** InfoLumi Co.

210-202, 421 Pangyo-ro, Bundang-gu, Seongnam 13522, Korea

Tel: +82-70-8839-8800 E-mail: [infolumi.chang@gmail.com](mailto:infolumi.chang@gmail.com)

Front cover image: Expressions of tau and  $\beta$ -amyloid in primary age-related tauopathy compared with those in high-Alzheimer's disease neuropathologic change (Fig. 1). p161.

© Copyright 2019 by the Korean Society of Pathologists/the Korean Society for Cytopathology

© Journal of Pathology and Translational Medicine is an Open Access journal under the terms of the Creative Commons Attribution Non-Commercial License (<https://creativecommons.org/licenses/by-nc/4.0>).

© This paper meets the requirements of KS X ISO 9706, ISO 9706-1994 and ANSI/NISO Z.39.48-1992 (Permanence of Paper).

This journal was supported by the Korean Federation of Science and Technology Societies Grant funded by the Korean Government.

## CONTENTS

---

### REVIEWS

- 153 **Provisional Guideline Recommendation for *EGFR* Gene Mutation Testing in Liquid Samples of Lung Cancer Patients: A Proposal by the Korean Cardiopulmonary Pathology Study Group**  
Dong Hoon Shin, Hyo Sup Shim, Tae Jung Kim, Heae Surng Park, Yun La Choi, Wan Seop Kim, Lucia Kim, Sun Hee Chang, Joon Seon Song, Hyo Jin Kim, Jung Ho Han, Chang Hun Lee, Geon Kook Lee, Se Jin Jang, Korean Cardiopulmonary Pathology Study Group
- 159 **Primary Age-Related Tauopathy: An Elderly Brain Pathology Frequently Encountered during Autopsy**  
Daru Kim, Hyung-Seok Kim, Seong-Min Choi, Byeong C. Kim, Min-Cheol Lee, Kyung-Hwa Lee, Jae-Hyuk Lee

### ORIGINAL ARTICLES

- 164 **Potential Role for a Panel of Immunohistochemical Markers in the Management of Endometrial Carcinoma**  
Amany Salama, Mohammad Arafa, Eman ElZahaf, Abdelhadi Mohamed Shebl, Azmy Abd El-Hameed Awad, Sylvia A. Ashamalla, Reda Hemida, Anas Gamal, Abd AlRahman Foda, Khaled Zalata, El-Said M. Abdel-Hady
- 173 **Prognostic Role of Claudin-1 Immunohistochemistry in Malignant Solid Tumors: A Meta-Analysis**  
Jung-Soo Pyo, Nae Yu Kim, Won Jin Cho
- 180 **Association between p53 Expression and Amount of Tumor-Infiltrating Lymphocytes in Triple-Negative Breast Cancer**  
Miseon Lee, In Ah Park, Sun-Hee Heo, Young-Ae Kim, Gyungyub Gong, Hee Jin Lee

### CASE REPORTS

- 188 **A Rare Case of Adenosquamous Carcinoma Arising in the Background of IgG4-Related Lung Disease**  
Sangjoon Choi, Sujin Park, Man Pyo Chung, Tae Sung Kim, Jong Ho Cho, Joungho Han
- 192 **Frozen Cytology of Meningeal Malignant Solitary Fibrous Tumor/Hemangiopericytoma**  
Myunghee Kang, Na Rae Kim, Dong Hae Chung, Gie-Taek Yie

**Instructions for Authors** for *Journal of Pathology and Translational Medicine* are available at <http://jpatholm.org/authors/authors.php>

# Provisional Guideline Recommendation for *EGFR* Gene Mutation Testing in Liquid Samples of Lung Cancer Patients: A Proposal by the Korean Cardiopulmonary Pathology Study Group

Dong Hoon Shin · Hyo Sup Shim<sup>1</sup>  
Tae Jung Kim<sup>2</sup> · Heae Surng Park<sup>3</sup>  
Yun La Choi<sup>4</sup> · Wan Seop Kim<sup>5</sup>  
Lucia Kim<sup>6</sup> · Sun Hee Chang<sup>7</sup>  
Joon Seon Song<sup>8</sup> · Hyo Jin Kim<sup>9</sup>  
Jung Ho Han<sup>4</sup> · Chang Hun Lee  
Geon Kook Lee<sup>10</sup> · Se Jin Jang<sup>8</sup>  
Korean Cardiopulmonary Pathology  
Study Group

Department of Pathology, Pusan National University School of Medicine, Yangsan;  
<sup>1</sup>Department of Pathology, Yonsei University College of Medicine, Seoul; <sup>2</sup>Department of Hospital Pathology, College of Medicine, The Catholic University of Korea, Seoul;  
<sup>3</sup>Department of Pathology, Ewha Womans University Mokdong Hospital, Seoul;  
<sup>4</sup>Department of Pathology, Samsung Medical Center, Sungkyunkwan University School of Medicine, Seoul; <sup>5</sup>Department of Pathology, Konkuk University School of Medicine, Seoul;  
<sup>6</sup>Department of Pathology, Inha University School of Medicine, Incheon; <sup>7</sup>Department of Pathology, Inje University Ilsan Paik Hospital, Inje University College of Medicine, Goyang; <sup>8</sup>Department of Pathology, Asan Medical Center, University of Ulsan College of Medicine, Seoul; <sup>9</sup>Department of Pathology, Seoul National University Bundang Hospital, Seongnam; <sup>10</sup>Department of Pathology, National Cancer Center, Goyang, Korea

**Received:** November 29, 2018

**Revised:** February 7, 2019

**Accepted:** February 20, 2019

## Corresponding Author

Se Jin Jang, MD, PhD  
Department of Pathology, Asan Medical Centre,  
University of Ulsan College of Medicine,  
88 Olympic-ro 43-gil, Songpa-gu, Seoul 05505,  
Korea  
Tel: +82-2-3010-5966  
Fax: +82-2-472-7898  
E-mail: jangsejin@amc.seoul.kr

Liquid biopsy for detection of mutation from circulating tumor DNA is a new technology which is attractive in that it is non-invasive. Epidermal growth factor receptor (EGFR) tyrosine kinase inhibitors (TKI) is an effective first line drug for advanced non-small cell lung cancer patients who harbor activating *EGFR* mutation. During the course of treatment, resistance against TKI arises which can be contributed to *EGFR* T790M mutation in about 50–60% of patients. Third generation TKI may overcome the resistance. In patients who cannot undergo tissue biopsy due to variable reasons, liquid biopsy is an excellent alternative for the detection of *EGFR* T790M mutation. However, this relatively novel method requires standardization and vigorous quality insurance. Thus, a standard set of guideline recommendations for liquid biopsy for *EGFR* mutation testing suitable for the Korean medical community is necessary. In this article, we propose a set of provisional guideline recommendations that was discussed and approved by the Cardiopulmonary Pathology Study Group of the Korean Society of Pathologists.

**Key Words:** Carcinoma, non-small-cell lung; Epidermal growth factor receptor; T790M; Circulating tumor DNA; Liquid biopsy

After the discovery of activating epidermal growth factor receptor (*EGFR*) gene mutation, *EGFR* tyrosine kinase inhibitors (TKI) became the first line of treatment in advanced non-small cell lung cancer (NSCLC) with mutated *EGFR*.<sup>1-3</sup> These *EGFR* TKIs such as gefitinib, erlotinib, and afatinib show consistently better response rate and prolonged progression-free survival in *EGFR* mutant NSCLC patients.<sup>1-3</sup> However, most patients receiving *EGFR* TKI treatment may develop acquired resistance.<sup>4-6</sup> Although various mechanisms are involved in this resistance, secondary T790M mutation of *EGFR* gene illustrates 50%–60% of the resistance.<sup>7,8</sup> A recently developed third generation TKIs can effectively target T790M, and so it is very critical to detect this mutation in patients who has developed acquired resistance against first- or second-line *EGFR* TKIs.<sup>9-11</sup>

Liquid biopsy is an emerging tool that detects genetic changes in circulating tumor DNA (ctDNA) shed from the tumor cells.<sup>12-14</sup> Recently, Cobas *EGFR* mutation test V2 (Roche, Indianapolis, IN, USA) has been approved by Food and Drug Administration (FDA) for the detection of *EGFR* mutations from the blood of NSCLC patients.<sup>15</sup> Although this non-invasive technique is fascinating and promising, it is still a developing method which needs further improvements. Hence, it is necessary to have guidelines for its usage. Korean cardiopulmonary study group has prepared the first guideline of *EGFR* mutation detection in blood for clinicians and pathologists who actively take part in the diagnosis and treatment of lung cancer.

## PATIENT ELIGIBILITY

Liquid biopsy for the detection of *EGFR* mutation can play many roles in cancer diagnostics.<sup>12-14,16,17</sup> Patients diagnosed with lung adenocarcinoma harboring *EGFR* mutation will be the first candidates when they develop resistance against first-line TKIs. Especially, when the tumor is too small or located in a challenging region to be sampled, liquid biopsy can be a good alternative.<sup>14-18</sup> Patients with poor performance status can also benefit from this technique.

**Table 1.** Comparison of specialized tubes for collection of ctDNA

Company	Trade name	Volume (mL)	Temperature (°C)	Storage duration (day)
Streck	ctDNA BCT	10	6–37	14
Roche	Cell-Free DNA Collection Tube	8.5	18–25	7
Qiagen	PAXgene Blood ccfDNA Tube	10	18–25	7

ctDNA, circulating tumor DNA.

## SAMPLE COLLECTION

Sample collection and processing is a critical step in liquid biopsy. Since ctDNA is rapidly degraded by the nuclease in blood and contaminated by genomic DNA from blood cells, it is essential to separate plasma from the sample.<sup>13,14</sup> The routine venipuncture technique will be sufficient to collect blood from the patients. The sample collection tube should be chosen considering each institution's setting. Conventional ethyldiaminetetraacetic acid (EDTA) tube can be used if the samples are processed without delay.<sup>19,20</sup> Recently, specialized tubes for delaying degradation of ctDNA are commercially available.<sup>19,20</sup> The tube from Streck (Omaha, NE, USA) has been the most widely used collection tube. Roche diagnostics and Qiagen have also marketed specialized tubes. According to a study,<sup>19</sup> conventional EDTA tube and Streck tube do not show much difference in their performance when samples are processed within 6 hours. When incubated longer in EDTA tube, cell-free DNA may be released from the blood cells, and EDTA will hinder the polymerase chain reaction (PCR).<sup>20</sup> Tubes from Roche and Qiagen showed similar performance, and they are slightly better than Streck tube.<sup>20</sup> Specialized tubes can sustain sample quality for several days at room temperature before processing further (Table 1).

## CIRCULATING TUMOR DNA ISOLATION

Before ctDNA extraction, blood should be processed into plasma through double centrifugation. Plasma samples are better than serum samples, which can be contaminated by DNA released from immune cells.<sup>15</sup> Since a small amount of ctDNA is present in plasma, isolation is a critical step in the process for saving tumor DNA. Several commercial kits for isolation are available in the market (Table 2).<sup>21,22</sup> These are manual, semiautomatic, and fully

**Table 2.** Commercially available ctDNA extraction kits

Company	Trade name	Method	Automation
ThermoFisher	MagMAX	Magnetic beads	Semiauto
Promega	Maxwell RSC	Magnetic beads	Semiauto
Roche	Cobas	Silica membrane	Manual
Qiagen	QIAamp	Silica membrane	Semiauto

ctDNA, circulating tumor DNA.

automatic. Manual protocol uses column-based method while semi-automatic instrument works with magnetic beads. Previous studies showed variable results depending on the extraction kits, though they all had similar performances.<sup>21,22</sup> The technician's skill and protocol optimization may be one of the critical factors for yielding better ctDNA. Table 1 summarizes commercial ctDNA extraction kits.

## MUTATION DETECTION METHODS

High sensitivity detection methods are required to detect *EGFR* mutations from liquid samples. Kits for detecting mutations have been developed and are commercially available.<sup>23-25</sup> Each kit requires different quality and amount of DNA (Table 3). They depend on real time PCR technology with their own variations. Roche Cobas uses real time PCR with Taqman like probe and Qiagen has released ARMS based kits, Therascreen *EGFR* RGQ. Another PCR based technique uses peptide nucleic acid clamping and Panamutyper (Panagene, Daejeon, Korea). The Roche and Qiagen systems use their own PCR machine from Roche and Qiagen while Panamutyper can run on any qualified PCR machines. The number of mutations these kits can detect are different; however, together they include exon 19 deletion, T790M and L858R. Currently, only Roche kit has acquired FDA approval. The most important element of these kits is how sensitively and specifically they can detect mutations in liquid samples. There are certain studies to evaluate their performance and report sensitivities ranging from 62% to 67.5% and specificities ranging from 88% to 97%.<sup>26-29</sup> In the ASSESS study, these three kits showed high specificity, however, sensitivity was equal to or less than 75%.<sup>25</sup> For T790M, sensitivity was 41% and 29% for Cobas and Therascreen, respectively, and specificity was 100% for both kits from the patients enrolled in AURA trial.<sup>10</sup> Therefore, deciding the best kit will depend on the laboratory's choice with consideration of their requirements. Features of these products are summarized in Table 3. Other platforms using digital PCR and next generation sequencing are still far from widespread use in clinical setting.<sup>24</sup>

**Table 3.** *EGFR* mutation detection kits in plasma

Company	Trade Name	Method	Detectable mutations
Roche	Cobas	Real time PCR	EX19Del, S768I, T790M, L858R, L861Q, G719X, EX20Ins
Qiagen	Therascreen RGQ	ARMS	Ex19Del, T790M, L858R
Panagene	Mutyper	PNA clamp	EX19Del, S768I, T790M, L858R, L861Q, G719X, EX20Ins
Bio-Rad	rimePCR ddPCR Mutation Assay	Digital PCR	Ex19Del, T790M, L858R, L861Q
Symex-Inostics	OncoBEAM	Digital PCR	Ex19Del, T790M, L858R, C797S

EGFR, epidermal growth factor receptor; PCR, polymerase chain reaction; PNA, peptide nucleic acid.

## REPORTING FORMAT

Once liquid biopsy for detecting T790M mutation is done, the reports should contain the following information: pathologic number, age, sex, hospital unit number, sample source, requesting physician, requesting department, adequacy for testing (amount of DNA extracted), receipt day, report day, storage tube, methodology used, exons tested and associated range of detectable mutations, mutation status, comments, testing technician, and corresponding pathologist. Since the patients already have sensitizing *EGFR* mutation, it is recommended to include the type of original *EGFR* alteration and previous histologic diagnosis.

## PROPOSAL FOR AN EXTERNAL QUALITY ASSESSMENT PROGRAM

Since liquid biopsy technique has not been validated yet, vigorous quality assurance is necessary. Although there is no recommended program for external quality assessment (EQA), one pilot trial for *EGFR* testing in blood is ongoing in Germany.<sup>30</sup> Another program for *BRAF* and *KRAS* is also being conducted.<sup>31</sup> Since patient derived standard sample is difficult to store and distribute, artificial sample mimicking the real one can be used instead.<sup>30,31</sup> We are in the process of developing Korean EQA program.

## ROLE OF PATHOLOGISTS

Performance and interpretation of liquid biopsy require broad knowledge in lung cancer pathology. Pathologists have an important role in the diagnosis and management of cancer and thus can interpret liquid biopsy results in conjunction with the histologic diagnosis, previous status of *EGFR*-activating mutation, and clinical situation. The liquid biopsy in lung cancer is usually performed in patients whose previous *EGFR* mutation status has been known. The sole purpose of this technique is to detect a T790M mutation responsible for TKI resistance. Unlike tissue specimens, in which the pathologists can determine the percentage of tumor

cells, it is extremely difficult to estimate whether the blood sample contains a sufficient amount of tumor DNA. If the sample is adequate, the test generally finds the original *EGFR*-activating mutation, which may act as an internal control for the presence of ctDNA.<sup>13</sup> When it has not detected any *EGFR*-activating mutation including previously existing one or reported mutations other than the preexisting ones or T790M, pathologists should be able to interpret the result. In the former, test should be repeated because the samples might have been degraded and contain insufficient ctDNA. In the latter, the newly emerged mutation, in the presence of newly developed lesion, may indicate a metachronous primary tumor. The communication between pathologists, clinicians, and radiologists is important for further diagnosis and management of cancer. Moreover, lung adenocarcinoma undergoes frequent transformation into small cell carcinoma when it is treated with TKI, while maintaining the original *EGFR* mutation.<sup>7,8,32</sup> Recommended interpretation is suggested in Table 4.

## PERSPECTIVES AND ADDITIONAL RECOMMENDATIONS

*EGFR* mutation testing performed with blood or other liquid sample is a non-invasive method, which can be more widely adopted. Laboratories must get familiar with liquid samples and develop their own protocols to handle these specimens. They can choose appropriate sample tubes, extraction kits, detection methods, and other instruments. They should select the most suitable combination in accordance with their requirements, unless the detection kits indicate specific methods and instruments.<sup>31</sup> Although sensitivity of tissue biopsy is higher than liquid biopsy, both are far from perfection and T790M mutation can be detected only in one of the two methods. Reportedly, allele fraction of T790M mutation tends to correlate with treatment efficacy of osimertinib.<sup>33</sup> Therefore, absence of T790M in tumor tissue while it is detected in plasma might reflect low allele frequency and lead to poor response. Therefore, the two methods are complementary to each other and should be selected according to each patient's condition (Fig. 1).

## CONCLUSIONS

Liquid biopsy is a promising method, which is safe and convenient. Before more experiences and data are accumulated, liquid biopsy should be performed with great caution. There are a few steps in liquid biopsy, which can produce false negative or false positive results. Interpretation requires profound knowledge of

**Table 4.** Recommended interpretation of *EGFR* mutation test from blood

Sensitizing mutation	T790M	Interpretation
Detected	Detected	T790M positive: start treatment with third generation TKI
Detected	Not detected	T790M negative: tissue biopsy recommended
Not detected	Detected	T790M positive: confirmation is necessary
Not detected	Not detected	Non-informative: tissue biopsy strongly recommended

*EGFR*, epidermal growth factor receptor; TKI, tyrosine kinase inhibitor.

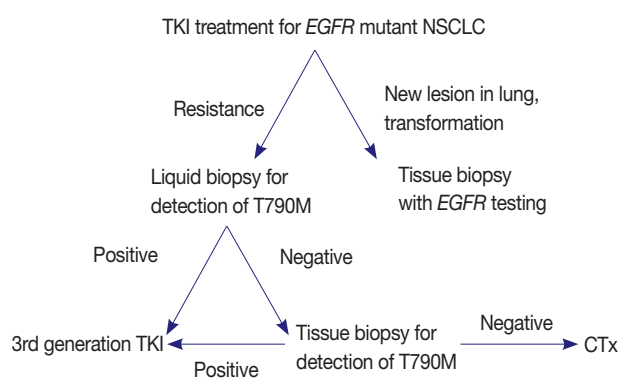


**Fig. 1.** Proposed diagnostic algorithm for the detection of epidermal growth factor receptor (*EGFR*) T790M mutation. NSCLC, non-small cell lung cancer; TKI, tyrosine kinase inhibitor; CTx, chemotherapy.

lung cancer including diagnosis, treatment, and prognosis. However, in debatable cases, discussion between pathologists, physicians, and radiologists is critical. This method will soon play a major role in early diagnosis, monitoring of treatment, and detection of minimal residual disease. Currently, it cannot replace the conventional pretreatment tissue diagnosis.<sup>14</sup> It is important to validate and improve the performance of this technique before it is widely used in clinical practice. Liquid biopsy performed in *EGFR* has provided a platform for determining gene mutations in *KRAS*, *ALK*, *PI3CA*, and *BRAF* as well.

## ORCID

Dong Hoon Shin: <https://orcid.org/0000-0002-4980-9295>

Hyo Sup Shim: <https://orcid.org/0000-0002-5718-3624>

Tae Jung Kim: <https://orcid.org/0000-0003-3140-3681>

Heae Surng Park: <https://orcid.org/0000-0003-1849-5120>

Yun La Choi: <https://orcid.org/0000-0002-5788-5140>

Wan Seop Kim: <https://orcid.org/0000-0001-7704-5942>

Lucia Kim: <https://orcid.org/0000-0002-4100-6607>

Sun Hee Chang: <https://orcid.org/0000-0002-7775-4711>  
 Joon Seon Song: <https://orcid.org/0000-0002-7429-4254>  
 Hyo Jin Kim: <https://orcid.org/0000-0001-9201-8328>  
 Jung Ho Han: <https://orcid.org/0000-0003-4424-7008>  
 Chang Hun Lee: <https://orcid.org/0000-0003-4216-2836>  
 Geon Kook Lee: <https://orcid.org/0000-0003-3138-3908>  
 Se Jin Jang: <https://orcid.org/0000-0001-8239-4362>

### Author Contributions

Conceptualization: DHS, HSS, TJK, HSP, YLC, WSK, LK, SHC, JSS, HJK, JHH, CHL, GKL, SJJ.

Data curation: DHS.

Formal analysis: DHS, HSS, TJK.

Investigation: DHS, HSP, YLC, WSK, LK.

Methodology: DHS, SHC, JSS, HJK, JHH.

Project administration: JHH, CHL, GKL, SJJ.

Writing—original draft: DHS.

Writing—review & editing: DHS, HSS, TJK, HSP, YLC, WSK, LK, SHC, JSS, HJK, JHH, CHL, GKL, SJJ.

### Conflicts of Interest

The authors declare that they have no potential conflicts of interest.

## REFERENCES

- Lynch TJ, Bell DW, Sordella R, et al. Activating mutations in the epidermal growth factor receptor underlying responsiveness of non-small-cell lung cancer to gefitinib. *N Engl J Med* 2004; 350: 2129-39.
- Paez JG, Janne PA, Lee JC, et al. EGFR mutations in lung cancer: correlation with clinical response to gefitinib therapy. *Science* 2004; 304: 1497-500.
- Mok TS, Wu YL, Thongprasert S, et al. Gefitinib or carboplatin-paclitaxel in pulmonary adenocarcinoma. *N Engl J Med* 2009; 361: 947-57.
- Balak MN, Gong Y, Riely GJ, et al. Novel D761Y and common secondary T790M mutations in epidermal growth factor receptor-mutant lung adenocarcinomas with acquired resistance to kinase inhibitors. *Clin Cancer Res* 2006; 12: 6494-501.
- Thress KS, Paweletz CP, Felip E, et al. Acquired EGFR C797S mutation mediates resistance to AZD9291 in non-small cell lung cancer harboring EGFR T790M. *Nat Med* 2015; 21: 560-2.
- Sequist LV, Waltman BA, Dias-Santagata D, et al. Genotypic and histological evolution of lung cancers acquiring resistance to EGFR inhibitors. *Sci Transl Med* 2011; 3: 75ra26.
- Sequist LV, Waltman BA, Dias-Santagata D, et al. Genotypic and histological evolution of lung cancers acquiring resistance to EGFR inhibitors. *Sci Transl Med* 2011; 3: 75ra26.
- Yu HA, Arcila ME, Rekhtman N, et al. Analysis of tumor specimens at the time of acquired resistance to EGFR-TKI therapy in 155 patients with EGFR-mutant lung cancers. *Clin Cancer Res* 2013; 19: 2240-7.
- Goss G, Tsai CM, Shepherd FA, et al. Osimertinib for pretreated EGFR Thr790Met-positive advanced non-small-cell lung cancer (AURA2): a multicentre, open-label, single-arm, phase 2 study. *Lancet Oncol* 2016; 17: 1643-52.
- Yang JC, Ahn MJ, Kim DW, et al. Osimertinib in pretreated T790M-positive advanced non-small-cell lung cancer: AURA study phase II extension component. *J Clin Oncol* 2017; 35: 1288-96.
- Ballard P, Yates JW, Yang Z, et al. Preclinical comparison of osimertinib with other EGFR-TKIs in EGFR-mutant NSCLC brain metastases models, and early evidence of clinical brain metastases activity. *Clin Cancer Res* 2016; 22: 5130-40.
- Diehl F, Schmidt K, Choti MA, et al. Circulating mutant DNA to assess tumor dynamics. *Nat Med* 2008; 14: 985-90.
- Wan JCM, Massie C, Garcia-Corbacho J, et al. Liquid biopsies come of age: towards implementation of circulating tumour DNA. *Nat Rev Cancer* 2017; 17: 223-38.
- Sholl LM, Aisner DL, Allen TC, et al. Liquid biopsy in lung cancer: a perspective from members of the Pulmonary Pathology Society. *Arch Pathol Lab Med* 2016; 140: 825-9.
- Cobas EGFR Mutation Test v2, PMA 150047. FDA summary of safety and effectiveness data [Internet]. Silver Spring: US Food and Drug Administration, 2016 [cited 2018 Jan 2]. Available from: [https://www.accessdata.fda.gov/cdrh\\_docs/pdf15/P150047B.pdf](https://www.accessdata.fda.gov/cdrh_docs/pdf15/P150047B.pdf).
- Mino-Kenudson M. Cons: Can liquid biopsy replace tissue biopsy?: the US experience. *Transl Lung Cancer Res* 2016; 5: 424-7.
- Ilie M, Hofman P. Pros: can tissue biopsy be replaced by liquid biopsy? *Transl Lung Cancer Res* 2016; 5: 420-3.
- Mock TS, Carbone DP, Hirsch FR. IASLC atlas of EGFR testing in lung cancer. Aurora: International Association for the Study of Lung Cancer, 2017.
- Alidousty C, Brandes D, Heydt C, et al. Comparison of blood collection tubes from three different manufacturers for the collection of cell-free DNA for liquid biopsy mutation testing. *J Mol Diagn* 2017; 19: 801-4.
- Kang Q, Henry NL, Paoletti C, et al. Comparative analysis of circulating tumor DNA stability in K3EDTA, Streck, and CellSave blood collection tubes. *Clin Biochem* 2016; 49: 1354-60.
- Fleischhacker M, Schmidt B, Weickmann S, et al. Methods for isolation of cell-free plasma DNA strongly affect DNA yield. *Clin Chim Acta* 2011; 412: 2085-8.

22. Sorber L, Zwaenepoel K, Deschoolmeester V, et al. A comparison of cell-free DNA isolation kits: isolation and quantification of cell-free DNA in plasma. *J Mol Diagn* 2017; 19: 162-8.
23. Vendrell JA, Mau-Them FT, Beganton B, Godreuil S, Coopman P, So-llassol J. Circulating cell free tumor DNA detection as a routine tool for lung cancer patient management. *Int J Mol Sci* 2017; 18: E264.
24. Thress KS, Brant R, Carr TH, et al. *EGFR* mutation detection in ctDNA from NSCLC patient plasma: a cross-platform comparison of leading technologies to support the clinical development of AZD9291. *Lung Cancer* 2015; 90: 509-15.
25. Reck M, Hagiwara K, Han B, et al. ctDNA determination of *EGFR* mutation status in European and Japanese patients with advanced NSCLC: the ASSESS study. *J Thorac Oncol* 2016; 11: 1682-9.
26. Bernabe R, Hickson N, Wallace A, Blackhall FH. What do we need to make circulating tumour DNA (ctDNA) a routine diagnostic test in lung cancer? *Eur J Cancer* 2017; 81: 66-73.
27. Qiu M, Wang J, Xu Y, et al. Circulating tumor DNA is effective for the detection of *EGFR* mutation in non-small cell lung cancer: a meta-analysis. *Cancer Epidemiol Biomarkers Prev* 2015; 24: 206-12.
28. Luo J, Shen L, Zheng D. Diagnostic value of circulating free DNA for the detection of *EGFR* mutation status in NSCLC: a systematic review and meta-analysis. *Sci Rep* 2014; 4: 6269.
29. Wu Y, Liu H, Shi X, Song Y. Can *EGFR* mutations in plasma or serum be predictive markers of non-small-cell lung cancer? A meta-analysis. *Lung Cancer* 2015; 88: 246-53.
30. Fassunke J, Ihle MA, Lenze D, et al. *EGFR* T790M mutation testing of non-small cell lung cancer tissue and blood samples artificially spiked with circulating cell-free tumor DNA: results of a round robin trial. *Virchows Arch* 2017; 471: 509-20.
31. Haselmann V, Ahmad-Nejad P, Geilenkeuser WJ, et al. Results of the first external quality assessment scheme (EQA) for isolation and analysis of circulating tumour DNA (ctDNA). *Clin Chem Lab Med* 2018; 56: 220-8.
32. Oser MG, Niederst MJ, Sequist LV, Engelman JA. Transformation from non-small-cell lung cancer to small-cell lung cancer: molecular drivers and cells of origin. *Lancet Oncol* 2015; 16: e165-72.
33. Oxnard GR, Thress KS, Alden RS, et al. Association between plasma genotyping and outcomes of treatment with osimertinib (AZD9291) in advanced non-small-cell lung cancer. *J Clin Oncol* 2016; 34: 3375-82.

# Primary Age-Related Tauopathy: An Elderly Brain Pathology Frequently Encountered during Autopsy

Daru Kim · Hyung-Seok Kim<sup>1</sup>  
Seong-Min Choi<sup>2</sup> · Byeong C. Kim<sup>2</sup>  
Min-Cheol Lee · Kyung-Hwa Lee  
Jae-Hyuk Lee

Departments of Pathology, <sup>1</sup>Forensic Medicine, and <sup>2</sup>Neurology, Chonnam National University Medical School, Hwasun, Korea

**Received:** February 14, 2019  
**Revised:** March 12, 2019  
**Accepted:** March 14, 2019

## Corresponding Author

Kyung-Hwa Lee, MD, PhD  
Department of Pathology, Chonnam National University Medical School, 264 Seoyang-ro, Hwasun 58128, Korea  
Tel: +82-61-379-7050  
Fax: +82-61-379-7099  
E-mail: mdkaylee@jnu.ac.kr

Jae-Hyuk Lee, MD, PhD  
Department of Pathology, Chonnam National University Medical School, 264 Seoyang-ro, Hwasun 58128, Korea  
Tel: +82-61-379-7073  
Fax: +82-61-379-7099  
E-mail: jhlee@chonnam.ac.kr

Due to the progressive aging of Korean society and the introduction of brain banks to the Korean medical system, the possibility that pathologists will have access to healthy elderly brains has increased. The histopathological analysis of an elderly brain from a subject with relatively well-preserved cognition is quite different from that of a brain from a demented subject. Additionally, the histology of elderly brains differs from that of young brains. This brief review discusses primary age-related tauopathy; this term was coined to describe elderly brains with Alzheimer's disease-type neurofibrillary tangles mainly confined to medial temporal structures, and no  $\beta$ -amyloid pathology.

**Key Words:** Autopsy; Cognition; Dementia; Tauopathies; Amyloid beta-peptides

Even before the term “primary age-related tauopathy (PART)” was proposed in 2014, pathologists had observed localized neurofibrillary degeneration in brains from aged people with relatively well-preserved cognitive function that was mostly restricted to medial temporal regions. These findings were somewhat informally described as “aging changes” because the features were considered insufficient for a diagnosis of Alzheimer disease (AD). The newly proposed consensus term (i.e., PART) includes features that range from the presence of isolated neurofibrillary tangles (NFTs) in cognitively normal aged brains to a subtype of frontotemporal lobe degeneration (FTLD) known as FTLD-tau, which is also referred to as tangle-only dementia, tangle-predominant senile dementia (TPSD), and preferential development of NFT without senile plaques.<sup>1,2</sup> However, these previous designations tended to accentuate unnecessarily the clinical aspects of

cognitive impairment, leading to a biased understanding of the disease entity.<sup>1</sup> Although the word dementia is included in these terms, profound cognitive impairment that interferes with daily activities occurs in only a minority of affected individuals within this population.<sup>1</sup>

Thus, the consensus term PART was suggested by researchers of neurodegenerative diseases as a more objective and quantitative description of pathological disease status separate from the clinical presentation. The term PART was inspired by the pathological classification system for AD of the National Institute on Aging-Alzheimer's Association.<sup>1,3</sup> Since being introduced, the clinicopathological traits of PART have been clarified more precisely.<sup>4-8</sup> This review aims to increase recognition of this disease entity by Korean pathologists through a literature review and discussion of the clinicopathological implications of PART, and via a figu-

rative presentation of a PART case recently diagnosed at Chonnam National University Hospital brain bank.

### DEFINITION AND HISTOLOGICAL SPECTRUM OF PRIMARY AGE-RELATED TAUOPATHY

The diagnosis of PART is histological in nature and can be applied to patients exhibiting mild-to-moderate tau-positive NFTs but without, or with few,  $\beta$ -amyloid ( $A\beta$ ) plaques.<sup>1,9</sup> The gross features of a brain with PART may include minimal atrophy that is primarily located in the medial temporal lobe; however, diffuse neocortical atrophy is also present in some cases. AD-type NFTs, including ghost tangles, are mainly distributed in the hippocampus and medial temporal lobe (Fig. 1A, in comparison with advanced AD, Fig. 1B), and correspond to Braak stages I–III in the majority of patients and to stage IV in rare cases.<sup>9</sup> The neuronal tauopathy of PART may also extend to granule cells of the dentate gyrus and neurons in the CA4 subregion of the hippocampus (Fig. 1C).<sup>9</sup> Other than PART, the presence of ghost tangles or tau involvement in the dentate gyrus and CA4 are typically considered to be features of advanced AD (Fig. 1D).<sup>9</sup> In addition to the hippocampus and medial temporal lobe, NFTs may also be observed in subcortical structures, such as the amygdala, nucleus basalis of Meynert, nucleus accumbens, hypothalamus, thalamus, and olfactory system (bulb and cortex), and in the brainstem, including the substantia nigra, locus coeruleus, dorsal raphe nucleus, and medulla oblongata, where NFTs develop at a younger age, sometimes even in teenagers.<sup>1,10,11</sup> Biochemical and immunohistochemical studies have revealed that the NFTs in PART contain mixed three-repeat (3R) and four-repeat (4R) isoforms of tau proteins, as seen in AD.<sup>1,9</sup>

The presence of NFTs in Braak stage IV or lower is a basic requirement for a histological diagnosis of PART; when combined with Thal  $A\beta$  phase 0, PART can be diagnosed definitively (Fig. 1E–G). If the required distribution of NFTs is observed together with Thal  $A\beta$  phase 1 or 2, then the pathology is categorized as possible PART.<sup>1</sup> The following is an example pathological diagnosis of PART: “Primary age-related tauopathy (PART), Definite, Braak stage III.”<sup>1</sup> Although Braak stage IV is considered a requirement for PART diagnosis, Braak stage IV pathology in the absence of  $A\beta$  plaques is rare and the possibility that cases such as these represent FTLD-tau needs to be considered.<sup>1</sup>

### GENETIC AND CLINICAL ASPECTS OF PART

PART brains are deficient in the apolipoprotein E (*APOE*)  $\epsilon 4$  allele, which is highly associated with the risk of AD.<sup>2</sup> The frequency of *APOE*  $\epsilon 4$  in PART is approximately 10%,<sup>1,6</sup> whereas its prevalence in AD exceeds 45%.<sup>12,13</sup> A major genetic risk factor for PART is the microtubule-associated protein tau (*MAPT*) gene H1 haplotype, which is also an accepted risk factor of progressive supranuclear palsy (PSP), corticobasal degeneration (CBD), and argyrophilic grain disease (AGD).<sup>2,14</sup>

By definition, patients with the PART pathology present with a lack of, or minimal, cognitive impairment.<sup>2</sup> However, greater impairment has been noted as an aspect of TSPD, where the initial symptoms typically include memory disturbances.<sup>15</sup> During disease progression, deficits in cognitive function may extend to mild cognitive impairment (MCI) with a relatively well-preserved personality.<sup>15</sup> Mental derangements, such as disorientation (or rarely, delirium), depression and paranoid thinking have also been observed.<sup>15,16</sup> One feature of PART is that cases with higher NFT stages (Braak stage III or IV) are more likely to be associated with subjective memory impairments, which is a common complaint among the elderly population.<sup>17,18</sup>

### DEBATE REGARDING WHETHER PART IS ON THE ALZHEIMER DISEASE CONTINUUM

Considering PART as being on the AD continuum, and especially comparing it with the limbic-predominant form of AD, has been discouraged for several reasons.<sup>6,9,16,19</sup> First, PART is associated with lower Braak NFT stages and fewer, or an absence of,  $A\beta$  plaques. Second, patients with PART have an older age of onset, shorter disease duration, and less severe cognitive impairment. Third, the frequency of *APOE*  $\epsilon 4$  is much lower in PART than in the normal elderly population and the frequency of TDP-43 proteinopathy is higher in patients with limbic-predominant AD (67%) than in those with definite PART (29%) (Table 1).<sup>20</sup>

A discussion on the role that  $A\beta$  plays in tauopathy is inevitable when PART is compared with AD. In the absence of  $A\beta$ , as seen in definite PART, the severity of tau-positive NFTs tends to be greater with older age at death.<sup>6</sup> A proposed pathological step in late-onset AD is tauopathy, corresponding to PART, which is purported to occur at some point in the life cycle of almost every individual; amyloidosis may also occur as an independent event.<sup>21</sup> In this model,  $A\beta$  is not a catalyst for tau deposition in the brain, but rather serves to promote the spread of tauopathy. This hypothesis is supported by a study that used an established cell biosensor

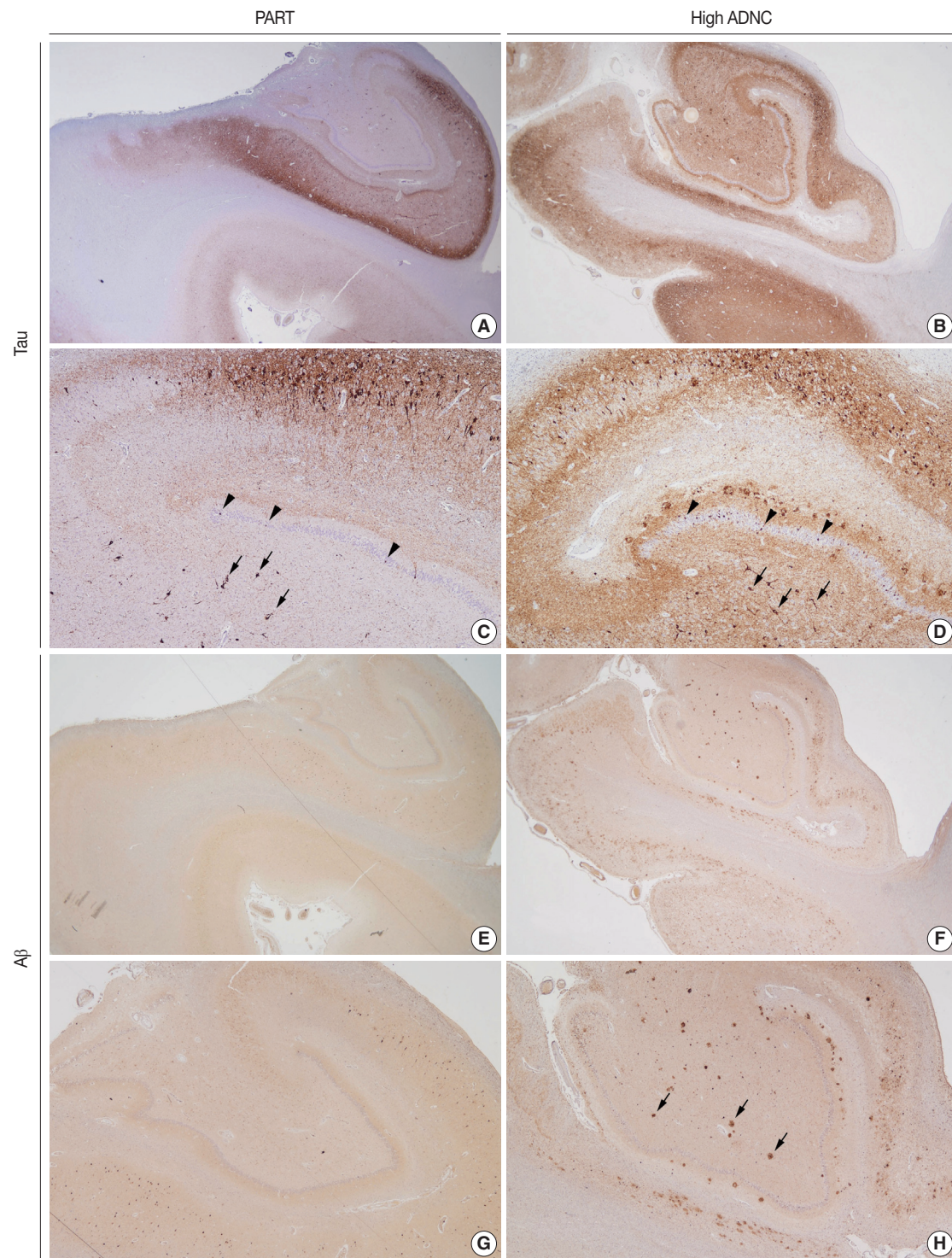


**Fig. 1.** Histopathological findings of primary age-related tauopathy (PART) in a 92-year-old woman (A, C, E, G) compared with those of high-Alzheimer's disease (AD) neuropathologic change (ADNC) in an 82-year-old man (B, D, F, H). Tau immunohistochemistry analyses revealed marked tauopathy centered in the hippocampus and subiculum of the PART brain (A) and the extension of tauopathy into the temporal neocortex of the high-ADNC brain (B) (AT8 immunohistochemistry). At a higher magnification, the granule cells of the dentate gyrus (arrowheads) and the neurons of the CA4 subregion (arrows) exhibited tau involvement in the PART brain (C), as well as in the brain of the advanced AD case (D) (AT8 immunohistochemistry). Although the hippocampus in the PART brain did not reveal any  $\beta$ -amyloid ( $A\beta$ )-positive plaques (E, G) ( $A\beta$  immunohistochemistry), the high ADNC brain showed  $A\beta$  deposition in the temporal neocortex through the CA4 subregion (arrows) that corresponded to Thal  $A\beta$  phase 4 (F, H) ( $A\beta$  immunohistochemistry).

**Table 1.** Comparison of PART with AD

Variable	PART	AD
Primary pathology		
Tau-positive NFTs	Medial temporal region-restricted Braak stage ≤ IV (usually I–III)	Diffuse cortical distribution Braak stage ≥ III (usually IV–VI)
Aβ plaques	Thal phase 0–2 Definite PART: Thal phase 0 Possible PART: Thal phase 1–2	Thal phase ≥ 3
Tau isoforms	Mixed 3R and 4R tau	Mixed 3R and 4R tau
Genetic association	MAPT H1 haplotype	APOE ε4
Clinical features		
Cognition	Normal-to-mild impairment	Dementia
Duration (yr)	5	9 <sup>16</sup>
Age at death (yr)	86	79 <sup>14,19</sup>
Prevalence at ≥ 80 yr (%)	20	80 <sup>8,11</sup>
Other co-existing pathology		
TDP-43 proteinopathy (%)	30	67 <sup>14,19,20</sup>
Hippocampal sclerosis (%)	10	3 <sup>16,20</sup>
α-Synuclein positive Lewy bodies (%)	10	30 <sup>14,20</sup>

PART, primary age-related tauopathy; AD, Alzheimer's disease; NFTs, neurofibrillary tangles; Aβ, β-amyloid; 3R, three-repeat; 4R, four-repeat.

assay to show that the seeding activity of tauopathy is enhanced in the presence of Aβ-positive plaques.<sup>4</sup> However, another report found no clear distinction in tau seeding activity between PART and AD subjects.<sup>7</sup> The functional interaction between tau and Aβ, as well as the relationship between PART and AD, remain to be elucidated.<sup>2,22</sup>

### COEXISTING PATHOLOGIES IN ELDERLY INDIVIDUALS WITH PRIMARY AGE-RELATED TAUOPATHY

Previous studies focused on brain pathology in the elderly have identified several pathological trends.<sup>8,11,18</sup> Roughly 20% of aged people in their 80s or older have PART,<sup>8,11,18,23</sup> while the remaining 80% exhibit some degree of AD-type pathology characterized by both NFTs and neuritic plaques.<sup>11</sup> Moreover, there are few cases that are Aβ-positive only; most cases of Aβ deposition show some tau-positive NFTs.<sup>8,11</sup> These observations are consistent with prior reports showing that approximately 25% of elderly people with well-preserved cognitive function lack brain amyloidosis.<sup>1</sup> Even among a carefully selected group of centenarians, 20% were relatively free of Aβ deposition as detected by immunohistochemistry.<sup>11</sup> Thus, the relative proportions of PART and

AD appear to be maintained in centenarian populations.<sup>8,11</sup>

It has been proposed that a neuropathological diagnosis of TPSD or PART should be conservatively applied to cases where NFTs mainly affect the hippocampal/limbic area, and where there is a scarcity of Aβ deposits and no evidence of any other dementia characterized by NFTs.<sup>15</sup> The limits of the PART diagnosis explain the exclusion of PSP, CBD, and even Lewy body disease cases in previous studies on PART.<sup>6</sup> Despite the proposed limitations to its diagnostic criteria, PART has been shown to co-exist with other pathologies. For example, TDP-43 proteinopathy, including cerebral age-related TDP-43 with sclerosis, and AGD have been identified in approximately 30% of cases with definite PART.<sup>6</sup> Similarly, hippocampal sclerosis has been identified in approximately 10% of cases,<sup>16</sup> while α-synuclein-positive Lewy bodies have been observed in fewer than 10% of PART cases.<sup>6</sup>

### CONCLUSIONS

PART can be diagnosed in cases showing neurofibrillary degeneration restricted to the medial temporal region, an absence (or scarcity) of Aβ deposition, and a lack of cognitive impairment or MCI. However, several unanswered issues remain regarding the “gray zone” between PART and AD. The definition of clinicopathological PART requires refinement due to the presence of clinical PART in cases with higher Thal Aβ phases and moderate-to-frequent neuritic plaques.<sup>18</sup> The implications of the association of PART with diffuse amyloid and neuritic plaques also remain to be clarified, although a quantitative margin of Aβ deposition, up to Thal phase 2, has been proposed.<sup>1</sup> Neither an exact diagnostic threshold for Aβ deposition nor the methodology with which to detect its presence has been clearly defined. Furthermore, the term “age-related” is somewhat ambiguous. For example, the accumulation of abnormally phosphorylated tau proteins can begin before puberty and Braak stage I or II may be seen in individuals in their 20s.<sup>11</sup> Determining a common pathology in aged brains, with recognition of PART, will provide a firm foundation for a more profound understanding of age-related neurodegenerative changes. Additionally, accumulated neuropathology data reflecting the epidemiology of the Korean population will be a good resource for future neuroscientific research.

### ORCID

Daru Kim: <https://orcid.org/0000-0001-5382-1206>

Hyung-Seok Kim: <https://orcid.org/0000-0002-8297-9747>

Seong-Min Choi: <https://orcid.org/0000-0003-3138-1881>

Byeong C. Kim: <https://orcid.org/0000-0001-6827-6730>  
 Min-Cheol Lee: <https://orcid.org/0000-0002-0799-2976>  
 Kyung-Hwa Lee: <https://orcid.org/0000-0002-3935-0361>  
 Jae-Hyuk Le: <https://orcid.org/0000-0002-8934-0145>

### Author Contributions

Conceptualization: MCL.  
 Funding acquisition: KHL.  
 Investigation: SMC.  
 Methodology: HSK, DK.  
 Project administration: JHL.  
 Supervision: JHL.  
 Validation: MCL, KHL.  
 Visualization: DK, KHL.  
 Writing—original draft: DK.  
 Writing—review & editing: HSK, SMC, BCK, KHL.

### Conflicts of Interest

The authors declare that they have no potential conflicts of interest.

### Acknowledgments

This work was supported by a National Research Foundation of Korea (NRF) grant funded by the government of Korea (MSIT; No. 2016R1A2B1014597, 2018R1A5A2024181).

## REFERENCES

- Crary JF, Trojanowski JQ, Schneider JA, et al. Primary age-related tauopathy (PART): a common pathology associated with human aging. *Acta Neuropathol* 2014; 128: 755-66.
- Irwin DJ. Tauopathies as clinicopathological entities. *Parkinsonism Relat Disord* 2016; 22 Suppl 1: S29-33.
- Hyman BT, Phelps CH, Beach TG, et al. National Institute on Aging-Alzheimer's Association guidelines for the neuropathologic assessment of Alzheimer's disease. *Alzheimers Dement* 2012; 8: 1-13.
- Bennett RE, DeVos SL, Dujardin S, et al. Enhanced tau aggregation in the presence of amyloid beta. *Am J Pathol* 2017; 187: 1601-12.
- Crary JF. Primary age-related tauopathy and the amyloid cascade hypothesis: the exception that proves the rule? *J Neurol Neuromedicine* 2016; 1: 53-7.
- Josephs KA, Murray ME, Tosakulwong N, et al. Tau aggregation influences cognition and hippocampal atrophy in the absence of beta-amyloid: a clinico-imaging-pathological study of primary age-related tauopathy (PART). *Acta Neuropathol* 2017; 133: 705-15.
- Kaufman SK, Del Tredici K, Thomas TL, Braak H, Diamond MI. Tau seeding activity begins in the transentorhinal/entorhinal regions and anticipates phospho-tau pathology in Alzheimer's disease and PART. *Acta Neuropathol* 2018; 136: 57-67.
- Neltner JH, Abner EL, Jicha GA, et al. Brain pathologies in extreme old age. *Neurobiol Aging* 2016; 37: 1-11.
- Kovacs GG. Invited review: neuropathology of tauopathies: principles and practice. *Neuropathol Appl Neurobiol* 2015; 41: 3-23.
- Braak H, Del Tredici K. The pathological process underlying Alzheimer's disease in individuals under thirty. *Acta Neuropathol* 2011; 121: 171-81.
- Braak H, Thal DR, Ghebremedhin E, Del Tredici K. Stages of the pathologic process in Alzheimer disease: age categories from 1 to 100 years. *J Neuropathol Exp Neurol* 2011; 70: 960-9.
- Jicha GA, Parisi JE, Dickson DW, et al. Age and apoE associations with complex pathologic features in Alzheimer's disease. *J Neurol Sci* 2008; 273: 34-9.
- Alzheimer's Association. 2016 Alzheimer's disease facts and figures. *Alzheimers Dement* 2016; 12: 459-509.
- Janocko NJ, Brodersen KA, Soto-Ortolaza AI, et al. Neuropathologically defined subtypes of Alzheimer's disease differ significantly from neurofibrillary tangle-predominant dementia. *Acta Neuropathol* 2012; 124: 681-92.
- Yamada M. Senile dementia of the neurofibrillary tangle type (tangle-only dementia): neuropathological criteria and clinical guidelines for diagnosis. *Neuropathology* 2003; 23: 311-7.
- Jellinger KA, Attems J. Neurofibrillary tangle-predominant dementia: comparison with classical Alzheimer disease. *Acta Neuropathol* 2007; 113: 107-17.
- Kryscio RJ, Abner EL, Jicha GA, et al. Self-reported memory complaints: a comparison of demented and unimpaired outcomes. *J Prev Alzheimers Dis* 2016; 3: 13-9.
- Nelson PT, Trojanowski JQ, Abner EL, et al. "New old pathologies": AD, PART, and cerebral age-related TDP-43 with sclerosis (CARTS). *J Neuropathol Exp Neurol* 2016; 75: 482-98.
- Murray ME, Graff-Radford NR, Ross OA, Petersen RC, Duara R, Dickson DW. Neuropathologically defined subtypes of Alzheimer's disease with distinct clinical characteristics: a retrospective study. *Lancet Neurol* 2011; 10: 785-96.
- Josephs KA, Whitwell JL, Tosakulwong N, et al. TAR DNA-binding protein 43 and pathological subtype of Alzheimer's disease impact clinical features. *Ann Neurol* 2015; 78: 697-709.
- Jack CR Jr. PART and SNAP. *Acta Neuropathol* 2014; 128: 773-6.
- Duyckaerts C, Braak H, Brion JP, et al. PART is part of Alzheimer disease. *Acta Neuropathol* 2015; 129: 749-56.
- Robinson JL, Corrada MM, Kovacs GG, et al. Non-Alzheimer's contributions to dementia and cognitive resilience in The 90+ Study. *Acta Neuropathol* 2018; 136: 377-88.

## Potential Role for a Panel of Immunohistochemical Markers in the Management of Endometrial Carcinoma

Amany Salama<sup>1</sup>  
Mohammad Arafa<sup>1,2</sup> · Eman ElZahaf<sup>3</sup>  
Abdelhadi Mohamed Shebl<sup>1</sup>  
Azmy Abd El-Hameed Awad<sup>1</sup>  
Sylvia A. Ashamallah<sup>1</sup>  
Reda Hemida<sup>4</sup> · Anas Gamal<sup>4</sup>  
Abd AlRahman Foda<sup>1</sup>  
Khaled Zalata<sup>1</sup>  
El-Said M. Abdel-Hady<sup>4</sup>

<sup>1</sup>Department of Pathology, Faculty of Medicine, Mansoura University, Mansoura, Egypt;

<sup>2</sup>Department of Pathology, College of Medicine and Health Sciences, Sultan Qaboos University, Muscat, Oman; <sup>3</sup>Clinical Oncology and Nuclear Medicine and <sup>4</sup>Obstetrics and Gynecology, Faculty of Medicine, Mansoura University, Mansoura, Egypt

Received: August 31, 2018  
Revised: February 11, 2019  
Accepted: February 12, 2019

### Corresponding Author

Mohammad Arafa, MD, PhD  
Department of Pathology, Faculty of Medicine,  
Mansoura University, 35516 Mansoura, Egypt  
Tel: +2-050-226-59-22  
Fax: +2-050-226-37-17  
E-mail: marafa8@yahoo.com

This study was partially presented as an abstract in the XXXI Congress of the International Academy of Pathology and the 28th Congress of the European Society of Pathology, Cologne, Germany, 2016.

**Background:** In order to improve the efficacy of endometrial carcinoma (EC) treatment, identifying prognostic factors for high risk patients is a high research priority. This study aimed to assess the relationships among the expression of estrogen receptors (ER), progesterone receptors (PR), human epidermal growth factor receptor 2 (HER2), Ki-67, and the different histopathological prognostic parameters in EC and to assess the value of these in the management of EC. **Methods:** We examined 109 cases of EC. Immunohistochemistry for ER, PR, HER2, and Ki-67 were evaluated in relation to age, tumor size, International Federation of Gynecology and Obstetrics (FIGO) stage and grade, depth of infiltration, cervical and ovarian involvement, lymphovascular space invasion (LVSI), and lymph node (LN) metastasis. **Results:** The mean age of patients in this study was 59.8±8.2 years. Low ER and PR expression scores and high Ki-67 expression showed highly significant associations with non-endometrioid histology ( $p=.007$ ,  $p<.001$ , and  $p<.001$ , respectively) and poor differentiation ( $p=.007$ ,  $p<.001$ , and  $p<.001$ , respectively). Low PR score showed a significant association with advanced stage ( $p=.009$ ). Low ER score was highly associated with LVSI ( $p=.006$ ), and low PR scores were associated significantly with LN metastasis ( $p=.026$ ). HER2 expression was significantly related to advanced stages ( $p=.04$ ), increased depth of infiltration ( $p=.02$ ), LVSI ( $p=.017$ ), ovarian involvement ( $p=.038$ ), and LN metastasis ( $p=.038$ ). There was a close relationship between HER2 expression and uterine cervical involvement ( $p=.009$ ). Higher Ki-67 values were associated with LN involvement ( $p=.012$ ). **Conclusions:** The over-expression of HER2 and Ki-67 and low expression of ER and PR indicate a more malignant EC behavior. An immunohistochemical panel for the identification of high risk tumors can contribute significantly to prognostic assessments.

**Key Words:** Endometrial neoplasms; Prognosis; Steroid receptors; HER2; Ki-67

Endometrial carcinoma (EC) is the most common gynaecologic malignancy among women worldwide with 287,000 new cases and 74,000 mortalities per year.<sup>1</sup> EC is the fourth most common type of cancer in females.<sup>2,3</sup> Traditionally, ECs have been classified into two types. The more common is type I, mostly endometrioid carcinomas, which are estrogen-dependent cancers with a relatively good prognosis. On the other hand, type II tumours are not estrogen-driven and affect older age groups. These tumours have a poor prognosis and demonstrate more common extrauterine spread.

The prototype for this group is serous carcinoma.<sup>1,4,5</sup> In order to improve the efficacy of EC treatment, identification of high-risk prognostic factors is a high research priority. Early assessment could enable conservative therapy in patients with favorable prognosis as well as reserve effective and more radical therapy for patients with aggressive forms of the tumor.<sup>6</sup> The use of estrogen receptor (ER), progesterone receptor (PR), human epidermal growth factor receptor 2 (HER2), and Ki-67 have been routinely used in breast cancer cases for molecular subtyping and guiding

treatment. However, unlike breast cancer, there is no molecular classification for EC based on such markers.<sup>7</sup> Recently, integrated genomic characterization of EC revealed four genomic classes; however, receptor status is not involved in this molecular classification.<sup>8</sup>

Numerous studies showed that the EC prognosis is closely related to patient age, tumour grade, depth of invasion and/or cervical involvement, and the occurrence of lymph node metastases.<sup>9</sup> Some potential biological markers including hormone receptors, oncogenes, and tumour suppressor genes are also involved. However, no single marker was found to be indicative of EC often enough to allow routine use in the sub-classification of EC.<sup>10</sup> Therefore, in the current study, a panel of immunohistochemical markers (ER, PR, Her-2, and Ki-67) was tested to ascertain their relationships with the histopathological prognostic parameters of EC. The aim was to identify suitable markers to guide treatment and assess prognosis of EC patients.

## MATERIALS AND METHODS

### Sample selection

Archival material of randomly-selected hysterectomy specimens of 109 EC cases were retrieved from the Pathology Department. These cases were diagnosed in the period between 2005 and 2017. Corresponding files of these cases were retrieved from the Clinical Oncology and Nuclear Medicine Departments at Mansoura University. The histological types were endometrioid (89 cases), serous (12 cases), undifferentiated (one case), dedifferentiated (one case), and carcinosarcoma (three cases). The remaining three cases showed mixed patterns. The major component in two was endometrioid; the other was serous carcinoma. Hematoxylin and eosin (H&E) stained slides for every case were reviewed by two independent pathologists. International Federation of Gynecology and Obstetrics (FIGO) revised criteria in 2009 were used for grading and staging of cases.<sup>11</sup> All procedures performed in the current study were approved by the ethical committee of Mansoura University (Institutional Review Board [IRB] code number MD15.09.08, dated 18/09/2015) in accordance with the 1964 Declaration of Helsinki and its later amendments. Formal written informed consent was not required with a waiver by the IRB.

### Tissue microarray construction

The tissue microarray (TMA) was constructed as previously published.<sup>12</sup> Briefly, a representative slide for each tumor was selected and an area of the tumor was circled. Using the manual tissue arrayer (MTA-1, Estigen, Tartu, Estonia), the areas of interest

of a donor block were cored using tissue punches of 0.6 mm diameter. The cores were then transferred into the recipient block. Three cores were taken from each tumour. In carcinosarcoma cases, only the epithelial component was assessed. Sections from these microarrays were then H&E stained and tested for spot adequacy.

### Immunohistochemistry

Sections from the microarray were stained with antibodies against ER, PR, HER2 (Rabbit, monoclonal, Genemed, South San Francisco, CA, USA) and Ki-67 (mouse, monoclonal, Genemed) according to the instructions of the manufacturers. The positive control for ER and PR in this study was normal endometrial glands and stroma where these receptors show nuclear expression. The positive control for HER2 was positive breast carcinoma tissue. The positive internal control for Ki-67 was tonsillar lymphoid follicles.

### Evaluation of the staining

Slides were examined by two independent pathologists blinded to patient characteristics and outcome. For ER and PR, we applied a scoring system that depended on immunoreactivity distribution and intensity.<sup>13,14</sup> The percentage of stained cells was scored as follows: 1, 0%–25%; 2, 26%–75%, and 3, ≥76%. The intensity of staining was also reported as 1, absent or weak; 2, moderate; and 3, strong. The sum of the two values equalled the score. Tumours were then subdivided into three categories depending on this immunohistochemical score. Category I corresponded to a score of 2, category II to a score of 3–4, and category III to a score of 5–6.

U.S. Food and Drug Administration criteria were used for evaluation of HER2 scoring.<sup>15</sup> The scoring was 3+ if complete with strong membranous staining in more than 10% of tumor cells; 2+ if complete, weak to moderately intense staining of the membrane was seen in greater than 10% of tumor cells; 1+ if incomplete staining of the membrane was found in more than 10% of tumor cells and a score of 0 was assigned when no staining or membranous staining in less than 10% of tumor cells was present. A score of 3+ was considered positive, a score of 2+ was equivocal positive and scores of 1+ and 0 were negative.

Ki-67 was evaluated as the percentage of cells showing positive nuclear reactivity in at least 500 histologically recognized tumour cells counted at ×400 magnification.

For TMA validation purposes, the originally recorded immunohistochemical results from the initial routine histopathology reports of ten patients were compared to those of the current experiment. Similar findings were observed in the TMAs compared to

full tissue sections.

### Statistical analysis

Data were analysed by IBM SPSS software package ver. 20.0 (IBM Corp., Armonk, NY, USA). Qualitative data were described as number and percent. Quantitative data were described using median (minimum and maximum) and interquartile range for non-parametric data and mean and standard deviation for parametric data after testing for normality using the Kolmogorov-Smirnov test. The significance of the results obtained was judged at the 5% level. The tests used were chi-square, Monte Carlo, Fisher exact, Student t-, F- (ANOVA), Mann-Whitney, Kruskal-Wallis, and Spearman correlation.

## RESULTS

### Clinicopathological features of the studied cases

Patient ages ranged from 37 to 79 years with a mean age of  $59.8 \pm 8.2$  years. Most of the cases (88 patients, 80.7%) in this study were postmenopausal.

Tumors ranged from 1 to 14 cm in largest dimension with a median value of 3 cm. There were 36 cases of grade 1 (33%), 43 cases of grade 2 (39.4%), and 30 cases were high grade carcinomas (27.5%) including grade 3 endometrioid, serous, mixed, undifferentiated and dedifferentiated carcinomas, and carcinosarcomas. In three cases (2.7%) the tumour was limited to the endometrium, 69 (63.3%) cases showed infiltration of the inner myometrial half, the tumour infiltrated the outer half in 26 cases (24%), and the serosa was infiltrated in three cases (2%). Cervical involvement was found in 20 cases (18%), 71 cases (65%) were free from cervical infiltration and in 14 cases (12.8%) cervical involvement was not determined due to suboptimal surgery. Adnexal metastases were found in 11 cases (10%), 83 cases (76%) were free from adnexal infiltration, and in 15 cases (13.7%) adnexal infiltration was unknown due to suboptimal surgery. There were 71 cases (65.1%) in stage I (56 stage IA and 15 stage IB), 15 cases in stage II (13.8%), 10 cases (9%) in stage IIIA, only two cases were stage IIIB, and one case was stage IVA. Lymphovascular emboli were found in 29 cases (26.6%).

**Table 1.** ER expression score in relation to histopathological parameters

	ER score			Test of significance
	Category 1 (n=45)	Category 2 (n=40)	Category 3 (n=20)	
Grade				
G1	10 (22.2)	20 (50.0)	6 (30.0)	MC, p=.021
G2	15 (33.3)	13 (32.5)	11 (55.0)	$\chi^2 = 2.9$ , p=.233
G3	20 (44.4)	7 (17.5)	3 (15.0)	$\chi^2 = 2.67$ , p=.007
Stage				MC, p=.057
I & II	32 (78.0)	35 (94.6)	16 (94.1)	
III & IV	9 (22.0)	2 (5.4)	1 (5.9)	
Depth				$\chi^2 = 1.97$ , p=.362
Inner half	27 (65.9)	28 (73.7)	15 (83.3)	
Outer half	14 (34.1)	10 (26.3)	3 (16.7)	
Cervical involvement				$\chi^2 = 5.1$ , p=.081
Absent	30 (75.0)	26 (72.2)	15 (100)	
Present	10 (25.0)	10 (27.8)	0	
LVI				$\chi^2 = 10.13$ , p=.006
Present	19 (42.2)	7 (17.5)	2 (10.0)	
Absent	26 (57.8)	33 (82.5)	18 (90.0)	
Lymph node involvement				MC, p=.161
Absent	15 (71.4)	18 (94.7)	3 (75.0)	
Present	6 (28.6)	1 (5.3)	1 (25.0)	
Ovarian involvement				MC, p=.025
Absent	30 (76.9)	35 (97.2)	14 (93.3)	
Present	9 (23.1)	1 (2.8)	1 (6.7)	
Histology				MC, p=.007
Non-endometrioid	15 (33.3)	3 (2.5)	2 (10.0)	
Endometrioid	30 (66.7)	37 (92.5)	18 (90.0)	

Values are presented as number (%).

ER, estrogen receptor;  $\chi^2$ , chi-square test; MC, Monte Carlo test; LVI, lymphovascular invasion.

### The association of immunohistochemical results with histopathological prognostic parameters

The distribution of immunohistochemical data in relation to individual histopathological parameters is presented in Tables 1–4. The relationships among ER, PR expression, and other markers (HER2-neu and Ki-67) as well as the relationship between HER2-neu expression and Ki-67 expression are presented in Tables 5. Representative examples of the different expression patterns are shown in Fig. 1.

ER and PR scores were statistically associated ( $p < .001$ ). There were significant relationships between low ER scores and non-endometrioid histology ( $p = .007$ ) and higher grade of endometrial cancer ( $p = .007$ ). The ER score tended to decrease with advanced stage ( $p = .057$ ). Low ER score was associated with ovarian involvement ( $p = .025$ ), lymphovascular space invasion (LVSI) ( $p = .006$ ), and higher Ki-67 values ( $p = .024$ ).

Low PR expression score was associated with non-endometrioid histology ( $p < .001$ ), higher tumour grade ( $p < .001$ ), advanced stage ( $p = .009$ ), and ovarian involvement ( $p < .007$ ). The PR score decreased with LVSI ( $p = .06$ ), and lower score was associated with

lymph node metastasis ( $p = .026$ ). Ki-67 values were higher with low PR score ( $p = .025$ ).

HER2 expression was significantly associated with advanced tumour stages ( $p = .04$ ), increased depth of myometrial infiltration ( $p = .02$ ), greater incidence of LVSI ( $p = .017$ ), ovarian involvement ( $p = .038$ ), and lymph node metastasis ( $p = .038$ ). There was a notable relationship between HER2 expression and cervical involvement ( $p = .009$ ).

A positive correlation was found between tumour size and Ki-67 index ( $p = .02$ ). Higher Ki-67 index was linked to more aggressive features such as non-endometrioid histotype ( $p < .001$ ) and poor differentiation grade ( $p < .001$ ). There was a strong relationship between higher Ki-67 values and lymph node involvement ( $p = .012$ ).

Median Ki-67 index value was higher in HER2-neu-positive cases than that of negative cases ( $p = .482$ , Mann-Whitney test).

## DISCUSSION

EC is the most common gynaecologic cancer worldwide and

**Table 2.** PR expression score in relation to histopathological parameters

	PR score			Test of significance
	Category 1 (n=35)	Category 2 (n=33)	Category 3 (n=37)	
Grade				
G1	2 (5.7)	12 (36.4)	22 (59.5)	MC, $p < .001$
G2	13 (37.1)	13 (39.4)	13 (35.1)	MC, $p = .901$
G3	20 (57.1)	8 (24.2)	2 (5.4)	MC, $p < .001$
Stage				
I & II	25 (73.5)	28 (93.3)	30 (96.8)	MC, $p = .009$
III & IV	9 (26.5)	2 (6.7)	1 (3.2)	
Depth				
Inner half	21 (63.6)	24 (77.4)	25 (75.8)	$\chi^2 = 1.83$ , $p = .401$
Outer half	12 (36.4)	7 (22.6)	8 (24.2)	
Cervical involvement				
Absent	23 (69.7)	21 (75.0)	27 (90.0)	$\chi^2 = 3.9$ , $p = .162$
Present	10 (30.3)	7 (25.0)	3 (10.0)	
LVI				
Present	13 (37.1)	10 (30.3)	5 (13.5)	$\chi^2 = 5.46$ , $p = .063$
Absent	22 (62.9)	23 (59.7)	32 (86.5)	
Lymph node involvement				
Absent	11 (64.7)	10 (83.3)	15 (100)	MC, $p = .026$
Present	6 (35.3)	2 (16.7)	0	
Ovarian involvement				
Absent	24 (75.0)	25 (89.3)	30 (100)	MC, $p = .007$
Present	8 (25.0)	3 (10.7)	0	
Histology				
Non-endometrioid	15 (42.9)	5 (15.2)	0	$\chi^2 = 21.89$ , $p < .001$
Endometrioid	20 (57.1)	28 (84.8)	37 (100)	

Values are presented as number (%).

PR, progesterone receptor; MC, Monte Carlo test;  $\chi^2$ , chi-square test; LVI, lymphovascular invasion.

the incidence is increasing.<sup>2,3,16</sup> EC may not always fit into the dual model of type I and type II cancers: those can be vague clinico-pathological designations rather than firm diagnostic entities. Tumours display varying degrees of conformity with both types and have different behaviours and prognoses.<sup>17-19</sup> According to the National Cancer Comprehensive Network guidelines for management of EC, the treatment strategy depends on surgical staging, depth of infiltration and the presence of adverse risk factors

**Table 3.** The expression of HER2 in relation to histopathological parameters

	HER2		Fisher exact test p-value
	Negative (n=102)	Positive (n=3)	
Grade			
G1	36 (35.3)	0	.321
G2	38 (37.3)	1 (33.3)	> .992
G3	28 (27.5)	2 (66.7)	.192
Stage			
I & II	82 (89.1)	1 (33.3)	.042
III & IV	10 (10.9)	2 (66.7)	
Depth			
Inner half	70 (74.5)	0	.022
Outer half	24 (25.5)	3 (100)	
Cervical involvement			
Absent	71 (80.7)	0	.009
Present	17 (19.3)	3 (100)	
LVI			
Present	25 (24.5)	3 (100)	.017
Absent	77 (75.5)	0	
Lymph node involvement			
Absent	36 (85.7)	0	.032
Present	6 (14.3)	2 (100)	
Ovarian involvement			
Absent	78 (89.7)	1 (33.3)	.038
Present	9 (10.3)	2 (66.7)	
Histology			
Non-endometrioid	19 (18.6)	1 (33.3)	.473
Endometrioid	83 (81.4)	2 (66.7)	

Values are presented as number (%).  
HER2, human epidermal growth factor receptor 2; LVI, lymphovascular invasion.

such as age, tumour size, LVSI and lower uterine involvement. Adjuvant therapy determinations are made on the basis of pathologic findings in the postoperative specimen. Superficially invasive, low grade (G 1–2) carcinomas in the absence of adverse risk factors can be treated by surgery with post-operative observation. However, in the presence of adverse risk factors, patients need adjuvant radiotherapy. High grade carcinomas with no adverse risk factors may be spared from adjuvant chemotherapy.<sup>20</sup>

Both breast and endometrial cancers are among the commonest

**Table 4.** The expression of Ki-67 in relation to histopathological parameters

	Ki-67	
	Median (min–max)	Test of significance
Grade		
G1	15.0 (0.5–90.0)	KW, p<.001
G2	15.0 (0.5–75.0)	
G3	35.0 (0.5–80.0)	
Stage		
I & II	20.0 (0.5–90.0)	Z=1.5, p=0.132
III & IV	35.0 (2.0–80.0)	
Depth		
Inner half	17.0 (0.5–90.0)	Z=0.11, p=.921
Outer half	23.0 (0.5–80.0)	
Cervical involvement		
Absent	20.0 (0.5–90.0)	Z=0.18, p=.862
Present	20.0 (0.5–70.0)	
LVI		
Present	30.0 (0.5–80.0)	Z=1.58, p=.113
Absent	18.5 (0.5–90.0)	
Lymph node involvement		
Absent	20.0 (0.5–70.0)	Z=2.5, p=.012
Present	50.0 (8.0–80.0)	
Ovarian involvement		
Absent	20.0 (0.5–90.0)	Z=1.36, p=.171
Present	30.0 (5.0–80.0)	
Histology		
Non-endometrioid	50.0 (5.0–80.0)	Z=4.4, p<.001
Endometrioid	15.0 (0.5–90.0)	

KW, Kruskal-Wallis test; Z, Mann-Whitney U test; LVI, lymphovascular invasion.

**Table 5.** Relationship between ER, PR expression and other markers (HER2 and Ki-67)

	ER score			Test of significance	PR score			Test of significance
	Category 1 (n=45)	Category 2 (n=40)	Category 3 (n=20)		Category 1 (n=35)	Category 2 (n=33)	Category 3 (n=37)	
HER2				MC, p=.812				MC, p=.193
Negative	43 (95.6)	39 (97.5)	20 (100)		34 (97.1)	31 (93.3)	37 (100)	
Positive	2 (4.4)	1 (2.5)	0	1 (2.9)	2 (6.1)	0		
Ki-67				KW, p=.024				KW, p=.025
Median (min–max)	30 (0.5–80)	10 (0.5–80)	25 (1–90)		35.0 (0.5–80)	15 (0.5–70)	10 (0.5–90)	

Values are presented as number (%).  
ER, estrogen receptor; PR, progesterone receptor; HER2, human epidermal growth factor receptor 2; MC, Monte Carlo test; KW, Kruskal-Wallis test.

cancers in females, and both are largely considered to be hormone-dependent tumours. In breast cancer, a simple immunohistochemical panel of ER, PR, HER2, and Ki-67 is routinely per-

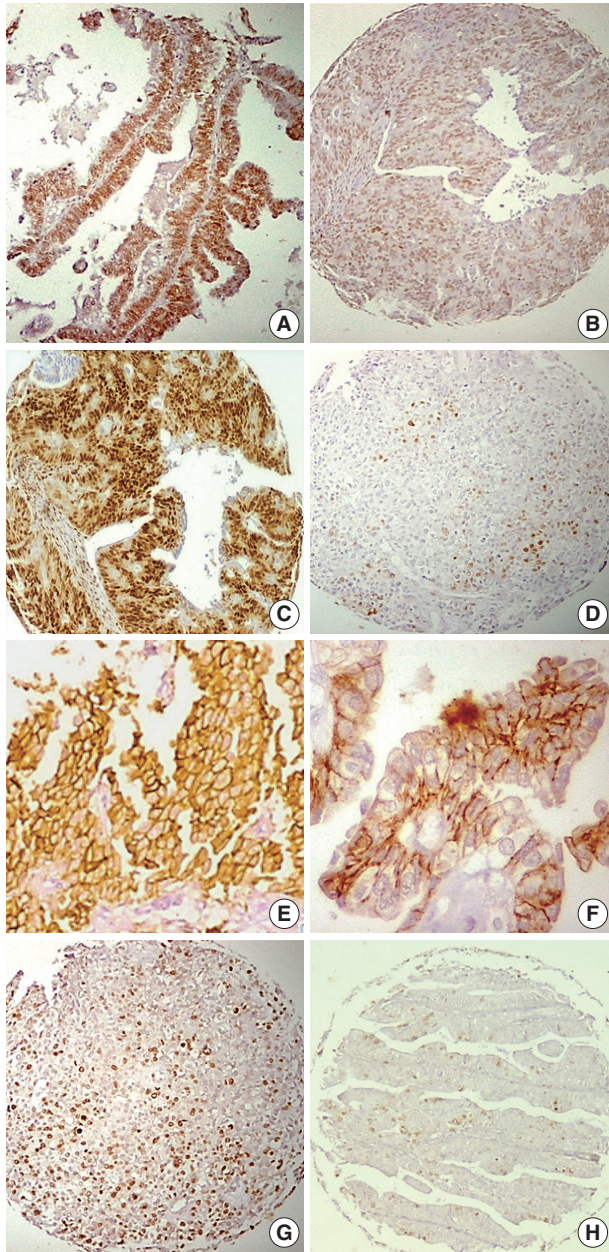


**Fig. 1.** Examples of different patterns of immunohistochemical expression in endometrial carcinomas. (A) Estrogen receptor (ER) expression score (6) in a case of well differentiated endometrial carcinoma (EC). (B) ER expression score (4) in a poorly differentiated EC. (C) progesterone receptor (PR) expression score (6) in a moderately differentiated EC. (D) PR expression score (2) in a poorly differentiated EC. (E) Positive human epidermal growth factor receptor 2 (HER2) overexpression (score +3) in a case of poorly differentiated EC. (F) HER2 score (+1), which is considered negative, in a well differentiated EC. (G) High Ki-67 index in a poorly differentiated EC. (H) Low Ki-67 index in a well differentiated EC.

formed on preoperative or postoperative specimens yielding valuable therapeutic and prognostic information. Similar to breast cancer, this panel may be of value when assessing EC specimens. The information attained may be helpful in guiding patient management and in providing prognostic information about tumour behaviour.<sup>7</sup>

In the current work, we assessed the immunohistochemical expression of the same panel of biological markers (ER, PR, HER2, and Ki-67) on 109 cases of EC and their association with histopathological prognostic characteristics. The presence of hormone receptors in ECs correlates with the clinical disease stage, histological grade, and overall survival. The absence of hormone receptors is considered to indicate aggressive tumour behaviour and poor prognosis.<sup>21,22</sup> A recent systematic review and meta-analysis revealed that higher levels of ER and PR were associated with favourable prognosis and longer overall survival.<sup>23</sup> This study showed close associations between low ER and PR scores, non-endometrioid histology and high grade endometrial cancer. Moreover, low PR score was significantly associated with advanced tumour stage. These findings agree with previous studies.<sup>21,24,25</sup> While not statistically significant, the ER score tended to be lower with advanced stage. Some studies failed to show associations between ER and PR expression and tumour stage.<sup>26,27</sup> Our data revealed significant associations between ovarian involvement and low ER and PR scores, an observation in contrast to previous observations.<sup>6,28</sup> This discrepancy may be due to differences in sample size, primary antibody used, and the method of scoring the immunohistochemical results. ER and PR did not show significant association with the depth of myometrial invasion or cervical infiltration as previously reported.<sup>25,26</sup> Low ER score was significantly associated with LVSI; low PR score tended to be associated with LVSI as well, but the strength of the low PR association did not match that of low ER. This agrees with the findings of a previous study.<sup>24</sup> Low PR scores were significantly associated with lymph node metastasis as reported earlier.<sup>26</sup> Consistent with previous studies, high ER and PR scores were highly associated while lower scores were associated with higher Ki-67 values.<sup>24,27,29</sup>

The increased expression of HER2 correlates with worse prognosis in various malignant tumours. In their extensive study (483 cases), Morrison et al.<sup>30</sup> demonstrated that the over-expression of HER2 was an independent prognostic factor that correlated with worse survival. Our work confirms a close relationship between HER2 overexpression and some of the traditional prognostic factors of endometrial cancer. In partial agreement with previous studies, we found HER2 expression to be associated with advanced tumour stages and increased depth of myometrial invasion.<sup>31-33</sup> We have

not observed, however, any substantial relationship between HER2 overexpression and the grading of ECs. Some previous studies did not show a significant association between HER2 expression and the prognostic parameters.<sup>6,33</sup> In contrast to this, our study revealed that HER2 overexpression was significantly associated with a greater incidence of ovarian and cervical involvement, lympho-vascular emboli and LN metastasis, findings in line with a previous observation.<sup>4</sup> We did not find HER2 over-expression to be significantly associated with ER, PR, or Ki-67 expression, a finding inconsistent with that of a study showing significant correlation between HER2 over-expression and high Ki-67 index.<sup>4</sup>

Increased Ki-67 expression indicates higher mitotic activity and greater tumour cell proliferation. Some studies revealed that Ki-67 could be an independent prognostic marker of survival in EC.<sup>34,35</sup> On the other hand, Pansare et al.<sup>36</sup> did not find correlations between Ki-67, histological type, grading, and tumour clinical staging. An elevated Ki-67 expression in this study was strongly related to non-endometrioid histotype and poor differentiation. Higher Ki-67 index was also found to be associated with lymph node involvement but not tumour stage, depth of myometrial invasion, cervical infiltration, or ovarian involvement.

Our proposed immunohistochemical panel (ER, PR, HER2, and Ki-67) may be of value for preoperative biopsies. Results may indicate tumour behaviour characteristics, presence of adverse risk factors such as lympho-vascular emboli and cervical involvement, and the necessity for more radical surgery with pelvic and para-aortic lymph node dissection.<sup>37</sup> Moreover, the panel may also be performed on postoperative specimens. The panel may be included routinely as an adjunct consideration in the postoperative treatment decision making process. Low risk patients with low grade, superficially invasive tumours may be spared the morbidity of lymphadenectomy as well as the cost and morbidity of radiotherapy. The panel results can also assist in identifying high risk patients requiring more radical surgery, post-operative radiotherapy, and/or chemotherapy.<sup>38</sup>

In conclusion, low ER and PR expression scores (category I), together with HER2 overexpression (score + 3) and Ki-67 indices of more than 20%, were associated with more malignant behaviour of ECs. Further studies involving larger numbers of patients are needed to investigate the correlation between this immunohistochemical panel's results and the recent molecular classification of EC.

## ORCID

Amany Salama: <https://orcid.org/0000-0001-8433-9981>

Mohammad Arafa: <https://orcid.org/0000-0001-6514-3545>

Abdelhadi Mohamed Shebl:

<https://orcid.org/0000-0002-2624-0040>

Sylvia A. Ashamalla: <https://orcid.org/0000-0002-6395-769X>

Reda Hemida: <https://orcid.org/0000-0003-0841-0242>

Anas Gamal: <https://orcid.org/0000-0001-8381-5536>

Abd AlRahman Foda: <https://orcid.org/0000-0002-6858-9822>

Khaled Zalata: <https://orcid.org/0000-0002-6678-7438>

El-Said M. Abdel-Hady: <https://orcid.org/0000-0001-5010-1449>

## Author Contributions

Conceptualization: MA.

Data curation: AS, MA, AAF, SAA.

Formal analysis: AS, MA, AAF, SAA.

Funding acquisition: MA.

Investigation: AS, MA, AAF, SAA.

Methodology: AS, MA, AAF, SAA.

Project administration: MA, SAA, RH, AG, KZ, ESMHAH.

Resources: MA, SAA, RH, AG, KZ, ESMHAH.

Software: AS, MA, SAA.

Supervision: MA, AMS, EE, AAEHA.

Validation: AS, MA, SAA.

Visualization: AS, MA, AAF, SAA.

Writing—original draft: AS.

Writing—review & editing: AS, MA, AAF, SAA.

## Conflicts of Interest

The authors declare that they have no potential conflicts of interest.

## Acknowledgments

This study is the outcome of a research project (entitled: Impact of Genetic Alterations on the Management of Endometrial Carcinoma) supported by the research fund unit of Mansoura University.

## REFERENCES

1. Le Gallo M, Bell DW. The emerging genomic landscape of endometrial cancer. *Clin Chem* 2014; 60: 98-110.
2. Llaurodo M, Ruiz A, Majem B, et al. Molecular bases of endometrial cancer: new roles for new actors in the diagnosis and the therapy of the disease. *Mol Cell Endocrinol* 2012; 358: 244-55.
3. Backes FJ, Walker CJ, Goodfellow PJ, et al. Estrogen receptor-alpha as a predictive biomarker in endometrioid endometrial cancer. *Gynecol Oncol* 2016; 141: 312-7.

4. Yu CG, Jiang XY, Li B, Gan L, Huang JF. Expression of ER, PR, CerbB-2 and Ki-67 in endometrial carcinoma and their relationships with the clinicopathological features. *Asian Pac J Cancer Prev* 2015; 16: 6789-94.
5. Arafa M, Sonja J, Dehan P, et al. Current concepts in the pathology and epigenetics of endometrial carcinoma. *Pathology* 2010; 42: 613-7.
6. Markova I, Duskova M, Lubusky M, et al. Selected immunohistochemical prognostic factors in endometrial cancer. *Int J Gynecol Cancer* 2010; 20: 576-82.
7. Lapinska-Szumczyk S, Supernat A, Majewska H, et al. HER2-positive endometrial cancer subtype carries poor prognosis. *Clin Transl Sci* 2014; 7: 482-8.
8. Cancer Genome Atlas Research Network, Kandoth C, Schultz N, et al. Integrated genomic characterization of endometrial carcinoma. *Nature* 2013; 497: 67-73.
9. Faria SC, Sagebiel T, Balachandran A, Devine C, Lal C, Bhosale PR. Imaging in endometrial carcinoma. *Indian J Radiol Imaging* 2015; 25: 137-47.
10. Li M, Zhao L, Qi W, et al. Clinical implications and prognostic value of five biomarkers in endometrial carcinoma. *Chin Ger J Clin Oncol* 2013; 12: 586-91.
11. Pecorelli S. Revised FIGO staging for carcinoma of the vulva, cervix, and endometrium. *Int J Gynaecol Obstet* 2009; 105: 103-4.
12. Arafa M, Boniver J, Delvenne P. Progression model tissue microarray (TMA) for the study of uterine carcinomas. *Dis Markers* 2010; 28: 267-72.
13. Zannoni GF, Vellone VG, Arena V, et al. Does high-grade endometrioid carcinoma (grade 3 FIGO) belong to type I or type II endometrial cancer? A clinical-pathological and immunohistochemical study. *Virchows Arch* 2010; 457: 27-34.
14. Kounelis S, Kapranos N, Kouri E, Coppola D, Papadaki H, Jones MW. Immunohistochemical profile of endometrial adenocarcinoma: a study of 61 cases and review of the literature. *Mod Pathol* 2000; 13: 379-88.
15. Brunelli M, Manfrin E, Martignoni G, et al. HER-2/neu assessment in breast cancer using the original FDA and new ASCO/CAP guideline recommendations: impact on selecting patients for herceptin therapy. *Am J Clin Pathol* 2008; 129: 907-11.
16. Binder PS, Mutch DG. Update on prognostic markers for endometrial cancer. *Womens Health (Lond)* 2014; 10: 277-88.
17. Rutgers JK. Update on pathology, staging and molecular pathology of endometrial (uterine corpus) adenocarcinoma. *Future Oncol* 2015; 11: 3207-18.
18. Maiques O, Cuevas D, Garcia Dios DA, et al. FISH analysis of PTEN in endometrial carcinoma. Comparison with SNP arrays and MLPA. *Histopathology* 2014; 65: 371-88.
19. Garg K, Soslow RA. Strategies for distinguishing low-grade endometrioid and serous carcinomas of endometrium. *Adv Anat Pathol* 2012; 19: 1-10.
20. Koh WJ, Greer BE, Abu-Rustum NR, et al. Uterine neoplasms, version 1.2014. *J Natl Compr Canc Netw* 2014; 12: 248-80.
21. Ferrandina G, Ranelletti FO, Gallotta V, et al. Expression of cyclooxygenase-2 (COX-2), receptors for estrogen (ER), and progesterone (PR), p53, ki67, and neu protein in endometrial cancer. *Gynecol Oncol* 2005; 98: 383-9.
22. Jazaeri AA, Nunes KJ, Dalton MS, Xu M, Shupnik MA, Rice LW. Well-differentiated endometrial adenocarcinomas and poorly differentiated mixed mullerian tumors have altered ER and PR isoform expression. *Oncogene* 2001; 20: 6965-9.
23. Zhang Y, Zhao D, Gong C, et al. Prognostic role of hormone receptors in endometrial cancer: a systematic review and meta-analysis. *World J Surg Oncol* 2015; 13: 208.
24. Engelsen IB, Stefansson IM, Akslen LA, Salvesen HB. GATA3 expression in estrogen receptor alpha-negative endometrial carcinomas identifies aggressive tumors with high proliferation and poor patient survival. *Am J Obstet Gynecol* 2008; 199: 543.e1-7.
25. Tomica D, Ramic S, Danolic D, et al. A correlation between the expression of estrogen receptors and progesterone receptors in cancer cells and in the myometrium and prognostic factors in endometrial cancer. *Coll Antropol* 2014; 38: 129-34.
26. Srijaipracharoen S, Tangjitgamol S, Tanvanich S, et al. Expression of ER, PR, and Her-2/neu in endometrial cancer: a clinicopathological study. *Asian Pac J Cancer Prev* 2010; 11: 215-20.
27. Sivridis E, Giatromanolaki A, Koukourakis M, Anastasiadis P. Endometrial carcinoma: association of steroid hormone receptor expression with low angiogenesis and bcl-2 expression. *Virchows Arch* 2001; 438: 470-7.
28. Kobel M, Atenafu EG, Rambau PF, et al. Progesterone receptor expression is associated with longer overall survival within high-grade histotypes of endometrial carcinoma: a Canadian high risk endometrial cancer consortium (CHREC) study. *Gynecol Oncol* 2016; 141: 559-63.
29. Stoian SC, Simionescu C, Margaritescu C, Stepan A, Nurciu M. Endometrial carcinomas: correlation between ER, PR, Ki67 status and histopathological prognostic parameters. *Rom J Morphol Embryol* 2011; 52: 631-6.
30. Morrison C, Zanagnolo V, Ramirez N, et al. HER-2 is an independent prognostic factor in endometrial cancer: association with outcome in a large cohort of surgically staged patients. *J Clin Oncol* 2006; 24: 2376-85.
31. Ioffe OB, Papadimitriou JC, Drachenberg CB. Correlation of proliferation indices, apoptosis, and related oncogene expression (bcl-2

- and c-erbB-2) and p53 in proliferative, hyperplastic, and malignant endometrium. *Hum Pathol* 1998; 29: 1150-9.
32. Williams JA Jr, Wang ZR, Parrish RS, Hazlett LJ, Smith ST, Young SR. Fluorescence in situ hybridization analysis of HER-2/neu, c-myc, and p53 in endometrial cancer. *Exp Mol Pathol* 1999; 67: 135-43.
  33. Gul AE, Keser SH, Barisik NO, et al. The relationship of cerb B 2 expression with estrogen receptor and progesterone receptor and prognostic parameters in endometrial carcinomas. *Diagn Pathol* 2010; 5: 13.
  34. Salvesen HB, Iversen OE, Akslen LA. Prognostic significance of angiogenesis and Ki-67, p53, and p21 expression: a population-based endometrial carcinoma study. *J Clin Oncol* 1999; 17: 1382-90.
  35. Geisler JP, Geisler HE, Miller GA, Wiemann MC, Zhou Z, Crabtree W. MIB-1 in endometrial carcinoma: prognostic significance with 5-year follow-up. *Gynecol Oncol* 1999; 75: 432-6.
  36. Pansare V, Munkarah AR, Schimp V, et al. Increased expression of hypoxia-inducible factor 1alpha in type I and type II endometrial carcinomas. *Mod Pathol* 2007; 20: 35-43.
  37. Goebel EA, Vidal A, Matias-Guiu X, Blake Gilks C. The evolution of endometrial carcinoma classification through application of immunohistochemistry and molecular diagnostics: past, present and future. *Virchows Arch* 2018; 472: 885-96.
  38. Sundar S, Balega J, Crosbie E, et al. BGCS uterine cancer guidelines: Recommendations for practice. *Eur J Obstet Gynecol Reprod Biol* 2017; 213: 71-97.

# Prognostic Role of Claudin-1 Immunohistochemistry in Malignant Solid Tumors: A Meta-Analysis

Jung-Soo Pyo\* · Nae Yu Kim<sup>1</sup>\*  
Won Jin Cho<sup>2</sup>

Departments of Pathology and <sup>1</sup>Internal Medicine, Eulji University Hospital, Eulji University School of Medicine, Daejeon; <sup>2</sup>Department of Urology, Chosun University Hospital, Chosun University School of Medicine, Gwangju, Korea

Received: December 31, 2018

Revised: February 1, 2019

Accepted: February 3, 2019

## Corresponding Author

Won Jin Cho, MD

Department of Urology, Chosun University Hospital, Chosun University School of Medicine, 365 Pilmun-daero, Dong-gu, Gwangju 61453, Korea

Tel: +82-62-220-3210

Fax: +82-62-232-3210

E-mail: uro2097@gmail.com

\*Jung-Soo Pyo and Nae Yu Kim contributed equally to this work.

**Background:** Although the correlation between low claudin-1 expression and worse prognosis has been reported, details on the prognostic implications of claudin-1 expression in various malignant tumors remain unclear. The present study aimed to elucidate the prognostic roles of claudin-1 immunohistochemistry (IHC) in various malignant tumors through a meta-analysis. **Methods:** The study included 2,792 patients from 22 eligible studies for assessment of the correlation between claudin-1 expression and survival rate in various malignant tumors. A subgroup analysis based on the specific tumor and evaluation criteria of claudin-1 IHC was conducted. **Results:** Low claudin-1 expression was significantly correlated with worse overall survival (OS) (hazard ratio [HR], 1.851; 95% confidence interval [CI], 1.506 to 2.274) and disease-free survival (DFS) (HR, 2.028; 95% CI, 1.313 to 3.134) compared to high claudin-1 expression. Breast, colorectal, esophageal, gallbladder, head and neck, and lung cancers, but not cervical, liver or stomach cancers, were significantly correlated with worse OS. Breast, colorectal, esophageal, and thyroid cancers with low claudin-1 expression were associated with poorer DFS. In the lower cut-off subgroup (<25.0%) with respect to claudin-1 IHC, low claudin-1 expression was significantly correlated with worse OS and DFS. **Conclusions:** Taken together, low claudin-1 IHC expression is significantly correlated with worse survival in various malignant tumors. More detailed criteria for claudin-1 IHC expression in various malignant tumors are needed for application in daily practice.

**Key Words:** Claudin-1; Immunohistochemistry; Prognosis; Malignancy; Meta-analysis

Claudins comprise a large family of tetraspan trans-membrane proteins and are required for tight junction formation.<sup>1</sup> Claudin-1 expression is regulated by the  $\beta$ -catenin-T-cell factor/lymphoid enhancing factor signaling pathway.<sup>2,3</sup> Claudins have potentially different functions driven by the formation of homotypic or heterotypic interactions across the junction in various tissues.<sup>4-8</sup> The epithelial-to-mesenchymal transition, which is correlated with tumor invasiveness, is affected by the change of expression and the redistribution of tight junction proteins including claudin.<sup>9</sup> Expression patterns of claudins can differ by tumor or tissue type, which can affect tumor behavior and prognosis.<sup>10</sup> The prognostic roles of claudin-1 have been diverse in several studies involving various tumor types.<sup>9,11-31</sup> However, in stomach cancer, increased claudin-1 expression in tumor cells has been significantly correlated with worse prognosis in the intestinal type, but not in the diffuse type. In kidney and lung cancers, high claudin-1 expression has likewise been correlated with worse prognosis.<sup>12,14</sup> Although a correlation between low claudin-1

expression and worse prognosis has been reported, details on the prognostic implications of claudin-1 expression in various malignant tumors remain unclear.

To elucidate the prognostic role of claudin-1 immunohistochemistry (IHC), the correlation between claudin-1 IHC expression and survival rates was investigated in various malignant tumors. A subgroup analysis based on the evaluation criteria of claudin-1 IHC was conducted.

## MATERIALS AND METHODS

### Literature search and selection criteria

Relevant articles were obtained by searching the PubMed and MEDLINE databases through February 28, 2018. The search was performed using 'claudin-1' and 'survival' as search terms. The titles and abstracts of all returned articles were screened for exclusion. Review articles were also screened to find additional eligible studies. English language studies addressing claudin-1

IHC expression in human malignant tumors and the correlation between claudin-1 IHC expression and survival rate were included. Case reports were excluded. This meta-analysis did not require the approval of an institutional review board.

### Data extraction

The following information was collected and verified from the full texts of eligible studies:<sup>9,11-31</sup> first author's name, publication date, study location, number of patients analyzed, antibody manufacturer, dilution ratio, cut-offs for assessing high claudin-1 IHC expression, tumor type, and data allowing estimation of the impact of claudin-1 IHC expression on overall survival (OS) and disease-free survival (DFS). We did not define a minimum number of patients to be included in a study. Any disagreements were resolved by consensus.

### Statistical analyses

To perform the meta-analysis, all data were analyzed using the Comprehensive Meta-Analysis software package (Biostat, Englewood, NJ, USA). Correlations between claudin-1 IHC expression and survival were measured by hazard ratios (HR) obtained from the eligible study data. We aggregated the estimated HR and its standard error using given parameters, which were the HR point estimate, log-rank statistic or its p-value, O–E statistic (difference between numbers of observed and expected events), or its variance.<sup>32</sup> If the extractable data only included the survival curve, two persons independently extracted survival rates to reduce reading variability, according to Parmar's recommendation.<sup>32</sup> Meta-analysis was performed using fixed-effects and random-effects models. The values pooled using the random effects model were utilized for interpretation. Subsequently, a study showing results of an estimated HR > 1, with a 95% confidence interval (CI) that does not include 1, implied poor survival with a low or a loss of claudin-1 expression. Because eligible studies used various antibodies and evaluation criteria, a random-effects model was more suitable than a fixed-effects model. Subgroup analyses based on specific organs and cut-off value for high expression of claudin-1 IHC were performed. In addition, heterogeneous and sensitivity analyses were conducted to assess the heterogeneity of eligible studies and the impact of each study on the combined effect, respectively. Heterogeneity between studies was checked by the Q and I<sup>2</sup> statistics and demonstrated p-values. For assessment of publication bias, Begg's funnel plot and Egger's test were performed. The results were considered statistically significant when  $p < 0.05$ .

## RESULTS

### Selection and characteristics of studies

One hundred seventy reports were identified in the database search. Of these, 44 were excluded due to lack of sufficient information. Other studies were excluded because they reported the results of other diseases ( $n = 38$ ), used animals or cell lines ( $n = 57$ ), were not written in English ( $n = 5$ ), or were non-original articles ( $n = 3$ ) (Fig. 1). In addition, one article was excluded due to duplication. After applying the inclusion and exclusion criteria, 22 reports were finally included in the meta-analysis (Table 1). Eligible studies used various manufacturers' antibodies and variable dilution ratios, as shown in Table 1. The cut-off values to distinguish between low or high claudin-1 IHC expressions varied between 1% and 50%.

### The correlation between claudin-1 IHC expression and survival

The correlation between low expression of claudin-1 IHC and survival was investigated by subdividing data according to OS in 15 studies and according to DFS in 15 studies. Low expression of claudin-1 IHC was significantly correlated with worse OS (HR, 1.851; 95% CI, 1.506 to 2.274) (Fig. 2A) and DFS (HR, 2.028; 95% CI, 1.313 to 3.134) (Fig. 2B). Eligible studies showed significant heterogeneity in OS and DFS. Sensitivity analysis showed that eligible studies had no effect on the pooled HR. In sensitivity analysis, the ranges of HRs were 1.745–1.917 and

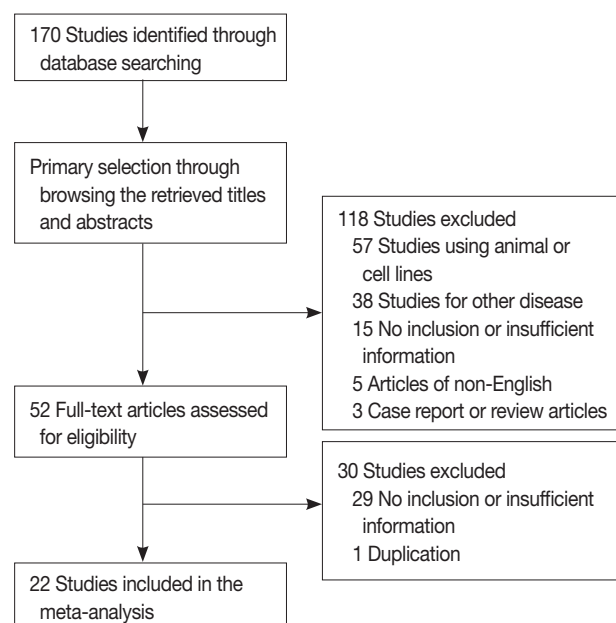


Fig. 1. Flow chart for study search and selection methods.

**Table 1.** Main characteristics of eligible studies

Study	Location	Antibody company	Dilution	Cut-off value (%)	Organ	Tumor type	Claudin-1 expression, n (%)	
							Low	High
Ma et al. (2014) <sup>19</sup>	China	Zymed	1:50	10	Breast	-	96 (55.5)	77 (44.5)
Morohashi et al. (2007) <sup>23</sup>	Japan	Zymed	1:50	10	Breast	-	104 (52.0)	96 (48.0)
Matsuoka et al. (2011) <sup>20</sup>	Japan	Spring Bioscience	ND	33.3	Colorectum	-	124 (79.5)	32 (20.5)
Resnick et al. (2005) <sup>24</sup>	USA	Zymed	1:125	ND <sup>a</sup>	Colorectum	-	32 (25.0)	96 (75.0)
Shibutani et al. (2013) <sup>26</sup>	Japan	Zymed	1:100	25	Colorectum	-	110 (32.0)	234 (68.0)
Yoshida et al. (2011) <sup>30</sup>	Japan	Zymed	1:400	30	Colorectum	-	92 (49.7)	93 (50.3)
Miyamoto et al. (2008) <sup>22</sup>	Japan	Zymed	1:100	10	Esophagus	SCC	11 (20.4)	43 (79.6)
Xiong et al. (2011) <sup>29</sup>	China	Fuzhou Maixin Biotech	ND	25	Gallbladder	-	37 (55.2)	30 (44.8)
Li et al. (2015) <sup>18</sup>	China	Beijing ZSGB-BIO	ND	40	H&N	SCC	26 (26.8)	71 (73.2)
Sappayatosok and Phattaratatip (2015) <sup>25</sup>	Thailand	Invitrogen	1:200	50	H&N	SCC	33 (73.3)	12 (26.7)
Fritzsche et al. (2008) <sup>14</sup>	Switzerland	Zymed	1:50	10	Kidney	Clear cell RCC	210 (75.5)	68 (24.5)
						Papillary RCC	6 (15.8)	32 (84.2)
Shin et al. (2011) <sup>27</sup>	Korea	Abcam	1:200	5	Kidney	Clear cell RCC	101 (84.9)	18 (15.1)
Bouchagier et al. (2014) <sup>11</sup>	Greece	Zymed	1:40	1 <sup>a</sup>	Liver	HCC	9 (13.4)	58 (86.6)
Higashi et al. (2007) <sup>15</sup>	USA	Zymed	1:50	ND	Liver	HCC	28 (50.9)	27 (49.1)
Chae et al. (2014) <sup>12</sup>	Korea	Abcam	1:500	50	Lung	AdCa	ND	ND
Chao et al. (2009) <sup>13</sup>	Taiwan	Zymed	ND	ND	Lung	AdCa	34 (50.7)	33 (49.3)
Merikallio et al. (2011) <sup>21</sup>	Finland	Zymed	1:50	25	Lung	SCC	15 (12.1)	109 (87.9)
						AdCa	2 (20.0)	8 (80.0)
Zhang et al. (2013) <sup>31</sup>	China	Zymed	ND	10	Lung	AdCa	33 (40.7)	48 (59.3)
Huang et al. (2014) <sup>9</sup>	China	Zymed	1:100	5	Stomach	-	63 (36.4)	110 (63.6)
Jung et al. (2011) <sup>17</sup>	Korea	Lab Vision	1:200	25	Stomach	-	31 (43.1)	41 (56.9)
Tzelepi et al. (2008) <sup>28</sup>	Greece	Zymed	1:100	5	Thyroid	-	24 (26.4)	67 (73.6)
Hoellen et al. (2017) <sup>16</sup>	Germany	Thermo Fisher Scientific Inc.	ND	>0	Uterine cervix	SCC	14 (13.2)	92 (86.8)

ND, non-description; SCC, squamous cell carcinoma; H&N, head and neck; RCC, renal cell carcinoma; HCC, hepatocellular carcinoma; AdCa, adenocarcinoma.

<sup>a</sup>Using criteria for intensity.

1.869–2.324 in OS and DFS, respectively. There was no evidence of publication bias in Egger's test ( $p = .505$  in OS and  $p = .956$  in DFS) and no asymmetry in Begg's funnel plot.

We conducted subgroup analysis based on specific tumors. In OS, low expression of claudin-1 IHC was significantly correlated with a lower survival rate in breast, colorectal, esophageal, gallbladder, head and neck, and lung cancers, but not in cervical, liver, or stomach cancers (Table 2). In addition, there was significant correlation between low expression of claudin-1 IHC and worse DFS in breast, colorectal, esophageal, and thyroid cancers, but not in liver, lung, kidney, or stomach cancers (Table 2). However, in DFS of head and neck cancer, low claudin-1 IHC expression showed a reverse correlation (HR, 0.396; 95% CI, 0.160 to 0.765). The cancer with the highest HR was breast cancer in both OS (HR, 3.364; 95% CI, 1.898 to 5.961) and DFS (HR, 5.182; 95% CI, 3.749 to 7.162).

Next, to evaluate the optimal criteria of low claudin-1 IHC expression, we created subgroups using the median value of cut-

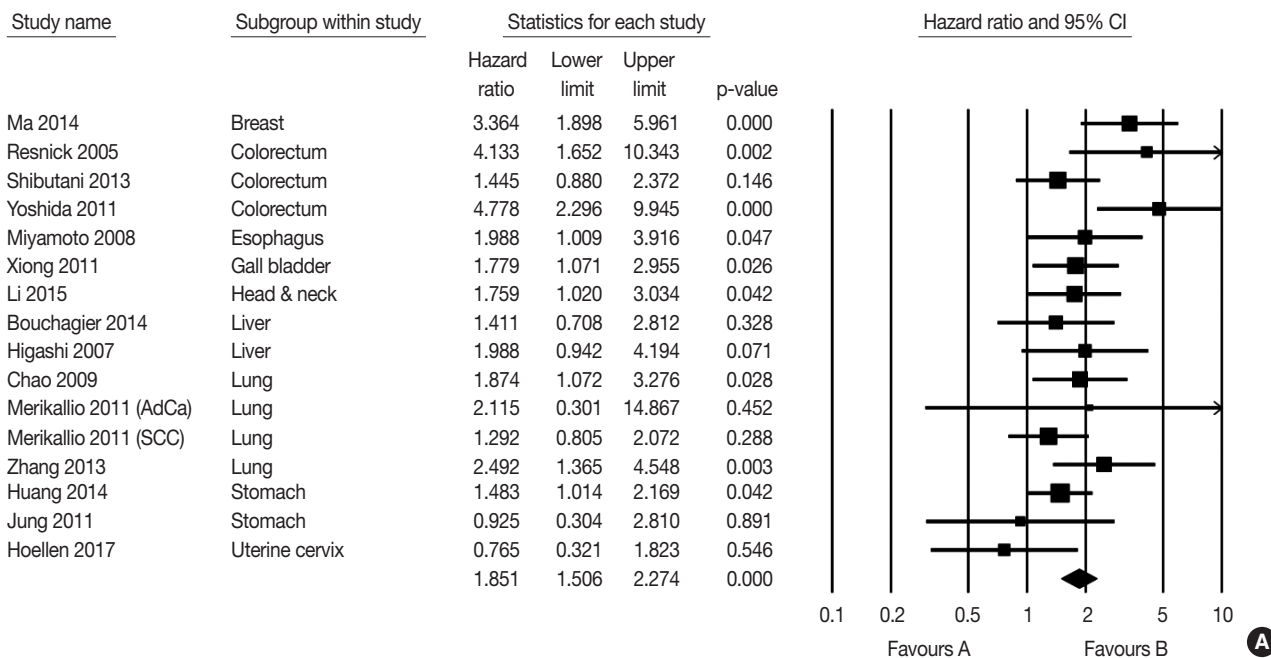
offs from eligible studies (25.0%). The results of subgroup analysis based on the evaluation criteria are shown in Fig. 3. In OS, HRs were 1.738 (95% CI, 1.251 to 2.415) and 1.805 (95% CI, 1.252 to 2.602) in the  $\geq 25.0\%$  and  $< 25.0\%$  cut-off subgroups, respectively. In DFS, HRs were 1.492 (95% CI, 0.808 to 2.753) and 2.611 (95% CI, 1.218 to 5.597) in subgroups with the  $\geq 25.0\%$  and  $< 25.0\%$  cut-offs, respectively.

## DISCUSSION

While claudin-1 has been studied in various malignant tumors, the prognostic role of claudin-1 IHC has not been fully elucidated and may vary.<sup>9,11-31</sup> The current study is the first meta-analysis of published studies on the prognostic role of claudin-1 IHC in various malignant tumors.

Although 27 subtypes of claudin are currently known in human tissues,<sup>33</sup> the expressions and functions of claudins in malignant tumors are not fully understood. In tumor cells, claudin-1 partic-

Overall survival



Disease-free survival

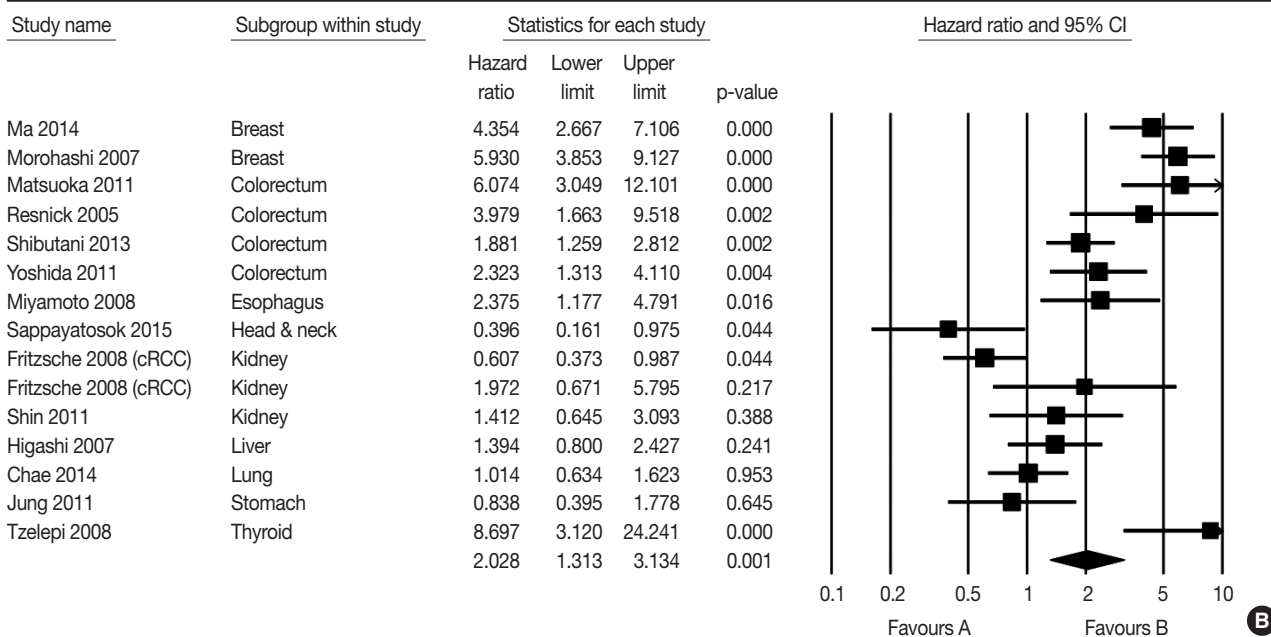


Fig. 2. Forest plot diagram showing the correlation between low claudin-1 immunohistochemical expression and overall survival (A) and disease-free survival (B).<sup>9,11-31</sup> CI, confidence interval.

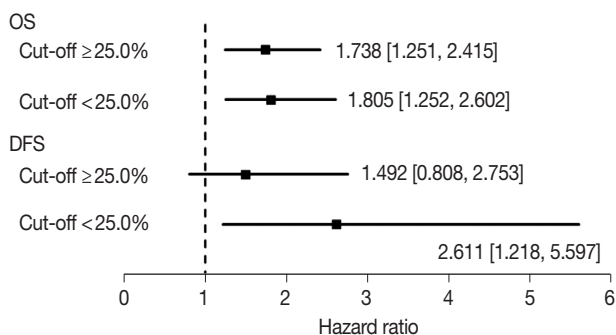
ipates in the up-regulation of ZEB-1, which induces reduction of E-cadherin expression and leads to invasive activity.<sup>34</sup> Loss of claudin-1 expression might induce loosening of tight junctions, which would alter the cohesion and invasiveness of tumor cells.<sup>1,7,8,35</sup> Furthermore, by loosening tight junctions, diffusion

of nutrients and other growth factors may be increased in tumor cells, which could induce proliferation of tumor cells. Claudin-1 overexpression inhibits the dissociation of cancer cells and suppresses migration, invasion, and metastasis.<sup>13,36</sup> Claudin-1 can also be expressed in normal cells, but the function and expression

**Table 2.** Meta-analysis for the correlation between low claudin-1 expression and overall and disease-free survival

	No. of subset	Fixed effect (95% CI)	Heterogeneity test p-value	Random effect (95% CI)	Egger's test p-value
Overall survival					
Breast*	1	3.364 (1.898–5.961)	>.99	3.364 (1.898–5.961)	-
Cervix	1	0.765 (0.321–1.823)	>.99	0.765 (0.321–1.823)	-
Colorectum*	3	2.354 (1.618–3.425)	.013	2.906 (1.244–6.786)	.286
Esophagus*	1	1.988 (1.009–3.916)	>.99	1.988 (1.009–3.916)	-
Gallbladder*	1	1.779 (1.071–2.955)	>.99	1.779 (1.071–2.955)	-
Head and neck*	1	1.759 (1.020–3.034)	>.99	1.759 (1.020–3.034)	-
Liver	2	1.652 (0.995–2.742)	.508	1.652 (0.995–2.742)	-
Lung*	4	1.731 (1.275–2.350)	.391	1.731 (1.275–2.350)	.648
Stomach	2	1.411 (0.985–2.022)	.431	1.411 (0.985–2.022)	-
Disease-free survival					
Breast*	2	5.182 (3.749–7.162)	.353	5.182 (3.749–7.162)	-
Colorectum*	4	2.599 (1.963–3.441)	.025	3.012 (1.763–5.146)	.178
Esophagus*	1	2.375 (1.177–4.791)	>.99	2.375 (1.177–4.791)	-
Head and neck*	1	0.396 (0.160–0.765)	>.99	0.396 (0.160–0.765)	-
Liver	1	1.394 (0.800–2.427)	>.99	1.394 (0.800–2.427)	-
Lung	1	1.014 (0.634–1.623)	>.99	1.014 (0.634–1.623)	-
Kidney	3	0.866 (0.589–1.274)	.056	1.072 (0.510–2.254)	.133
Stomach	1	0.838 (0.395–1.778)	>.99	0.838 (0.395–1.778)	-
Thyroid*	1	8.697 (3.120–24.241)	>.99	8.697 (3.120–24.241)	-

CI, confidence interval.

\* $p < .05$ .**Fig. 3.** Forest plot diagram for subgroup analysis based on cut-off value of low claudin-1 immunohistochemical expression. OS, overall survival; DFS, disease-free survival.

pattern of claudin-1 might vary in different organs. More studies are needed to clarify the potential gamut of functions.

In the present meta-analysis, low expression of claudin-1 IHC was significantly correlated with worse OS and DFS in human malignant tumors (HR, 1.851; 95% CI, 1.506 to 2.274 and HR, 2.028; 95% CI, 1.313 to 3.134, respectively). Unlike the results of most reports showing the correlation between low expression of claudin-1 IHC and a lower survival rate, inverse correlations or no correlations were found in stomach cancer, clear renal cell carcinoma, and lung adenocarcinoma. Among eligible studies with stomach cancers, Huang et al. reported that low claudin-1 expression was significantly correlated with better survival rate.<sup>17</sup>

The prognostic role of claudin-1 was different between intestinal and diffuse types of gastric cancer.<sup>10</sup> In addition, in meta-analysis for clear cell renal cell carcinoma, the estimated HR was 0.873 (95% CI, 0.385 to 1.981;  $p = .746$ ).<sup>14,27</sup> However, the estimated HR of papillary renal cell carcinoma was 1.972 (95% CI, 0.671 to 5.795), but there was no statistical significance ( $p = .217$ ). Although low claudin-1 IHC expression was significantly correlated with poor prognosis in lung cancer, significant correlation was found in adenocarcinoma, but not squamous cell carcinoma.<sup>12,13,21,31</sup> Cancers with an HR exceeding 1 in both OS and DFS were breast, colorectal, and esophageal cancers.

This meta-analysis included studies using IHC for the evaluation of claudin-1 expression. The rate of low claudin-1 IHC expression ranged from 15.8% to 84.9%, which varied according to specific tumor type. Various cut-off values (1%–50%) were used in eligible studies; therefore, the rates of low or high claudin-1 IHC expression could be largely affected by the cut-off value. Consequently, this discrepancy might affect the correlation between claudin-1 IHC expression and survival rate. In addition, discrepancies between investigators were possible concerning the rates of low claudin-1 IHC expression. Detailed evaluations, such as subgroup analysis based on median cut-off values, were required to elucidate the cause of the large difference between eligible studies. In OS, the HR of cases with low claudin-1 IHC expression was significantly higher in both cut-off subgroups (Fig. 3).

However, in the higher cut-off value subgroup, low claudin-1 IHC expression was not significantly correlated with worse DFS (HR, 1.492; 95% CI, 0.808 to 2.753). Our results suggest that a lower cut-off value might be more suitable for evaluation of low claudin-1 expression rather than a higher cut-off value. However, further studies based on specific tumor types will be needed to elucidate the effect of cut-off value on the correlation with survival.

There are a number of limitations in the current study. First, the study investigated the correlation between claudin-1 expression and prognosis in various malignant tumors. Although several studies have reported the prognostic roles of claudin-1, they were limited in their interpretive value because of the small number of studies for specific tumor types. Interestingly, in head and neck cancer, the prognostic roles of low claudin-1 IHC expression were different between OS and DFS.<sup>18,25</sup> The discrepancy between included studies could not be found due to the small number of studies. Second, the adequate antigenicity of included tissues in eligible studies could not be guaranteed due to the use of old specimens in some studies. Whether the low expression of claudin-1 reflected this problem could not be determined in the present study. Third, to avoid bias from follow-up periods, survival data were extracted at a 60-month follow-up. This follow-up period had no effect on the correlation between claudin-1 expression and survival in the present study, and the correlation between claudin-1 expression and survival could differ from those in previous reports.

In conclusion, low claudin-1 expression was significantly correlated with lower survival rates in various malignant tumors. Lower criteria for claudin-1 IHC expression could be suitable for prediction of a patient's prognosis. More detailed criteria for claudin-1 IHC expression in various malignant tumors is needed for application of claudin-1 IHC expression in daily practice.

## ORCID

Jung-Soo Pyo: <https://orcid.org/0000-0003-0320-8088>

Nae Yu Kim: <https://orcid.org/0000-0002-0461-6385>

Won Jin Cho: <https://orcid.org/0000-0001-9827-5173>

## Author Contributions

Conceptualization: JSP, NYK.

Data curation: JSP.

Formal analysis: JSP, NYK, WJC.

Funding acquisition: WJC.

Investigation: NYK.

Methodology: JSP, WJC.

Writing—original draft: JSP, NYK.

Writing—review & editing: JSP, WJC.

## Conflicts of Interest

The authors declare that they have no potential conflicts of interest.

## Acknowledgments

This study was supported by research funds from Chosun University Hospital, 2017.

## REFERENCES

1. Colegio OR, Van Itallie C, Rahner C, Anderson JM. Claudin extracellular domains determine paracellular charge selectivity and resistance but not tight junction fibril architecture. *Am J Physiol Cell Physiol* 2003; 284: C1346-54.
2. Miwa N, Furuse M, Tsukita S, Niikawa N, Nakamura Y, Furukawa Y. Involvement of claudin-1 in the beta-catenin/Tcf signaling pathway and its frequent upregulation in human colorectal cancers. *Oncol Res* 2001; 12: 469-76.
3. Bhat AA, Sharma A, Pope J, et al. Caudal homeobox protein Cdx-2 cooperates with Wnt pathway to regulate claudin-1 expression in colon cancer cells. *PLoS One* 2012; 7: e37174.
4. Tsukita S, Furuse M. The structure and function of claudins, cell adhesion molecules at tight junctions. *Ann N Y Acad Sci* 2000; 915: 129-35.
5. Günzel D, Fromm M. Claudins and other tight junction proteins. *Compr Physiol* 2012; 2: 1819-52.
6. Krug SM, Schulzke JD, Fromm M. Tight junction, selective permeability, and related diseases. *Semin Cell Dev Biol* 2014; 36: 166-76.
7. Koval M. Claudin heterogeneity and control of lung tight junctions. *Annu Rev Physiol* 2013; 75: 551-67.
8. Capaldo CT, Nusrat A. Claudin switching: physiological plasticity of the tight junction. *Semin Cell Dev Biol* 2015; 42: 22-9.
9. Huang J, Li J, Qu Y, et al. The expression of claudin 1 correlates with beta-catenin and is a prognostic factor of poor outcome in gastric cancer. *Int J Oncol* 2014; 44: 1293-301.
10. Suh Y, Yoon CH, Kim RK, et al. Claudin-1 induces epithelial-mesenchymal transition through activation of the c-Abl-ERK signaling pathway in human liver cells. *Oncogene* 2013; 32: 4873-82.
11. Bouchagier KA, Assimakopoulos SF, Karavias DD, et al. Expression of claudins-1, -4, -5, -7 and occludin in hepatocellular carcinoma and their relation with classic clinicopathological features and patients' survival. *In Vivo* 2014; 28: 315-26.
12. Chae MC, Park CK, Keum DY, Hwang I, Kwon KY, Jang BC. Prog-

- nostic significance of claudin 4 in completely resected adenocarcinoma of the lung. *Korean J Thorac Cardiovasc Surg* 2014; 47: 262-8.
13. Chao YC, Pan SH, Yang SC, et al. Claudin-1 is a metastasis suppressor and correlates with clinical outcome in lung adenocarcinoma. *Am J Respir Crit Care Med* 2009; 179: 123-33.
  14. Fritzsche FR, Oelrich B, Johannsen M, et al. Claudin-1 protein expression is a prognostic marker of patient survival in renal cell carcinomas. *Clin Cancer Res* 2008; 14: 7035-42.
  15. Higashi Y, Suzuki S, Sakaguchi T, et al. Loss of claudin-1 expression correlates with malignancy of hepatocellular carcinoma. *J Surg Res* 2007; 139: 68-76.
  16. Hoellen F, Waldmann A, Banz-Jansen C, et al. Claudin-1 expression in cervical cancer. *Mol Clin Oncol* 2017; 7: 880-4.
  17. Jung H, Jun KH, Jung JH, Chin HM, Park WB. The expression of claudin-1, claudin-2, claudin-3, and claudin-4 in gastric cancer tissue. *J Surg Res* 2011; 167: e185-91.
  18. Li WJ, Zhang ZL, Yu XM, Cai XL, Pan XL, Yang XY. Expression of claudin-1 and its relationship with lymphatic microvessel generation in hypopharyngeal squamous cell carcinoma. *Genet Mol Res* 2015; 14: 11814-26.
  19. Ma F, Ding X, Fan Y, et al. A CLDN1-negative phenotype predicts poor prognosis in triple-negative breast cancer. *PLoS One* 2014; 9: e112765.
  20. Matsuoka T, Mitomi H, Fukui N, et al. Cluster analysis of claudin-1 and -4, E-cadherin, and beta-catenin expression in colorectal cancers. *J Surg Oncol* 2011; 103: 674-86.
  21. Merikallio H, Kaarteenoaho R, Pääkkö P, et al. Impact of smoking on the expression of claudins in lung carcinoma. *Eur J Cancer* 2011; 47: 620-30.
  22. Miyamoto K, Kusumi T, Sato F, et al. Decreased expression of claudin-1 is correlated with recurrence status in esophageal squamous cell carcinoma. *Biomed Res* 2008; 29: 71-6.
  23. Morohashi S, Kusumi T, Sato F, et al. Decreased expression of claudin-1 correlates with recurrence status in breast cancer. *Int J Mol Med* 2007; 20: 139-43.
  24. Resnick MB, Konkin T, Routhier J, Sabo E, Pricolo VE. Claudin-1 is a strong prognostic indicator in stage II colonic cancer: a tissue microarray study. *Mod Pathol* 2005; 18: 511-8.
  25. Sappayatosok K, Phattaratartip E. Overexpression of claudin-1 is associated with advanced clinical stage and invasive pathologic characteristics of oral squamous cell carcinoma. *Head Neck Pathol* 2015; 9: 173-80.
  26. Shibutani M, Noda E, Maeda K, Nagahara H, Ohtani H, Hirakawa K. Low expression of claudin-1 and presence of poorly-differentiated tumor clusters correlate with poor prognosis in colorectal cancer. *Anticancer Res* 2013; 33: 3301-6.
  27. Shin HI, Kim BH, Chang HS, Kim CI, Jung HR, Park CH. Expression of claudin-1 and -7 in clear cell renal cell carcinoma and its clinical significance. *Korean J Urol* 2011; 52: 317-22.
  28. Tzelepi VN, Tsamandas AC, Vlotinou HD, Vagianos CE, Scopa CD. Tight junctions in thyroid carcinogenesis: diverse expression of claudin-1, claudin-4, claudin-7 and occludin in thyroid neoplasms. *Mod Pathol* 2008; 21: 22-30.
  29. Xiong L, Wen Y, Miao X, Yang Z. Expressions of cell junction regulatory proteins and their association with clinicopathologic parameters in benign and malignant gallbladder lesions. *Am J Med Sci* 2011; 342: 388-94.
  30. Yoshida T, Kinugasa T, Akagi Y, et al. Decreased expression of claudin-1 in rectal cancer: a factor for recurrence and poor prognosis. *Anticancer Res* 2011; 31: 2517-25.
  31. Zhang Z, Wang A, Sun B, Zhan Z, Chen K, Wang C. Expression of CLDN1 and CLDN10 in lung adenocarcinoma in situ and invasive lepidic predominant adenocarcinoma. *J Cardiothorac Surg* 2013; 8: 95.
  32. Parmar MK, Torri V, Stewart L. Extracting summary statistics to perform meta-analyses of the published literature for survival endpoints. *Stat Med* 1998; 17: 2815-34.
  33. Mineta K, Yamamoto Y, Yamazaki Y, et al. Predicted expansion of the claudin multigene family. *FEBS Lett* 2011; 585: 606-12.
  34. Singh AB, Sharma A, Dhawan P. Claudin-1 expression confers resistance to anoikis in colon cancer cells in a Src-dependent manner. *Carcinogenesis* 2012; 33: 2538-47.
  35. Kinugasa T, Akagi Y, Ochi T, et al. Increased claudin-1 protein expression in hepatic metastatic lesions of colorectal cancer. *Anticancer Res* 2012; 32: 2309-14.
  36. Chang TL, Ito K, Ko TK, et al. Claudin-1 has tumor suppressive activity and is a direct target of RUNX3 in gastric epithelial cells. *Gastroenterology* 2010; 138: 255-65.e1-3.

# Association between p53 Expression and Amount of Tumor-Infiltrating Lymphocytes in Triple-Negative Breast Cancer

Miseon Lee<sup>1\*</sup> · In Ah Park<sup>1\*</sup>  
Sun-Hee Heo<sup>1,2</sup> · Young-Ae Kim<sup>1,2</sup>  
Gyungyub Gong<sup>1</sup> · Hee Jin Lee<sup>1</sup>

<sup>1</sup>Department of Pathology, Asan Medical Center, University of Ulsan College of Medicine, Seoul; <sup>2</sup>Asan Center for Cancer Genome Discovery, Asan Institute for Life Sciences, Asan Medical Center, University of Ulsan College of Medicine, Seoul, Korea

Received: November 20, 2018  
Revised: February 7, 2019  
Accepted: February 8, 2019

## Corresponding Author

Hee Jin Lee, MD, PhD  
Department of Pathology, University of Ulsan College of Medicine, Asan Medical Center, 88 Olympic-ro 43-gil, Songpa-gu, Seoul 05505, Korea  
Tel: +82-2-3010-5889  
Fax: +82-2-472-7898  
E-mail: backkila@gmail.com

\*Miseon Lee and In Ah Park contributed equally to this article.

**Background:** Most triple-negative breast cancers (TNBCs) have a high histologic grade, are associated with high endoplasmic stress, and possess a high frequency of *TP53* mutations. *TP53* missense mutations lead to the production of mutant p53 protein and usually show high levels of p53 protein expression. Tumor-infiltrating lymphocytes (TILs) accumulate as part of the anti-tumor immune response and have a strong prognostic and predictive significance in TNBC. We aimed to elucidate the association between p53 expression and the amount of TILs in TNBC. **Methods:** In 678 TNBC patients, we evaluated TIL levels and expression of endoplasmic stress molecules. Immunohistochemical examination of p53 protein expression was categorized into three groups: no, low, and high expression. **Results:** No, low, and high p53 expression was identified in 44.1% (n=299), 20.1% (n=136), and 35.8% (n=243) of patients, respectively. Patients with high p53 expression showed high histologic grade (p<.001), high TIL levels (p=.009), and high expression of endoplasmic reticulum stress-associated molecules (p-eIF2a, p=.013; XBP1, p=.007), compared to patients with low p53 expression. There was no significant difference in disease-free (p=.406) or overall survival rates (p=.444) among the three p53 expression groups. **Conclusions:** High p53 expression is associated with increased expression of endoplasmic reticulum stress molecules and TIL influx.

**Key Words:** p53; Breast neoplasms; Lymphocytes, Tumor-infiltrating

Triple-negative breast cancer (TNBC) is a molecular subtype of breast cancer that lacks expression of estrogen and progesterone receptors and does not show overexpression of human epidermal growth factor 2. This profile has no targeted therapy or standard biomarkers, and its aggressive phenotype, lower overall survival, and shorter relapse-free intervals than other breast cancer subtypes make its clinical management a challenge.<sup>1,2</sup> Different biomarkers for TNBC as prognostic or predictive indicators and possible targets for novel therapy have been studied.<sup>2,3</sup> Insight into the connection between the immune system and breast cancer may improve treatments and outcomes.

We previously demonstrated that TNBC tumors characteristically possess more tumor-infiltrating lymphocytes (TILs) than other breast cancer subtypes and TILs are positively correlated with endoplasmic reticulum stress-associated molecules.<sup>4-8</sup> The endoplasmic reticulum is responsible for protein folding in cells.<sup>9,10</sup>

In tumor environments, the combination of high cancer cell proliferation rates, nutrient deficiency, and hypoxia lead to accumulation of unfolded or misfolded proteins in the endoplasmic reticulum that induce endoplasmic reticulum stress. Tumor cells activate the unfolded protein response and various downstream endoplasmic reticulum stress signaling pathways to adapt to this environment.<sup>9,10</sup> Recent studies show that endoplasmic reticulum stress-associated molecules play important roles in tumorigenicity in TNBC.<sup>9</sup>

The *TP53* gene is a tumor suppressor gene that regulates the cell cycle, cell proliferation, DNA repair, cellular senescence, and death by apoptosis.<sup>11</sup> Cells with somatic *TP53* mutations can avoid apoptosis and progress to malignant tumor cells. Tumors with *TP53* mutations are highly invasive, poorly differentiated, and have a high histologic grade, showing poor response to chemotherapy.<sup>2,12</sup> In solid cancers, mutations affecting the protein-

encoding reading frame, often referred to as null mutations, result in p53 protein absence.<sup>11</sup> On the contrary, *TP53* missense mutations may lead to the production of a mutant p53 protein, which has a prolonged half-life relative to the normal isoform that leads to its accumulation in tumor cells and makes it readily detectable by immunohistochemistry.<sup>11,13-15</sup> Mutant p53 proteins not only lose the tumor suppressor function of wild-type p53 but also acquire new functions not present in the wild-type protein, termed gain-of-function properties, that promote tumorigenesis. So far, mutant p53 gain-of-function properties have been shown to stimulate tumor cell proliferation, migration, invasion, survival, chemoresistance, cancer metabolism, and tissue architecture disruption.<sup>16</sup>

Both types of mutations (null and missense) have been observed in the same cancer type.<sup>11</sup> *TP53* mutations are seen in 18%–25% of primary breast cancers<sup>2,17</sup> and in approximately 80% of TNBCs, which is markedly more frequent than in other breast cancer subtypes.<sup>2,18,19</sup> Mutations in *TP53* are predominantly missense mutations, producing mutant p53 proteins. Furthermore, as the mutant protein in malignant cells is less susceptible to degradation than wild-type p53, its accumulation establishes the *TP53* mutation as an attractive therapeutic target for TNBC.<sup>20,21</sup>

Considering that TNBC is highly correlated with TIL levels, endoplasmic reticulum stress-associated molecules, and *TP53* mutation rate, we examined the correlations among TIL levels, endoplasmic reticulum stress-associated molecules, and expression of p53 in TNBC.

## MATERIALS AND METHODS

### Patients and tissue specimens

A total of 678 TNBC patients who underwent surgery for primary breast cancer between 2004 and 2010 at Asan Medical Center in Seoul, Korea were retrospectively selected. In this group, 470 patients did not present with lymph node metastasis, and they received four cycles of adjuvant anthracycline (60 mg/m<sup>2</sup> adriamycin) and cyclophosphamide (600 mg/m<sup>2</sup>). The remaining 208 patients presented with lymph node metastases and were treated with four cycles of adriamycin, followed by either four cycles of paclitaxel (175 mg/m<sup>2</sup>) or four cycles of docetaxel (75 mg/m<sup>2</sup>). In total, 548 patients (80.8%) received radiotherapy. The median follow-up period was 78.3 months. Clinicopathologic information and survival data were obtained from medical records and surgical pathology reports. Exemption from informed consent after de-identification of information was approved by the Institutional Review Board of Asan Medical Center (2013-0866).

### Histological evaluation

Two pathologists (H.J.L. and G.G.) reviewed whole sections of the hematoxylin and eosin-stained slides for histologic grade, pT category, pN category, and necrosis in the invasive area. Additionally, the levels of stromal TILs were evaluated, using full sections in 10% increments (defined as the mean percentage of plasma cells and lymphocytes in stroma of invasive carcinoma; if < 10% area, then 0, 1, or 5% level criteria were used).<sup>22</sup>

### Tissue microarray construction and immunohistochemical evaluation

Available formalin-fixed paraffin-embedded blocks of 678 cases were arrayed with a tissue-arraying instrument, as previously described.<sup>8</sup> Tissue microarray sections were stained with an automatic immunohistochemical staining device (Benchmark XT, Ventana Medical Systems, Tucson, AZ, USA). Antibodies to target phospho-eukaryotic initiation factor 2a (p-eIF2a), protein kinase RNA-like endoplasmic reticulum kinase (PERK), X-box binding protein-1 (XBP1), and CD8 were used, and their expressions in the tumor cells were determined, as previously described.<sup>8,23</sup> An additional antibody to target p53 (1:1,500, Dako, Glostrup, Denmark) was also used. The level of p53 expression was ranked on a 4-point intensity scale (0, none; 1, mild; 2, moderate; and 3, intense). The percentage of nuclear expression of the p53 was also measured. An “immunoreactive score” was generated as the product of the intensity and the percentage of positive cells.

### Statistical analysis

All statistical analyses were performed using SPSS statistical software ver. 18.0 (SPSS, Chicago, IL, USA). The chi-squared test, linear-by-linear association test, Spearman’s correlation, Mann-Whitney U test, and log-rank test were used to evaluate the data. All tests were two-sided and statistical significance was set at  $p < .05$ .

## RESULTS

### Clinicopathologic characteristics of the study population

All 678 patients were female, and their median age was 47 years at diagnosis (range, 23 to 76 years). Histologic grades 1 and 2 occurred in 160 cases (23.6%), and grade 3 in 518 cases (76.4%). There were 299 pT1 tumors (44.1%), 353 pT2 tumors (52.1%), 25 pT3 tumors (3.7%), and one pT4 tumor (0.1%). Most ( $n = 470$ ) of the patients did not have pathologic lymph node metastasis (pN0, 69.3%) while 120 tumors (17.7%) were

pN1, 46 tumors (6.8%) were pN2, and 42 tumors (6.2%) were pN3. The tumors were categorized into four groups based on TIL amounts: < 10% TILs (164 patients, 24.2%), ≥ 10%; < 30% TILs (154 patients, 22.7%); ≥ 30%; and < 60% TILs (148 patients, 21.8%), ≥ 60% TILs (212 patients, 31.3%). Necrosis in the invasive area was identified in 488 of the patients (72.0%).

**Classifying p53 expression as none, low, or high**

Immunohistochemical analysis of p53 expression was scored as follows (Fig. 1): 0, no expression (299 cases, 44.1%); > 0 to 240, low expression (136 cases, 20.1%); and > 240 to 300, high expression (243 cases, 35.8%).

**Characteristics of tumors according to p53 expression**

Compared to the low p53 expression group, the high p53 expression group was significantly associated with higher histologic grade ( $p < .001$ ), higher TIL levels ( $p = .009$ ), increased presence of necrosis in the invasive area ( $p = .010$ ), and higher expression

of two endoplasmic reticulum stress-associated molecules (p-eIF2a,  $p = .013$  and XBP1,  $p = .007$ ) (Table 1, Fig. 2). Compared to the no p53 expression group, the high p53 expression

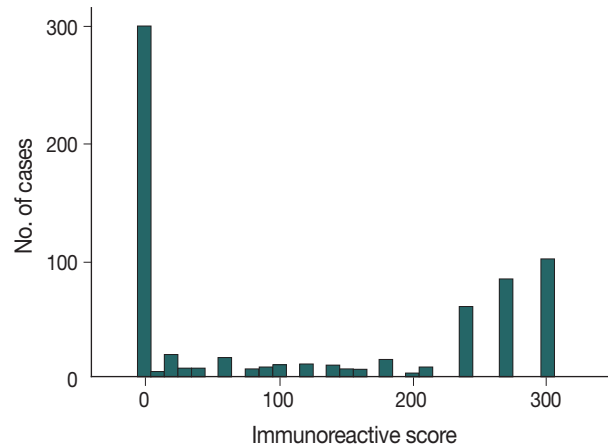


**Fig. 1.** Distribution of triple-negative breast cancer patients by immunoreactive scores for p53 expression.

**Table 1.** Comparison of clinicopathologic variables according to p53 expression level

Parameter	p53 expression level			p-value		
	Low (%)	No (%)	High (%)	Low vs no	Low vs high	No vs high
Histologic grade						
1 and 2	48 (35.3)	70 (23.4)	42 (17.3)	.011	< .001	.088
3	88 (64.7)	229 (76.6)	201 (82.7)			
pT category				.103	.430	.408
1	70 (51.4)	121 (40.5)	108 (44.5)			
2	61 (44.9)	168 (56.2)	124 (51.0)			
3	5 (3.7)	9 (3.0)	11 (4.5)			
4	0	1 (0.3)	0			
pN category				.510	.636	.161
0	95 (69.9)	199 (66.6)	176 (72.4)			
1-3	41 (30.1)	100 (33.4)	67 (27.6)			
TIL				.524	.009	.032
< 10%	39 (28.7)	72 (24.1)	53 (21.8)			
≥ 10% and < 30%	33 (24.3)	77 (25.8)	44 (18.1)			
≥ 30% and < 60%	33 (24.3)	65 (21.7)	50 (20.6)			
≥ 60%	31 (22.7)	85 (28.4)	96 (39.5)			
Necrosis in the invasive area				.579	.010	.015
Negative	46 (33.8)	92 (30.8)	52 (21.4)			
Positive	90 (66.2)	207 (69.2)	191 (78.6)			
p-eIF2a				.174	.013	.191
Low	79 (59.0)	151 (51.4)	108 (45.4)			
High	55 (41.0)	143 (48.6)	130 (54.6)			
PERK				.300	.740	.487
Low	77 (57.0)	153 (51.5)	132 (54.8)			
High	58 (43.0)	144 (48.5)	109 (45.2)			
XBP1				.137	.007	.088
Low	86 (64.7)	167 (56.6)	119 (50.0)			
High	47 (35.3)	128 (43.4)	119 (50.0)			

TIL, tumor-infiltrating lymphocyte.

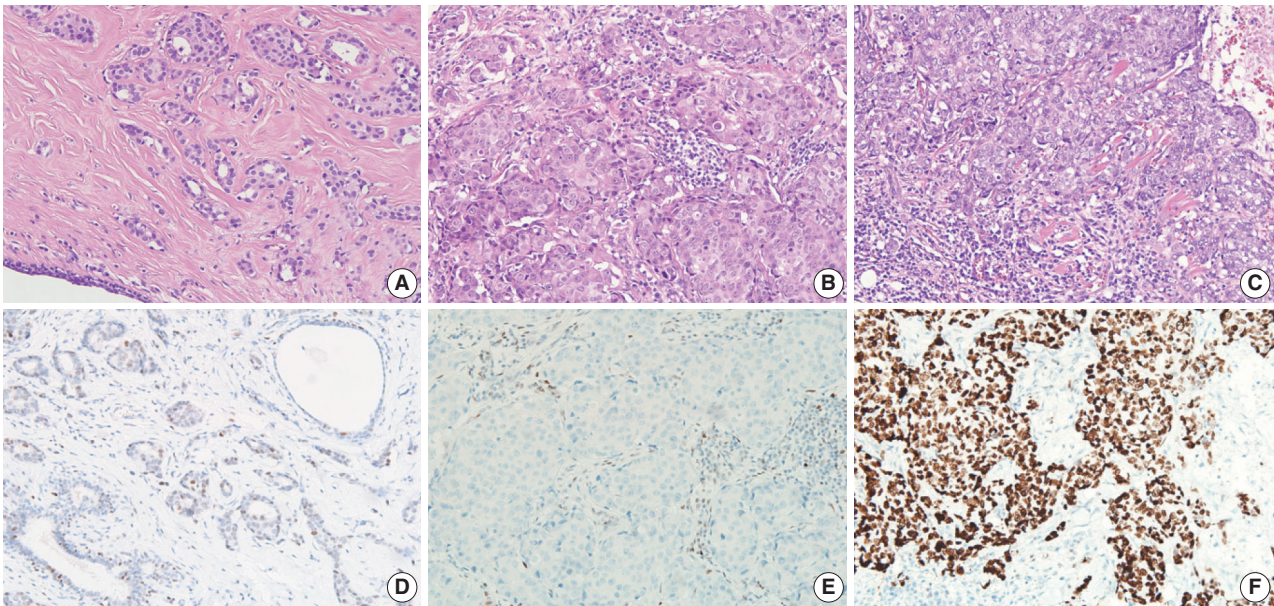


**Fig. 2.** Histologic features and p53 expression in triple-negative breast cancer tumors. A tumor with low histologic grade shows sparse tumor-infiltrating lymphocytes (TILs) and low p53 expression (A, D). Tumors with high histologic grade show abundant TILs and no p53 expression (B, E) or high p53 expression (C, F).

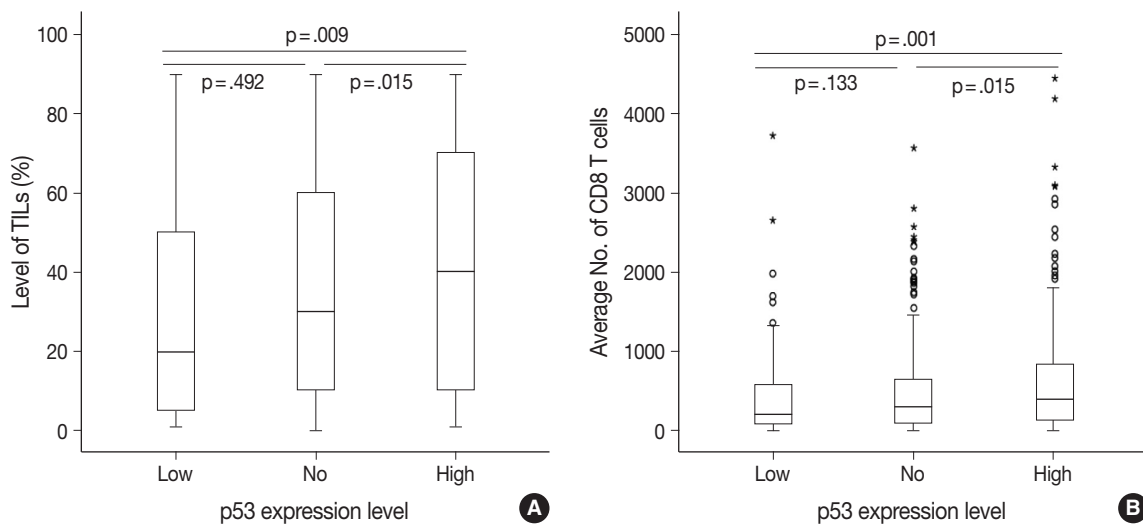


**Fig. 3.** Differences in the level of tumor-infiltrating lymphocytes (TILs) (A) and the average number of CD8<sup>+</sup> T cells (B) among the three groups of triple-negative breast cancer patients categorized by p53 expression level.

group was significantly associated with higher TIL levels ( $p = .032$ ). Compared to the low p53 expression group, the no p53 expression group was significantly associated with higher histologic grade ( $p = .011$ ). The TIL levels of the no p53 expression group did not show significant differences from the TIL levels of the low p53 expression group ( $p = .524$ ).

There were differences in the amounts of TILs (Fig. 3A) and the average number of CD8<sup>+</sup> T cells (Fig. 3B) among the three groups of TNBC patients classified according to p53 expression

level. The high p53 expression group had significantly higher amounts of TILs ( $p = .009$  and  $p = .015$ ) and more CD8<sup>+</sup> T cells ( $p = .001$  and  $p = .015$ ) than the low and no expression groups, respectively. However, there was no significant difference between the no and low p53 expression groups in the amounts of stromal TILs ( $p = .492$ ) and the number of CD8<sup>+</sup> T cells ( $p = .133$ ).

### Association between high histologic grade and endoplasmic reticulum stress-associated molecules

Since tumors with high histologic grades have an increased proliferation rate, which induces endoplasmic reticulum stress, we also analyzed the relationship between histologic grade and expression of endoplasmic reticulum stress-associated molecules. High histologic grade was significantly associated with two out of three endoplasmic reticulum stress-associated molecules (p-eIF2a,  $p = .036$  and XBP1,  $p < .001$ , but not PERK,  $p = .928$ ) (Table 2).

### Prognostic significance of p53 expression in TNBC

Univariate analysis was undertaken to elucidate the prognostic significance of p53 expression. There was no significant difference in disease-free ( $p = .406$ ) or overall survival rates ( $p = .444$ ) among the three groups of no, low, and high p53 expression (Fig. 4).

**Table 2.** Comparison of pathologic variables according to histologic grade

Parameter	Histologic grade		p-value
	1 and 2	3	
p-eIF2a			.036
Low	92 (58.2)	246 (48.4)	
High	66 (41.8)	262 (51.6)	
PERK			.928
Low	85 (53.5)	277 (76.5)	
High	74 (46.5)	237 (46.1)	
XBP1			<.001
Low	109 (69.4)	263 (51.7)	
High	48 (30.6)	246 (48.3)	

Values are presented as number (%).

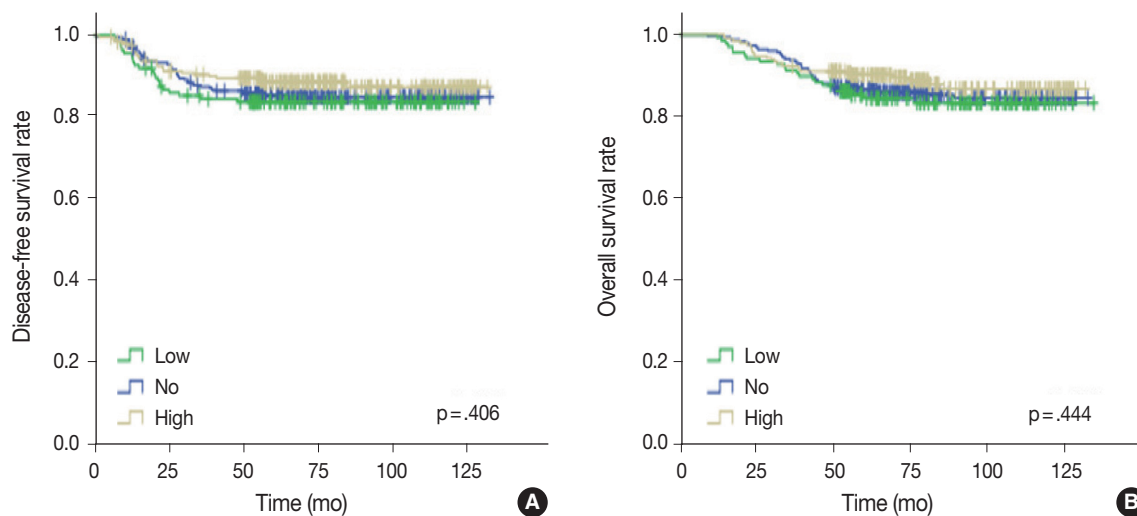


**Fig. 4.** (A, B) Kaplan-Meier survival analyses of triple-negative breast cancer patients categorized by p53 expression levels.

### Prognostic significance of TILs among groups based on p53 expression in TNBC

Since the level of TILs in TNBC patients has been recognized as a significant prognostic factor,<sup>24</sup> the effect of TILs in each p53 expression group was examined. In the high p53 expression group, the higher the TIL level, the better the disease-free ( $p = .006$ ) and overall survival rates ( $p = .005$ ) (Fig. 5). Disease-free ( $p = .001$ ) and overall survival curves ( $p = .001$ ) were more significantly separated when the TILs were divided by 10%. In the no p53 expression group, the higher the TIL level, the higher the disease-free ( $p = .044$ ) and overall survival rates ( $p = .046$ ). Conversely, in the low p53 expression group, disease-free ( $p = .092$ ) and overall survival rates ( $p = .108$ ) were not significantly different, according to the TIL levels.

## DISCUSSION

Our previous studies demonstrated that TILs are highly associated with interferon- and endoplasmic reticulum stress-associated molecules.<sup>5,8,25</sup> Based on these results, we hypothesized that high p53 expression, which is linked with a high histologic grade (frequent mitosis, large cell and nuclear size, and poor differentiation), might induce endoplasmic reticulum stress and subsequent interferon signaling pathway activation, as well as the influx of TILs. Moreover, high p53 expression, which is related to necrosis, might induce the release of damage-associated molecules, an immune response, and the influx of TILs. The present research analyzed the clinical and pathological significance of p53 expression in TNBC. In comparison to low p53 expression, high p53 expression was shown to be associated with high his-

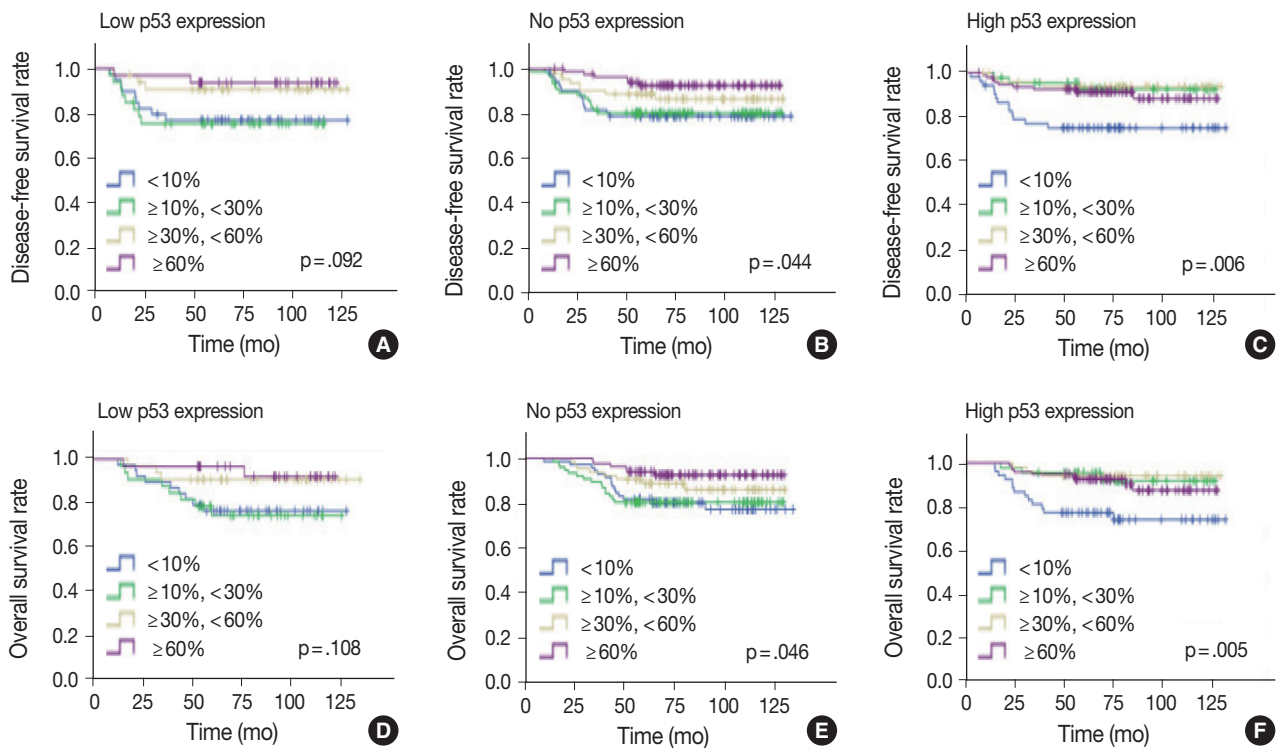


**Fig. 5.** Kaplan-Meier survival analyses of triple-negative breast cancer patients according to tumor-infiltrating lymphocytes levels in low (A, D), no (B, E), and high (C, F) p53 expression groups.

tologic grade, necrosis in the invasive area, and more TILs, supporting the study hypothesis.

Darb-Esfahani et al.<sup>26</sup> revealed a significant association between p53 protein expression characterized by immunohistochemical staining intensity (“wild-type pattern”, tumor cell nuclei stained as variable and weak intensity; “overexpression”,  $\geq 60\%$  of tumor cell nuclei stained as uniformly strong or moderate intensity; “loss,” tumor cell nuclei stained completely negative) and the *TP53* mutation, with 80% of the p53 overexpression group possessing the missense mutation. Also, in TNBC, missense *TP53* mutations were significantly linked with higher levels of stromal TILs ( $p = .028$ ) and *CD8A* gene expression ( $p = .020$ ), and tended to be associated with a better survival ( $p = .093$ ) compared to all other types of mutations.<sup>26</sup>

TNBC has a higher TIL level than other breast cancer subtypes. However, the level of TIL varies within TNBC. *TP53* mutations occur more frequently in TNBC (80%) than other breast cancer subtypes.<sup>2,10</sup> Of the *TP53* mutations, missense mutations produce a new mutant protein that can be presented on the cell surface via major histocompatibility complex (neoantigen), triggering the immune system and leading to a TIL response. This hypothesis is supported by our finding that the TIL levels of p53 overexpression group (probably due to missense muta-

tion) were significantly higher than the TIL levels in the p53 low expression group (wild-type *TP53*) ( $p = .009$ ). In contrast, null mutations of the *TP53* gene simply do not produce normal levels of p53 protein, and the p53 function is lost. Since it does not make a new mutant protein to act as a neoantigen, it does not trigger the immune response, resulting in unchanged TIL levels. This hypothesis is supported by our finding that the no p53 expression group (probably due to null mutation) did not show a significant difference in TIL levels compared to those of the low p53 expression group ( $p = .524$ ), while TIL levels in the no p53 expression group showed a significant difference compared to TIL levels in the high p53 expression group ( $p = .032$ ). Although TNBC has a high mutation burden and other gene mutations can enhance immunogenicity, our findings suggest an important role of *TP53* mutation in the immunogenicity of TNBC.

In TNBC patients, a high TIL level is associated with good prognosis.<sup>24</sup> In our study, p53 overexpression was related to TIL levels, but not with prognosis. Although there have been many attempts to correlate *TP53* mutation status and clinical outcomes, such as overall survival rates in TNBC patients, conflicting findings have often emerged, with either poor survival in TNBC patients with *TP53* mutation<sup>27-30</sup> or no significance.<sup>31,32</sup> This is

probably due to the beneficial effects of mutant p53 gain-of-function for tumorigenesis that offsets the favorable prognostic impacts of high TIL levels.

Mutant p53 proteins have been regarded as attractive targets for cancer therapy. Most of the strategies developed to target mutant p53 proteins involve restoration to wild-type p53 activity and depletion of the mutant p53 protein. Small molecules, such as 2,2-bis(hydroxymethyl)-quinuclidin-3-one or zinc metallo-chaperone-1, are representative restoration methods to wild-type p53 activity. Among exemplary methods for depletion of the mutant p53 protein, geldanamycin, 17AAG, and ganetespib are inhibitors of heat shock protein 90, which, in turn, inhibits the degradation of mutant p53 protein mediated by carboxyl terminus of heat shock cognate protein 70-interacting protein and murine double minute 2 (MDM2).<sup>16,33</sup>

In the current study, overall and disease-free survival rates were much better when the level of TILs was  $\geq 10\%$  compared with  $< 10\%$  in the high p53 expression group, suggesting that the *TP53* missense mutation is associated with TIL influx and some TILs can recognize mutant p53. Therefore, in the high p53 expression groups with TIL levels  $< 10\%$ , the identification of T cells with T cell receptors (TCRs) reactive to mutant p53 and development of engineered T cell adoptive immunotherapy targeting mutant p53 may lead to successful immunotherapy. For instance, Lheureux et al.<sup>33</sup> found immunogenic *TP53* “hotspot” mutations as well as T cells with mutant p53-reactive TCRs in seven ovarian cancer patients. Therefore, in TNBCs with *TP53* mutations, genetic transfer of the *TP53* mutation-specific TCRs into autologous lymphocytes could be used to generate cells for use in cancer adoptive cell transfer immunotherapy.

The present study demonstrated close associations between the expression of p53 and the molecules associated with endoplasmic reticulum stress and TIL influx. Further studies targeting mutant p53 could facilitate the development of efficient immunotherapeutic agents.

## ORCID

Miseon Lee: <https://orcid.org/0000-0002-6385-7621>

In Ah Park: <https://orcid.org/0000-0002-9542-9461>

Sun-Hee Heo: <https://orcid.org/0000-0002-3043-4139>

Young-Ae Kim: <https://orcid.org/0000-0002-5454-7816>

Gyungyub Gong: <https://orcid.org/0000-0001-5743-0712>

Hee Jin Lee: <https://orcid.org/0000-0002-4963-6603>

## Author Contributions

Conceptualization: HJL.

Data curation: IAP, ML, HJL.

Formal analysis: IAP, ML.

Funding acquisition: IAP, GG, HJL.

Investigation: HJL.

Methodology: HJL.

Project administration: ML.

Resources: GG, HJL.

Supervision: HJL.

Validation: HJL.

Visualization: IAP, ML.

Writing—original draft: IAP, ML.

Writing—review & editing: SHH, YAK, GG, HJL.

## Conflicts of Interest

The authors declare that they have no potential conflicts of interest.

## Acknowledgments

This study was funded by the Basic Science Research Program through the National Research Foundation of Korea (NRF) supported by the Ministry of Science, ICT & Future Planning (grant number 2017R1D1A1B03035491).

## REFERENCES

1. Yamashita N, Kondo M, Zhao S, et al. Picrasidine G decreases viability of MDA-MB 468 EGFR-overexpressing triple-negative breast cancer cells through inhibition of EGFR/STAT3 signaling pathway. *Bioorg Med Chem Lett* 2017; 27: 2608-12.
2. Yadav BS, Chanana P, Jhamb S. Biomarkers in triple negative breast cancer: a review. *World J Clin Oncol* 2015; 6: 252-63.
3. van Rooijen JM, Stutvoet TS, Schroder CP, de Vries EG. Immunotherapeutic options on the horizon in breast cancer treatment. *Pharmacol Ther* 2015; 156: 90-101.
4. Kim JY, Heo SH, Song IH, et al. Activation of the PERK-eIF2alpha pathway is associated with tumor-infiltrating lymphocytes in HER2-positive breast cancer. *Anticancer Res* 2016; 36: 2705-11.
5. Kim YA, Lee HJ, Heo SH, et al. MxA expression is associated with tumor-infiltrating lymphocytes and is a prognostic factor in triple-negative breast cancer. *Breast Cancer Res Treat* 2016; 156: 597-606.
6. Lee HJ, Park IA, Song IH, et al. Tertiary lymphoid structures: prognostic significance and relationship with tumour-infiltrating lymphocytes in triple-negative breast cancer. *J Clin Pathol* 2016; 69: 422-30.

7. Lee HJ, Song IH, Park IA, et al. Differential expression of major histocompatibility complex class I in subtypes of breast cancer is associated with estrogen receptor and interferon signaling. *Oncotarget* 2016; 7: 30119-32.
8. Park IA, Heo SH, Song IH, et al. Endoplasmic reticulum stress induces secretion of high-mobility group proteins and is associated with tumor-infiltrating lymphocytes in triple-negative breast cancer. *Oncotarget* 2016; 7: 59957-64.
9. Chen X, Iliopoulos D, Zhang Q, et al. XBP1 promotes triple-negative breast cancer by controlling the HIF1alpha pathway. *Nature* 2014; 508: 103-7.
10. Han CC, Wan FS. New insights into the role of endoplasmic reticulum stress in breast cancer metastasis. *J Breast Cancer* 2018; 21: 354-62.
11. Oros Klein K, Oualkacha K, Lafond MH, Bhatnagar S, Tonin PN, Greenwood CM. Gene coexpression analyses differentiate networks associated with diverse cancers harboring *TP53* missense or null mutations. *Front Genet* 2016; 7: 137.
12. Kandioler-Eckersberger D, Ludwig C, Rudas M, et al. *TP53* mutation and p53 overexpression for prediction of response to neoadjuvant treatment in breast cancer patients. *Clin Cancer Res* 2000; 6: 50-6.
13. Brosh R, Rotter V. When mutants gain new powers: news from the mutant p53 field. *Nat Rev Cancer* 2009; 9: 701-13.
14. Freed-Pastor WA, Prives C. Mutant p53: one name, many proteins. *Genes Dev* 2012; 26: 1268-86.
15. Muller PA, Vousden KH. p53 mutations in cancer. *Nat Cell Biol* 2013; 15: 2-8.
16. Yue X, Zhao Y, Xu Y, Zheng M, Feng Z, Hu W. Mutant p53 in cancer: accumulation, gain-of-function, and therapy. *J Mol Biol* 2017; 429: 1595-606.
17. Alsner J, Yilmaz M, Guldborg P, Hansen LL, Overgaard J. Heterogeneity in the clinical phenotype of *TP53* mutations in breast cancer patients. *Clin Cancer Res* 2000; 6: 3923-31.
18. Jin MS, Park IA, Kim JY, et al. New insight on the biological role of p53 protein as a tumor suppressor: re-evaluation of its clinical significance in triple-negative breast cancer. *Tumour Biol* 2016; 37: 11017-24.
19. Cancer Genome Atlas Network. Comprehensive molecular portraits of human breast tumours. *Nature* 2012; 490: 61-70.
20. Duffy MJ, Synnott NC, McGowan PM, Crown J, O'Connor D, Gallagher WM. p53 as a target for the treatment of cancer. *Cancer Treat Rev* 2014; 40: 1153-60.
21. Duffy MJ, Synnott NC, Crown J. Mutant p53 as a target for cancer treatment. *Eur J Cancer* 2017; 83: 258-65.
22. Kojima YA, Wang X, Sun H, Compton F, Covinsky M, Zhang S. Reproducible evaluation of tumor-infiltrating lymphocytes (TILs) using the recommendations of International TILs Working Group 2014. *Ann Diagn Pathol* 2018; 35: 77-9.
23. Park IA, Hwang SH, Song IH, et al. Expression of the MHC class II in triple-negative breast cancer is associated with tumor-infiltrating lymphocytes and interferon signaling. *PLoS One* 2017; 12: e0182786.
24. Adams S, Goldstein LJ, Sparano JA, Demaria S, Badve SS. Tumor infiltrating lymphocytes (TILs) improve prognosis in patients with triple negative breast cancer (TNBC). *Oncoimmunology* 2015; 4: e985930.
25. Lee HJ, Kim A, Song IH, et al. Cytoplasmic expression of high mobility group B1 (HMGB1) is associated with tumor-infiltrating lymphocytes (TILs) in breast cancer. *Pathol Int* 2016; 66: 202-9.
26. Darb-Esfahani S, Denkert C, Stenzinger A, et al. Role of *TP53* mutations in triple negative and HER2-positive breast cancer treated with neoadjuvant anthracycline/taxane-based chemotherapy. *Oncotarget* 2016; 7: 67686-98.
27. Maeda T, Nakanishi Y, Hirotani Y, et al. Immunohistochemical co-expression status of cytokeratin 5/6, androgen receptor, and p53 as prognostic factors of adjuvant chemotherapy for triple negative breast cancer. *Med Mol Morphol* 2016; 49: 11-21.
28. Wu M, Wei W, Xiao X, et al. Expression of SIRT1 is associated with lymph node metastasis and poor prognosis in both operable triple-negative and non-triple-negative breast cancer. *Med Oncol* 2012; 29: 3240-9.
29. Zhang J, Wang Y, Yin Q, Zhang W, Zhang T, Niu Y. An associated classification of triple negative breast cancer: the risk of relapse and the response to chemotherapy. *Int J Clin Exp Pathol* 2013; 6: 1380-91.
30. Biganzoli E, Coradini D, Ambrogio F, et al. p53 status identifies two subgroups of triple-negative breast cancers with distinct biological features. *Jpn J Clin Oncol* 2011; 41: 172-9.
31. Kashiwagi S, Yashiro M, Takashima T, et al. Advantages of adjuvant chemotherapy for patients with triple-negative breast cancer at Stage II: usefulness of prognostic markers E-cadherin and Ki67. *Breast Cancer Res* 2011; 13: R122.
32. Wang J, Zhang C, Chen K, et al. ERbeta1 inversely correlates with PTEN/PI3K/AKT pathway and predicts a favorable prognosis in triple-negative breast cancer. *Breast Cancer Res Treat* 2015; 152: 255-69.
33. Lheureux S, Denoyelle C, Ohashi PS, De Bono JS, Mottaghy FM. Molecularly targeted therapies in cancer: a guide for the nuclear medicine physician. *Eur J Nucl Med Mol Imaging* 2017; 44(Suppl 1): 41-54.

# A Rare Case of Adenosquamous Carcinoma Arising in the Background of IgG4-Related Lung Disease

Sangjoon Choi · Sujin Park  
Man Pyo Chung<sup>1</sup> · Tae Sung Kim<sup>2</sup>  
Jong Ho Cho<sup>3</sup> · Joungho Han

Departments of Pathology and Translational Genomics, <sup>1</sup>Internal Medicine, <sup>2</sup>Radiology, and <sup>3</sup>Thoracic and Cardiovascular Surgery, Samsung Medical Center, Sungkyunkwan University School of Medicine, Seoul, Korea

Received: December 3, 2018  
Revised: January 26, 2019  
Accepted: February 20, 2019

## Corresponding Author

Joungho Han, MD  
Department and of Pathology and Translational Genomics, Samsung Medical Center, Sungkyunkwan University School of Medicine, 81 Irwon-ro, Gangnam-gu, Seoul 06351, Korea  
Tel: +82-2-3410-2800  
Fax: +82-2-3410-0025  
E-mail: hanjho@skku.edu

IgG4-related disease is a systemic inflammatory disease and is known as IgG4-related lung disease (IgG4-RLD) when it involves the respiratory system. Primary lung cancer arising from a background of IgG4-RLD is very rare. Herein, we report a case of adenosquamous carcinoma arising from the background of IgG4-RLD and presenting as an interstitial lung disease pattern. A 66-year-old man underwent lobectomy under the impression of primary lung cancer. Grossly, the mass was ill-defined and gray-tan colored, and the background lung was fibrotic. Microscopically, tumor cells showed both squamous and glandular differentiation. Dense lymphoplasmacytic infiltration with fibrosis and obliterative phlebitis were seen in the background lung. IgG4 immunohistochemical stain showed diffuse positivity in infiltrating plasma cells. Primary lung adenosquamous carcinoma has not been reported in a background of IgG4-RLD. Due to the rarity of IgG4-RLD, physicians must follow patients with IgG4-RLD over long periods of time to accurately predict the risk of lung cancer.

**Key Words:** Lung; Neoplasm; IgG4-related disease; Autoimmune

IgG4-related disease (IgG4-RD) is a rare, chronic, systemic inflammatory disease with increased serum IgG4 levels that is characterized by dense lymphoplasmacytic infiltration, storiform fibrosis, and obliterative phlebitis with IgG4 immunoreactivity in plasma cells.<sup>1</sup> When IgG4-RD involves the lung, it is called IgG4-related lung disease (IgG4-RLD) and manifests in various histologic forms, such as solid nodular type, bronchovascular type, or interstitial lung disease type.<sup>2-4</sup> The association of lung cancer with IgG4-RLD remains unclear, and only a small number of adenocarcinoma-associated cases have been reported.<sup>4-6</sup> Herein, for the first time, we report a case of adenosquamous carcinoma in a 66-year-old male patient who was followed-up for IgG4-related cholangitis.

## CASE REPORT

A 66-year-old man who had a past medical history of idiopathic pulmonary fibrosis (IPF) and mass-forming IgG4-related autoimmune cholangitis was admitted to the hospital for a

newly-identified consolidative lung mass discovered during follow-up. Chest computed tomography revealed a subpleural nodule in the left lower lobe of the lung in a background of reticular and honeycomb fibrosis (Fig. 1A). <sup>18</sup>F-fluorodeoxyglucose uptake was detected in the subpleural nodule (Fig. 1B). The results of the pulmonary function tests were within normal range: forced vital capacity (FVC) 3.23 L (82% of the predicted value), forced expiratory volume in 1 second (FEV<sub>1</sub>) 2.35 L (80% of the predicted value), and FEV<sub>1</sub>/FVC 73%. Laboratory test showed an increased serum IgG4 level (232.4 mg/dL). The patient underwent lobectomy under the impression of lung cancer. Grossly, the tumor was ill-defined, gray-tan colored and measured 3.5 × 3.2 × 2.0 cm. The background lung was fibrotic and emphysematous (Fig. 1C). Microscopically, the background lung showed diffuse irregular interstitial fibrosis with dense lymphoplasmacytic infiltration and occasional obliterative phlebitis (Fig. 1D-F). Tumor cells showed both squamous and glandular differentiation. The squamous cell carcinoma component was composed of moderately to poorly differentiated tumor cells that contained keratin

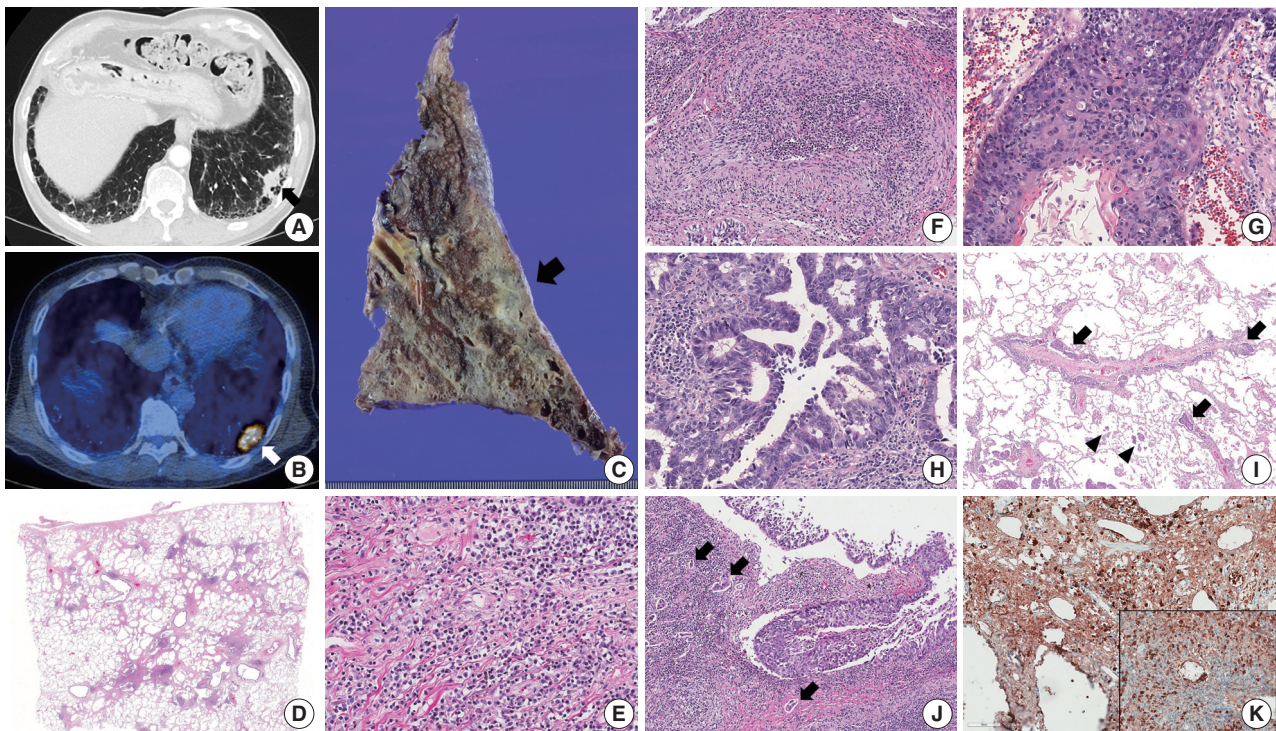


**Fig. 1.** (A, B) Chest computed tomography shows a consolidative nodule (arrow) in a background of subpleural reticulation and honeycomb fibrosis at both lung bases. Positron emission tomography reveals  $^{18}\text{F}$ -fluorodeoxyglucose uptake by the nodule. (C) The cut section of the lung showed an ill-defined and gray-tan colored mass (arrow). The background lung was emphysematous and fibrotic. (D–F) Histologic examination shows irregular interstitial fibrosis with patchy lymphoid aggregation, predominant lymphoplasmacytic infiltration, and occasional obliterative phlebitis. (G) The squamous cell carcinoma component shows keratinization and multifocal dyskeratosis. (H) The adenocarcinoma component was mainly composed of a moderately differentiated acinar pattern. (I) Diffuse spread through air space (arrowheads) and multifocal lymphangitic spread (arrow) of tumor cells are frequently found at the periphery of the mass. (J) Dense fibrosis and lymphoplasmacytic infiltration are found in the peritumoral area. Multifocal endolymphatic tumor emboli (arrows) are also noted. (K) Both IgG4 and IgG (inset) immunohistochemical stains show diffuse positivity in the infiltrating plasma cells. The IgG4/IgG ratio was over 40%.

pearls (Fig. 1G). The glandular component was mainly acinar pattern with focal micropapillary pattern (Fig. 1H). Diffuse spread through air space of tumor cells was frequently found at the periphery of the mass (Fig. 1I). Multifocal lymphangitic spreading of tumor cells and metastatic lymph nodes were found (Fig. 1I). Dense fibrosis and lymphoplasmacytic infiltration were adjacent to the tumor cells (Fig. 1J). The final pathologic stage was pT2aN2M0 by the American Joint Committee on Cancer seventh staging system. Immunohistochemistry (IHC) staining revealed the squamous cell carcinoma component was focally positive for p63 (1:200, Biocare, Concord, CA, USA), and the glandular component was negative for TTF-1 (1:50, Dako, Glostrup, Denmark). Additional tests for anaplastic lymphoma kinase (ALK) IHC staining (1:40, NCL-ALK, clone 5A4, Novocastra, Newcastle upon Tyne, UK) and epidermal growth factor receptor gene mutation analysis using a PNA clamping kit (Panagene, Inc., Daejeon, Korea) were negative, and up to 10% of the tumor cells showed membrane positivity for programmed death-

ligand 1 (RTU, 22C3, Dako). IgG4 (1:2,000, The Binding Site, Birmingham, UK) IHC stain showed diffuse positivity in infiltrating plasma cells (> 50 cells/high-power field), and the IgG4/IgG ratio was over 40% (Fig. 1K). Thus, the patient's IPF was thought to be a manifestation of IgG4-RLD, and we concluded that primary adenosquamous carcinoma had developed in the background of IgG4-RLD. This study was approved by the Institutional Review Board of the Samsung Medical Center with a waiver of informed consent (IRB No. 2018-11-053) and performed in accordance with the principles of the Declaration of Helsinki.

## DISCUSSION

IgG4-RD was first reported as autoimmune pancreatitis in 2001.<sup>7</sup> IgG4-RD is known to predominantly involve the pancreas, hepatobiliary tract, salivary glands, and lacrimal glands, and lung or pleural involvement can occur in up to 35% of patients.<sup>8</sup> The

**Table 1.** Clinicopathologic findings of previously reported cases of concurrent IgG4-RLD lung cancer

Reference	Sex	Age (yr)	Location	Type of tumor	Pattern of ADC	Radiologic finding	Pattern of IgG4-RLD	TNM stage	Other manifestations	Serum IgG4 (mg/dL)
Present case	M	66	LLL	ASC	Acinar and focal micropapillary	Subpleural nodule in a background of reticular and honeycomb fibrosis	Interstitial	pT2aN2M0	IHD	232
Zen et al. <sup>4</sup>	M	NA	RLL	ADC	Mixed, including acinar	Nodular lesion within the reticular shadow	Interstitial	pT1N2M0	No	NA
Inoue et al. <sup>5</sup>	M	78	RUL	ADC	Lepidic	Ground-glass opacity with central collapse and pleural indentation	Nodular	pT1bN0M0	Pancreas	983
Tashiro et al. <sup>6</sup>	M	72	RML	ADC	Lepidic	Spiculated nodule with pleural indentation	Nodular	pT1bN0M0	No	346

IgG4-RLD, IgG4-related lung disease; ADC, adenocarcinoma; M, male; LLL, left lower lobe; ASC, adenosquamous carcinoma; Interstitial, interstitial lung disease type; IHD, intrahepatic bile duct; RLL, right lower lobe; NA, not available; RUL, right upper lobe; Nodular, solid nodular type; RML, right middle lobe.

histologic patterns of IgG4-RLD are divided into three types: solid nodular type, bronchovascular type, and interstitial lung disease type.<sup>4</sup>

It is still debatable whether IgG4-RD is associated with malignancy. Yamamoto et al.<sup>9</sup> observed 106 IgG4-RD patients (primarily with Mikulicz's disease), and the high standardized incidence rate (SIR) of 3.83 supported the association between IgG4-RD and increased incidence of total malignancies. In a different study, Hirano et al.<sup>10</sup> observed 113 patients with IgG4-RD (primarily with autoimmune pancreatitis), and the SIR was not significant (1.04). These different outcomes likely result from whether the studies considered cases that simultaneously found malignancies and IgG4-RD.

However, none of these studies included patients with IgG4-RLD that involved the pulmonary system. The association of IgG4-RLD with lung cancer has not been studied, and only three lung cancer cases in IgG4-RLD patients have been reported with their histopathologic findings.<sup>4-6</sup>

The patient in the present case had primary adenosquamous carcinoma, which has not been reported alongside IgG4-RD in the previous literature. The adenosquamous carcinoma was characterized by poorly differentiated squamous and glandular tumor cells with lymph node metastases, and the IgG4-RLD background presented as interstitial lung disease. Inoue et al.<sup>5</sup> and Tashiro et al.<sup>6</sup> reported a well differentiated lepidic pattern of adenocarcinoma accompanied by IgG4-RLD as a solid nodule or ground glass opacity pattern. There were no lymph node metastases in these two cases. Zen et al.<sup>4</sup> reported a moderately differentiated, mixed pattern (including acinar pattern) adenocarcinoma in a background of IgG4-RLD presenting as interstitial pneumonia. Lymph node metastases were found, and the pathologic stage was pT1N2M0. In the present case, similar to Zen's report, moderately to poorly differentiated carcinoma occurred in a background of IgG4-RLD with an interstitial lung disease pat-

tern. Numerous lymphovascular invasions and lymph node metastases were found, and the final pathologic stage was pT2aN2M0. Table 1 summarizes the clinicopathologic and radiological characteristics of the reported cases of concurrent IgG4-RLD and lung cancer.

There have been no studies on whether IgG4-RLD increases the risk of malignancy. Although there have been a small number of cases, it is likely that lung cancer more frequently occurs in the solid nodular or interstitial lung disease type of IgG4-RLD rather than the bronchovascular type. Thus far, malignancy has not been reported in the bronchovascular type of IgG4-RLD. There is also a possibility that the differentiation or aggressiveness of the tumor may depend on the background type of IgG4-RLD, and the prognosis could be worse in patients with the interstitial lung disease background. Further studies with more cases are needed to elucidate the relationship between tumor aggressiveness and patterns of IgG4-RLD.

## ORCID

Sangjoon Choi: <https://orcid.org/0000-0003-2108-0575>

Sujin Park: <https://orcid.org/0000-0001-7819-5678>

Man Pyo Chung: <https://orcid.org/0000-0002-5548-0764>

Tae Sung Kim: <https://orcid.org/0000-0001-7512-0283>

Jong Ho Cho: <https://orcid.org/0000-0003-3362-4621>

Joungho Han: <https://orcid.org/0000-0003-4424-7008>

## Author Contributions

Conceptualization: SC.

Data curation: SC, JH.

Formal analysis: SC, SP.

Investigation: SC, SP.

Methodology: SC, SP, JH.

Project administration: SC, JH.

Resources: MPC, TSK, JHC.

Supervision: JH.

Validation: JH.

Writing—original draft: SC, JH.

Writing—review & editing: SC, SP, JH.

### Conflicts of Interest

The authors declare that they have no potential conflicts of interest.

### REFERENCES

1. Deshpande V, Zen Y, Chan JK, et al. Consensus statement on the pathology of IgG4-related disease. *Mod Pathol* 2012; 25: 1181-92.
2. Ahn JH, Hong SI, Cho DH, Chae EJ, Song JS, Song JW. A case of IgG4-related lung disease presenting as interstitial lung disease. *Tuberc Respir Dis* 2014; 77: 85-9.
3. Cho DH, An JH, Kang YM, Chae EJ, Song JS, Song JW. A case of IgG4-related lung disease mimicking non-specific interstitial pneumonia. *Korean J Med* 2015; 88: 308-12.
4. Zen Y, Inoue D, Kitao A, et al. IgG4-related lung and pleural disease: a clinicopathologic study of 21 cases. *Am J Surg Pathol* 2009; 33: 1886-93.
5. Inoue T, Hayama M, Kobayashi S, et al. Lung cancer complicated with IgG4-related disease of the lung. *Ann Thorac Cardiovasc Surg* 2014; 20 Suppl: 474-7.
6. Tashiro H, Takahashi K, Nakamura T, Komiya K, Kimura S, Sueoka-Aragane N. Coexistence of lung cancer and immunoglobulin G4-related lung disease in a nodule: a case report. *J Med Case Rep* 2016; 10: 113.
7. Hamano H, Kawa S, Horiuchi A, et al. High serum IgG4 concentrations in patients with sclerosing pancreatitis. *N Engl J Med* 2001; 344: 732-8.
8. Fei Y, Shi J, Lin W, et al. Intrathoracic involvements of immunoglobulin G4-related sclerosing disease. *Medicine (Baltimore)* 2015; 94: e2150.
9. Yamamoto M, Takahashi H, Tabeya T, et al. Risk of malignancies in IgG4-related disease. *Mod Rheumatol* 2012; 22: 414-8.
10. Hirano K, Tada M, Sasahira N, et al. Incidence of malignancies in patients with IgG4-related disease. *Intern Med* 2014; 53: 171-6.

# Frozen Cytology of Meningeal Malignant Solitary Fibrous Tumor/Hemangiopericytoma

Myunghee Kang · Na Rae Kim  
Dong Hae Chung · Gie-Taek Yie<sup>1</sup>

Departments of Pathology and <sup>1</sup>Neurosurgery,  
Gil Medical Center, Gachon University College of  
Medicine, Incheon, Korea

**Received:** January 28, 2019  
**Revised:** February 27, 2019  
**Accepted:** March 20, 2019

## Corresponding Author

Na Rae Kim, MD  
Department of Pathology, Gil Medical Center,  
Gachon University College of Medicine,  
21 Namdong-daero 774 beon-gil, Namdong-gu,  
Incheon 21565, Korea  
Tel: +82-32-460-3073  
Fax: +82-32-460-2394  
E-mail: clara\_nrk@gjilhospital.com

A 51-year-old woman presented with severe dizziness. The brain magnetic resonance image revealed a 5.5 cm multiloculated mass with a thick rim in the left temporal lobe. Cytological examination of frozen diagnosis of the mass showed hypercellular sheets of round and rhabdoid cells in a hemorrhagic background, and two mitotic figures were observed. Histologically, the excised dura-based mass consisted of predominantly round cells with small foci of rhabdoid tumor cells in a pseudoalveolar pattern in a hemorrhagic background, and the cells showed nuclear positivity for signal transducer and activator of transcription 6 as well as frequent mitosis. The mass was diagnosed as a grade 3 solitary fibrous tumor (SFT)/hemangiopericytoma (HPC). The cytological diagnosis of SFT/HPC is challenging because of the heterogeneous cytological findings, such as histological heterogeneity, and because there are no standardized cytological criteria for malignant SFT/HPC. Cytological findings, such as singly scattered small cells, hypercellularity, rare ropy collagen, and round and rhabdoid cells with pseudoalveolar pattern, may assist in the diagnosis of malignant SFT/HPC.

**Key Words:** Solitary fibrous tumors; Hemangiopericytoma; Frozen; Cytology; Central nervous system

A solitary fibrous tumor (SFT)/hemangiopericytoma (HPC) is uncommon and was first described as an angioblastic meningioma.<sup>1</sup> Currently, this combined term is used to describe a wide pathological spectrum of mesenchymal tumors that share molecular events such as paracentric inversion on chromosome 12q13, resulting in NGFI-A-binding protein 2 (*NAB2*)/signal transducer and activator of transcription 6 (*STAT6*) gene fusion with *STAT6* nuclear immunopositivity.<sup>2</sup> Dedifferentiation also occurs in SFT/HPC of the central nervous system (CNS), such as in those of extracranial soft tissue.<sup>3</sup>

Few studies have reported the cytological characteristics of SFT/HPC of the CNS.<sup>4</sup> Here, we present the cytology of a frozen, histologically-proven, grade 3, meningeal SFT/HPC.

## CASE REPORT

### Clinical summary

A 51-year-old woman visited an emergency center for abrupt onset of severe dizziness, sweating, and vomiting during sleep. The brain diffusion-weighted magnetic resonance image showed a 5.5-cm multiloculated mass with a thick hypointense rim,

hemorrhage, and surrounding edema in the left temporal lobe (Fig. 1). Cavernous hemangioma or other brain tumors with hemorrhage were considered, and surgical excision was performed. After complete surgical excision, the patient continued in good health for the next seven months.

### Pathological findings

For diagnosis of the frozen tissue, hemorrhagic and highly vascular crush smears composed of sheets of monotonous round cells with heterochromatic nuclei in a hemorrhagic background were obtained (Fig. 2A). Focal myxoid changes were also found (Fig. 2B). Small round cells were juxtaposed with abundant thin capillaries (Fig. 2C, D). In a background rich in red blood cells, only scant eosinophilic ropy collagen was found juxtaposed to the vessels (Fig. 2E). Small clusters or singly-dispersed round-to-rhabdoid cells with eccentric nuclei and eosinophilic, granular, inclusion-like cytoplasm were found (Fig. 2F). Based on the frozen cytology, the initial differential diagnoses of the frozen tissue were SFT/HPC and meningioma of focal rhabdoid type. Albeit rare, an oncocytic glomus tumor was also considered.

For the permanent diagnosis, formalin-fixed paraffin-embed-

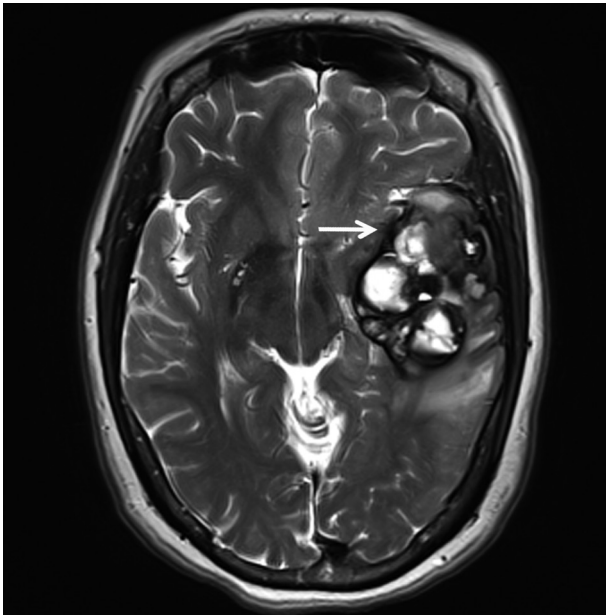


**Fig. 1.** T2-weighted magnetic resonance imaging reveals a 5.5 cm multiloculated mass (arrow) with a thick hypointense rim.

ded tissue sections of the entire resected mass were prepared, and they showed a highly vascular and hemorrhagic meningeal mass (Fig. 2G, H) composed of monotonous round cells with irregular nuclei and prominent single nucleoli and a scanty amount of eosinophilic cytoplasm (Fig. 2I). A peripheral solid portion was found, and blood-filled cavities with centrally detached cells, forming a pseudoalveolar and peritheliomatous arrangement, were observed throughout the mass (Fig. 2J). Mitotic activity was 9 mitoses/10 high power fields. Necrosis was not found. The congested portion showed myxoid changes in the loose edematous stroma and loose pseudoalveolar arrangements (Fig. 2K). Focal rhabdoid appearance was also observed, and these cells showed nuclear positivity for INI-1 (1:200, 25/BAF47, BD Bioscience, San Diego, CA, USA) (Fig. 2L, left). Both round and spindle cells showed positive staining for CD34 (1:50, QBEnd 10, Dako, Glostrup, Denmark) and nuclear positivity for STAT6 (1:150, S-20, sc-621, Santa Cruz Biotechnology, Santa Cruz, CA, USA) (Fig. 2L, right). The cells showed negative staining for glial fibrillary acidic antigen (prediluted, polyclonal, Dako), smooth muscle actin (1:100, 1A4, Dako), myogenin (1:50, LO26, Novocastra, Newcastle upon Tyne, UK), desmin (1:100, D33, Dako), epithelial membrane antigen (1:100, E29, Dako), S100 protein (1:600, polyclonal, Dako), synaptophysin (prediluted, DAK-SYNAP, Dako), and c-kit (1:30, T5P5, Novocastra).

Ultrathin sections revealed that the closely packed spindle-to-ovoid tumor cells had a moderate amount of cytoplasm con-

taining intermediate filaments and lysosomes with a well-formed Golgi apparatus (Fig. 3A). Occasionally, intermediate junctions and pinocytotic vesicles were found. The tumor cells also had cytoplasmic processes containing intermediate filaments (Fig. 3B). Basal lamina-like materials were found around the tumor cells (Fig. 3C). Microvillous processes were found, but paranuclear whorls of intermediate filaments were not observed. Isocitrate dehydrogenase 1 (*IDH1*) gene R132 mutation was tested on the resected specimen by real time polymerase chain reaction (PCR) using a PNA Clamp *IDH1* Mutation Detection Kit (Panagene Ltd., Daejeon, Korea) according to the manufacturer's instructions, and methylation of *O*<sup>6</sup>-methylguanine DNA methyltransferase (*MGMT*) was tested by methylation-specific PCR; *IDH1* R132 mutation was not detected, but promoter methylation of *MGMT* gene was detected. The tumor was diagnosed as a grade 3 SFT/HPC according to a 3-tier system based on the histopathological phenotype and mitotic count by the World Health Organization 2016 CNS tumor classification.<sup>4</sup>

Approval for this case report was obtained from our Institutional Review Board (No. GCIRB 2019-020) with a waiver of informed consent.

## DISCUSSION

In extracranial SFT/HPC cases, a preoperative, cytological, confirmative diagnosis can be established if STAT6 immunostaining of the cell block is performed.<sup>2</sup> However, cytologic examination of meningeal SFT/HPC cannot be performed until intraoperative frozen smears are made.<sup>5</sup> Therefore, cytological examination of frozen tissue is important for the correct diagnosis. Cytologic findings of SFT/HPC are nonspecific and include the so-called patternless pattern and various heterogeneous cytologic findings.<sup>6</sup> SFT/HPC with naked stripped nuclei has been shown to occur outside the CNS, and scattered ropy collagen fragments in the background are the most distinctive cytological findings.<sup>6</sup> Both intracranial and extracranial SFT/HPC shows scanty to moderate cellular smears of oval-to-spindle cells in a background of irregular ropy fragments of collagen or eosinophilic collagenous matrix.<sup>7</sup> Most of the cells are dispersed singly or in loose clusters enmeshed in vessels.<sup>8</sup> Individual tumor cells show uniform bland nuclei with even finely-granular chromatin in low-grade SFT/HPC.<sup>9</sup> The most consistent features are the presence of stripped nuclei in the background and thick ropy bands of matrix material.<sup>9</sup> The predominance of small round cells in the tumor should be used to distinguish SFT/HPC from neurocytoma or paraganglioma. Considering the heterogeneous and wide

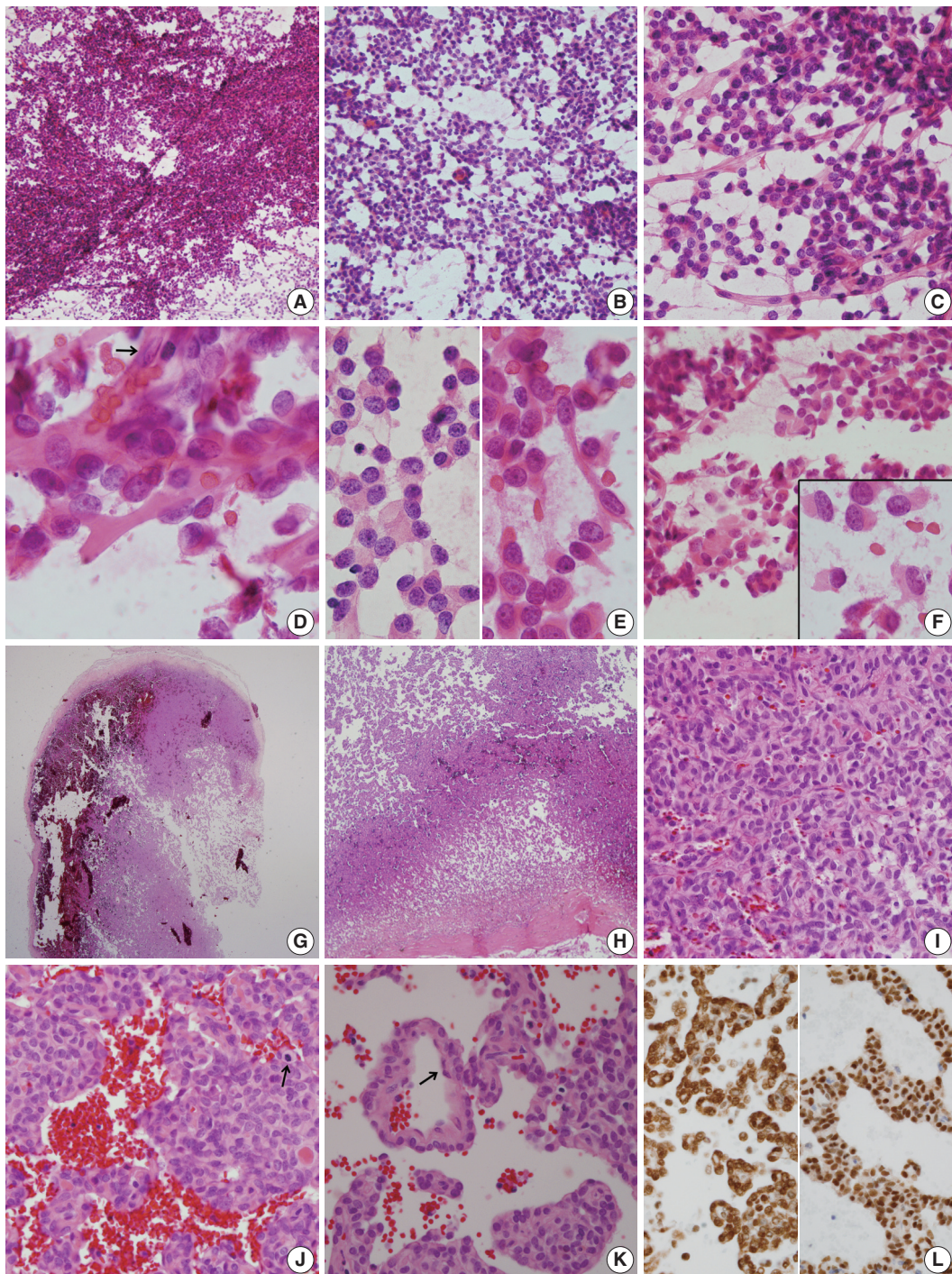


**Fig. 2.** (A–F) Frozen crush cytology. (A) Cellular smear shows sheets or singly scattered round to oval cells with cellular overlapping. (B) Round- to ovoid-shaped cells have bland nuclear chromatin with a moderate amount of cytoplasm with occasional rhabdoid features. (C) Endothelial cell-lined capillaries crossing the tumor cells. (D) High magnification shows several clusters of oval cells of a pseudoalveolar architecture, coarse chromatin pattern, small inconspicuous nucleoli, and irregular nuclear membranes. Arrow indicates nuclei of endothelial cells. (E) Small round cells (left) and ropy collagenous tails are found. (F) Round to ovoid cells had bland nuclear chromatin with a moderate amount of cytoplasm with occasional rhabdoid features. Inset indicates focal rhabdoid appearance. (G–L) Histological findings. (G, H) Patternless solid growth of spindle to round cells is present with intervening staghorn-like vessels. (I) High magnification shows congested tumor composed of round cells around blood vessels. (J) Pseudoalveolar pattern reveals hypercellularity, pleomorphism, and mitosis (arrow). (K) Congested pseudoalveolar pattern is arranged around blood vessels resembling a pseudorosette-like pattern. Arrow indicates endothelial cells. (L) The tumor cells retain INI-1 immunostainability (left) and nuclear positivity for STAT6 (right).

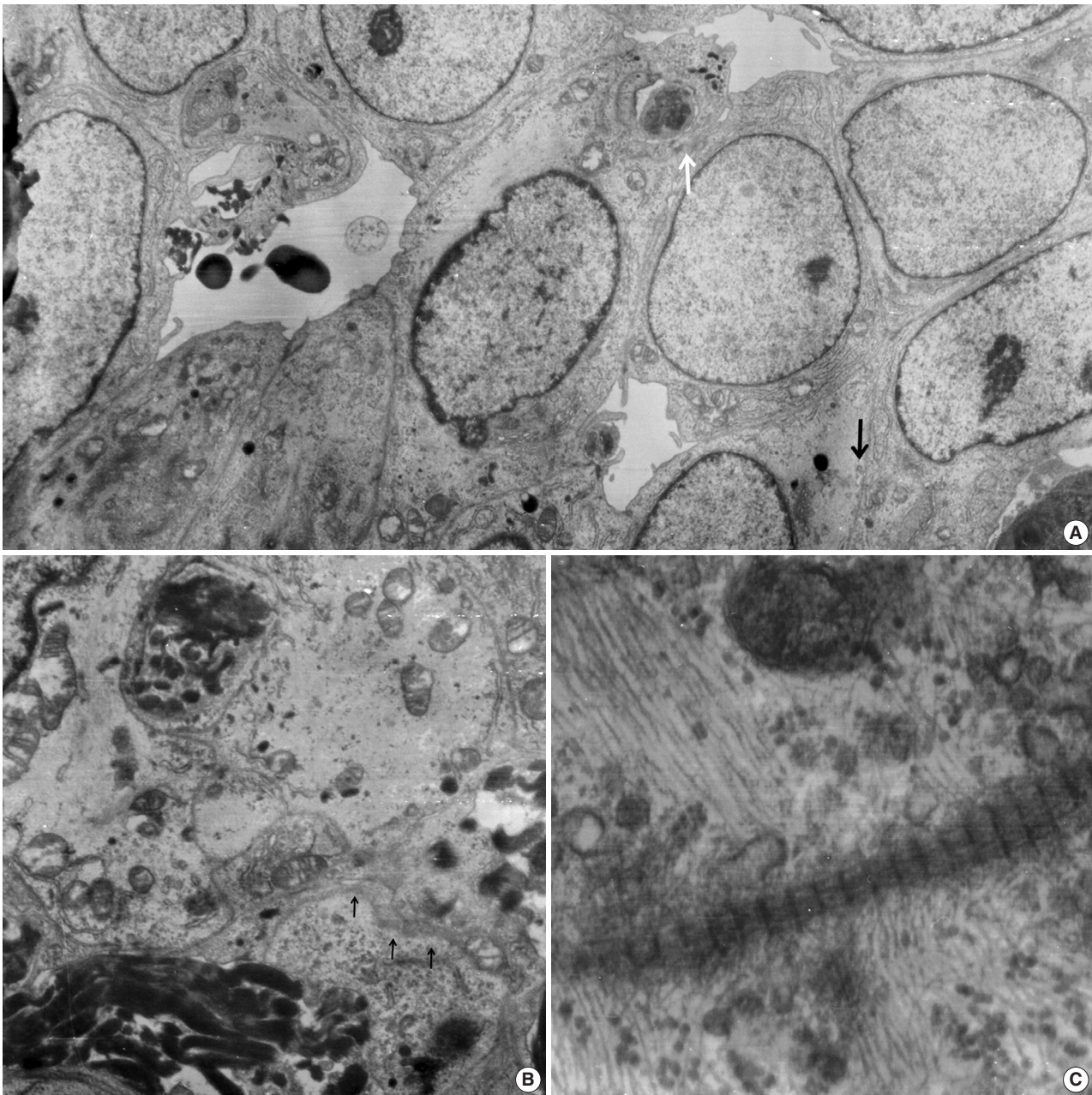


**Fig. 3.** Electron microscopic findings. (A) Round shaped tumor cells have a moderate amount of cytoplasm filled with intermediate filaments, lysosomes with well-formed Golgi apparatus. Note pinocytotic vesicles (black arrow), intermediate junctions (white arrow) and microvillous processes ( $\times 2,500$ ). (B) Basal lamina-like materials (arrows) surround the tumor cells filled with intermediate filaments ( $\times 5,000$ ). (C) Well-formed collagen bundles at the extracellular spaces and cytoplasmic intermediate filaments are found ( $\times 3,000$ ).

spectrum of histological findings observed in SFT/HPC, cytologic heterogeneity is comprehensible. SFT/HPC of the CNS is a poorly understood mesenchymal neoplasm,<sup>4</sup> and few reports of intraoperative cytological characteristics have been published.<sup>8,10</sup> Low to intermediate grade SFT/HPC, i.e., grades 1 and 2, shows cohesive hypercellular sheets of polygonal- to spindle-shaped tumor cells. The tumor cells have a scant amount of wispy cyto-

plasm and oval-to-short spindle-shaped nuclei with coarse chromatin, whereas SFT/HPC of higher grade shows increased nuclear pleomorphism with frequent mitoses.<sup>4</sup> Dense ropy collagen or dilated vascular structures are observed in almost all cases of benign SFT/HPC.<sup>2</sup> The present case showed scant ropy collagen, which made it difficult to diagnose SFT/HPC using frozen sections.<sup>11</sup> Despite the standardized cytological data for higher

grades of SFT/HPC, malignant SFT/HPC shows hypercellularity, pleomorphism, rare rosy collagen, and epithelioid or round cell features with occasional rosette-like structures as well as necrosis and mitosis, similar to high-grade SFT/HPC.<sup>9,11,12</sup> Some studies have suggested that a predominance of single cells confirms the presence of high-grade SFT/HPC.<sup>11,13</sup> Rare cases of extracranial malignant SFT/HPC have shown heterologous mesenchymal differentiation or lipomatous or rhabdomyosarcomatous differentiation.<sup>3,14</sup> In the present case, rhabdoid-featured cells retained INI-1 and showed negative staining for myogenin or desmin without ultrastructural demonstration of paranuclear whorls of intermediate filaments. In retrospect, the frozen cytology from the present case that showed a scanty amount of background rosy collagen and dispersed predominant round cells with an occasional rhabdoid appearance did not permit a correct frozen diagnosis. In our opinion, these focal rhabdoid features in the high-grade malignant SFT/HPC, which may be a high-grade component, may indicate the initial signs of dedifferentiation from low-grade SFT/HPC.

Besides, branching staghorn vasculature is one of the salient findings of SFT/HPC, and it is not commonly found in frozen cytology but instead in the cell block. Thus, the vascular pattern does not contribute to the frozen cytologic diagnosis of SFT/HPC.<sup>12</sup> Spindle cell predominant smears in SFT/HPC must be distinguished from nerve sheath tumors and fibrous histiocytoma. Meningeal SFT/HPC may show dispersed small monomorphic cells. Smears from a benign peripheral nerve-sheath tumor are composed of end-tapering spindle cells arranged in interlacing bundles in a myxoid background, and wavy nuclear buckling and thick hyalinized vessels may be found. In the present case, the frozen sections showed a myxoid edematous background, but this myxoid background is uncommon in the cytology of SFT/HPC with neither spindle cell nor round cell morphology.<sup>12</sup> A predominant spindle cell morphology and scattered background amorphous wispy magenta materials in a hemorrhagic background cause problems during diagnosis. A rarely-observed, monotonous, round cell-predominant SFT/HPC, like in the present case, should be distinguished from neurocytoma, paraganglioma, glomus tumor, and glomangiopericytoma, which are uncommon meningeal tumors.<sup>15</sup> A peritheliomatous or pseudoalveolar arrangement in cystic changes, which is unusual for SFT/HPC, is commonly found in glomus tumor/glomangiopericytoma or synovial sarcoma.<sup>16</sup> Capillaries crossing related to tumor cells as well as hemorrhagic cytological smears are shared cytological findings for glomus tumor, paraganglioma, and SFT/HPC. When compared with the knobby oval- to spindle-shaped

tumor cells of SFT/HPC, the cytology of glomus tumor or glomangiopericytoma is characterized by a fine vasculature surrounded by monotonous round cells with punched out nuclei and amphophilic cytoplasm with an indistinct cell border. Paraganglioma cytology also shows round cells with moderate nuclear pleomorphism and fine granular cytoplasm enveloped by thin vessels.<sup>17</sup>

It is important to differentiate SFT/HPC from meningioma. The indistinct cell border and stippled chromatin of meningioma differ from the cytology observed in the present case. Intraoperative cytologic findings of meningiomas have been well-described: nuclear grooves, intranuclear inclusions, and psammoma bodies as well as abundant wispy cytoplasm. However, similar to the present case, a predominance of epithelioid cells and small cell change or rhabdoid cells can be found in higher grade meningiomas. Rhabdoid meningioma shows eccentrically placed vesicular nuclei with eosinophilic plump hyaline cytoplasm and short broad processes.<sup>18</sup> The nuclei have occasional nuclear inclusions with no nuclear grooves and whorls. Oncocytic glomus tumor can be distinguished with the histological findings. Other CNS neoplasms showing rhabdoid cells are astrocytomas, glioblastomas, ependymomas and atypical teratoid/rhabdoid tumors, CNS embryonal tumors with rhabdoid features, choroid plexus carcinomas, sarcomas, and germ cell tumors.<sup>19</sup>

The present case showed MGMT methylation. Although a clear correlation between MGMT methylation status and response has not yet been clarified in SFT/HPC (unlike glioblastoma), SFT/HPC with or without MGMT methylation enhanced the response to alkylating agents by inhibiting DNA repair in a previous study using temozolomide or dacarbazine.<sup>20</sup>

The present tumor was diagnosed as grade 3 SFT/HPC, although the frozen smears did not show the typical cytological findings of SFT/HPC such as a paucity of collagenous stroma and rhabdoid cells masquerading as high grade meningioma, as well as a pseudoalveolar pattern, which are heterogeneous.

## ORCID

Myunghee Kang: <https://orcid.org/0000-0003-4083-888X>  
 Na Rae Kim: <https://orcid.org/0000-0003-2793-6856>  
 Dong Hae Chung: <https://orcid.org/0000-0002-4538-0989>  
 Gie-Taek Yie: <https://orcid.org/0000-0002-8706-7253>

## Author Contributions

Conceptualization: NRK.

Data curation: DHC.

Investigation: GTY.

Writing—original draft: MK, NRK.

Writing—review & editing: NRK, DHC.

### Conflicts of Interest

The authors declare that they have no potential conflicts of interest.

### REFERENCES

- Bailey P, Cushing H, Eisenhardt L. Angioblastic meningioma. *Arch Pathol Lab Med* 1928; 6: 953-90.
- Tani E, Wejde J, Åström K, Wingmo IL, Larsson O, Haglund F. FNA cytology of solitary fibrous tumors and the diagnostic value of STAT6 immunocytochemistry. *Cancer Cytopathol* 2018; 126: 36-43.
- Maekawa A, Kohashi K, Yamada Y, et al. A case of intracranial solitary fibrous tumor/hemangiopericytoma with dedifferentiated component. *Neuropathology* 2015; 35: 260-5.
- Giannini G, Rushing EJ, Hainfellner JA, et al. Solitary fibrous tumour/haemangiopericytoma. In: Louis DN, Ohgaki H, Wiestler OD, Cavenee WK, eds. *WHO classification of tumours of the central nervous system*. 4th ed. Lyon: IARC, 2016; 249-54.
- Samal S, Kalra R, Sharma J, Singh I, Panda D, Ralli M. Comparison between crush/squash cytology and frozen section preparation in intraoperative diagnosis of central nervous system lesions. *Oncol J India* 2017; 1: 25-30.
- Tihan T, Viglione M, Rosenblum MK, Olivi A, Burger PC. Solitary fibrous tumors in the central nervous system: a clinicopathologic review of 18 cases and comparison to meningeal hemangiopericytomas. *Arch Pathol Lab Med* 2003; 127: 432-9.
- Clayton AC, Salomao DR, Keeney GL, Nascimento AG. Solitary fibrous tumor: a study of cytologic features of six cases diagnosed by fine-needle aspiration. *Diagn Cytopathol* 2001; 25: 172-6.
- Gill SS, Bharadwaj R. Cytomorphologic findings of hemangiopericytoma of the meninges: a case report. *Indian J Pathol Microbiol* 2007; 50: 422-5.
- Baliga M, Flowers R, Heard K, Siddiqi A, Akhtar I. Solitary fibrous tumor of the lung: a case report with a study of the aspiration biopsy, histopathology, immunohistochemistry, and autopsy findings. *Diagn Cytopathol* 2007; 35: 239-44.
- Sandoh K, Ishida M, Okano K, et al. Cytological characteristics of meningeal solitary fibrous tumor metastatic to the lung: a case report with immunocytochemical analysis. *Mol Clin Oncol* 2018; 9: 17-20.
- Khanchel F, Driss M, Mrad K, Romdhane KB. Malignant solitary fibrous tumor in the extremity: cytopathologic findings. *J Cytol* 2012; 29: 139-41.
- Bishop JA, Rekhman N, Chun J, Wakely PE Jr, Ali SZ. Malignant solitary fibrous tumor: cytopathologic findings and differential diagnosis. *Cancer Cytopathol* 2010; 118: 83-9.
- Ali SZ, Hoon V, Hoda S, Heelan R, Zakowski MF. Solitary fibrous tumor: a cytologic-histologic study with clinical, radiologic, and immunohistochemical correlations. *Cancer* 1997; 81: 116-21.
- Kwon JH, Song JS, Jung HW, Lee JS, Cho KJ. Malignant solitary fibrous tumor with heterologous rhabdomyosarcomatous differentiation: a case report. *J Pathol Transl Med* 2017; 51: 171-5.
- Deb P, Kinra P, Bhatia HS. Intraoperative cytology of central neurocytoma mimicking oligodendroglioma. *J Cytol* 2011; 28: 219-22.
- Shetty KJ, Rao C, Prasad HL. Glomangiopericytoma versus solitary fibrous tumor: an omental tumor with unusual diagnostic dilemma. *Indian J Surg Oncol* 2016; 7: 475-8.
- Naniwadekar MR, Jagtap SV, Kshirsagar AY, Shinagare SA, Tata HR, Sahoo K. Fine needle aspiration diagnosis of carotid body tumor in a case of multiple paragangliomas presenting with facial palsy: a case report. *Acta Cytol* 2010; 54: 635-9.
- Xiao GQ, Burstein DE. Cytologic findings of rhabdoid meningioma in cerebrospinal fluid. *Acta Cytol* 2008; 52: 118-9.
- Louis DN, Perry A, Reifenberger G, et al. The 2016 World Health Organization Classification of tumors of the central nervous system: a summary. *Acta Neuropathol* 2016; 131: 803-20.
- Stacchiotti S, Tortoreto M, Bozzi F, et al. Dacarbazine in solitary fibrous tumor: a case series analysis and preclinical evidence vis-à-vis temozolomide and antiangiogenics. *Clin Cancer Res* 2013; 19: 5192-201.

